Development of chitosan-based bioactive coating enriched with trans-cinnamaldehyde essential oil for enhancing postharvest quality of fresh produce

闫, 僖芮

Development of chitosan-based bioactive coating enriched with *trans*-cinnamaldehyde essential oil for enhancing postharvest quality of fresh produce

Yan Xirui

2024

Development of chitosan-based bioactive coating enriched with *trans*-cinnamaldehyde essential oil for enhancing postharvest quality of fresh produce

by

Yan Xirui

A dissertation submitted to the Laboratory of Postharvest Science in fulfillment of the requirements for the degree of

DOCTOR OF PHILOSOPHY

Graduate School of Bioresource and Bioenvironmental Sciences

Kyushu University

Japan

July 2024

Acknowledgements

I would like to express my deepest and sincere appreciation to my supervisor Professor Fumihiko Tanaka for his kindness, illuminating guidance and profound knowledge throughout my Ph.D. period. He always made me feel confident in my skills. Learning and working under his guidance and encouragement was the best experience ever. Furthermore, it is my honor to benefit from his personality and diligence, which I will treasure my whole life. My gratitude to him knows no bounds. Also, I would like to express my heartfelt gratitude to the responsible Assistant Professor Fumina Tanaka for her considerate care for my study and life.

I would like to take this opportunity to express my deep gratitude and respect to the review committees: Professor Takashi Okayasu and Associate Professor Yasumaru Hirai.

I would like to thank all the faculty members and staff, especially Ms. Kanae Iwasaki for their kindness, patience, and support during my studies.

I would like to express my heartfelt thanks to Professor Tungalag Dong and Associate Professor Xueyan Yun, who taught me how to start an experiment and write scientific articles since I was a novice. Without their enlightenment, it is unfeasible for me to complete all these tough works.

I would like to give my heartfelt thanks to my parents, for their endless love and care for me. Whatever I need and wherever I go, they are always supporting me without any requirement in return. I thank my loving family and family is where I can forever turn.

Special thanks to my husband, Fanze Meng, who made my study abroad life rich and colorful. I am grateful for his meticulous care, constant support, and patient encouragement. For me, all the days together have become precious memories. Hope, hold your hand and grow old with you.

I also want to thank to all those who have helped me, cared about me and wished me well, especially to Dr. Ata Aditya Wardana, Dr. Laras Putri Wigati, Dr. Phuong Thi Hang Nguyen, Dr. Arisa Koga, Ms. Tran Thi Van, Mr. Francis Ngwane Nkede, Mr. Mohammad Hamayoon Wardak and all the members of the Postharvest Sciences laboratory at Kyushu University. This is a testament to our cooperation, our diligence, persistence and perpetual friendship.

I would like to thank The Ministry of Education, Culture, Sports, Science and Technology of Japan (MEXT) for granting me this valuable scholarship allowing me to continue my studies in Japan for my Ph.D. degree.

Ultimately, I would like to thank myself for always sticking to dreams. I traveled to Japan for the first time in 2018, and since then the seed of my dream has been buried deep in my heart. It has not been easy to make it all the way to this day, but luckily the gods of fortune have favored me. May always remember the way I came, run as hard as I can and become the person I want to be.

Fukuoka

April 2024

Yan Xirui

ABSTRACT

Edible polysaccharide coatings have been used to improve the shelf life of postharvest products by regulating gas permeability through the formation of strong hydrogen bonds with solvents. Meanwhile, the preparation process of coating/film packaging depends on the properties of the ingredients, the preparation method and the final commercial value. The aim of this study was to prepare bioactive films/coatings for fresh fruit storage using chitosan (CS) as a substrate in different combinations (blending, cross-linked). The study was divided into three points as follows:

1) Diepoxy- (ethylene glycol) (PEG) was prepared by cross-linked method and then combined with chitosan (CS)/*trans*-cinnamaldehyde (CIN) to form a polymer composite coating to prolong the shelf-life of postharvest bananas.

2) Bioactive films of chitosan (CS)/ polyvinyl alcohol (PVA)/*trans*-cinnamaldehyde (CIN) were prepared by co-blending and the effects of different concentrations (0.5%, 1.0% and 1.5%) of CIN on the physicochemical properties of the ternary films were investigated.

3) To improve the storage life and regulate reactive oxygen species (ROS) metabolism of these tomatoes by utilizing chitosan (CS), polyvinyl alcohol (PVA), and *trans*-cinnamaldehyde (CIN) water barrier coatings and the potential mechanisms were investigated.

In the first work, development of bioactive coatings containing 1% (w/v) CS, 0.6% (w/v) PEG, and CIN was achieved. The tensile strength, light transmission, water vapor permeability (WVP), and antibacterial properties were enhanced by the incorporation of CIN. The CIN-containing films appeared compact and rough, as observed using scanning electron microscopy (SEM) and atomic force microscopy (AFM). In addition, the quality attributes of the bananas were evaluated at room temperature for 24 days, and the results showed that the CS/PEG/CIN coating

delayed the respiration peak, weight loss, sugar content loss, and maintained firmness, color, total soluble solids (TSS), titratable acid (TA), and the appearance of the bananas. Principal component analysis (PCA) revealed that the bioactive coating significantly affected the respiration rate and weight loss of bananas.

Further work, bioactive films of CS / PVA/ CIN were prepared by co-blending, and the impact of varying concentrations (0.5, 1.0 and 1.5 %) of CIN on the physicochemical properties of the ternary films was investigated. The ATR/FT-IR analysis revealed that the bioactive film is modulated by Schiff base (C=N) and hydrogen-bond interactions of CS, PVA, and CIN. Inclusion of CIN into the film improved mechanical properties with tensile strength increased from 0.5 % (68.52 MPa) to 1.5 % (76.95 MPa). The presence of CIN within the CS/PVA film also remarkably affected oxygen permeability and improved light transmittance. Additionally, the water barrier and contact angle properties were improved with increasing CIN content. The morphology of the CIN-containing films appeared non-stratified and dense when observed by SEM and AFM. Moreover, spore germination and in vitro assays confirmed strong antifungal activity of the CIN-containing film against *P. italicum* (~90 %) and *B. cinerea* (~85 %). The ternary films also exhibited excellent antioxidant activity, as evidenced by DPPH radical scavenging activity (31.43%) and ferric reducing power ($OD_{700\ nm}$ = 0.172) at the highest CIN concentration tested.

Lastly, aimed to extend the shelf life of tomatoes while controlling reactive oxygen species (ROS) metabolism through the application of water barrier coatings containing CS, PVA, and CIN. The results showed that the addition of CIN increased the structural density, water barrier properties, and *B. cinerea* resistance of the coatings. The CIN-containing coating significantly improved water loss, firmness, TA value, color, and appearance; decreased lipid peroxidation; and modulated the ROS scavenging system. Principal component analysis and correlation revealed that

the CIN-coated material, characterized by water-barrier properties, contributed positively to the preservation of tomatoes during refrigeration. Water barrier coating facilitates the enzymatic ROS scavenging system in tomatoes, thereby extending their senescence.

To summarize, different treatment combinations based on CS can greatly extend the shelf-life of fruits and vegetables and delay post-harvest senescence, which are expected to become the new preservation technology.

CONTENTS

LIST OF FIGURES

LIST OF TABLES

ABBREVIATIONS

ATR/FTIR	Attenuated total reflection /Fourier-transform infrared spectroscopy
AFM	Atomic Force Microscope
APX	Ascorbate peroxidase
A_w	Water activity
B. cinerea	*Botrytis cinerea*
CLSM	Confocal Laser Scanning Microscope
CS	Chitosan
CAT	Catalase
CMC	Carboxymethyl cellulose
CIN	*trans*-Cinnamaldehyde
DPPH	2,2-diphenyl-1-picrylhy-drazyl
EAB	Elongation at break
EOs	Essential oils
E. coli	*Escherichia coli*
EDTA	Ethylenediamine tetraacetic acid
FRAP	Ferric reducing antioxidant power
FS	Film swelling
GR	Glutathione reductase
H_2O_2	Hydrogen peroxide
LOX	Lipoxygenase

MAP	Modified atmosphere packaging
MDA	Malondialdehyde
MC	Moisture content
O_2^-	Superoxide anion
OTR	Oxygen transmission rate
OP	Oxygen permeability
PCA	Principal component analysis
PDA	Potato dextrose agar
PEG	epoxidized-Polyethylene glycol
P. italicum	*Penicillium italicum*
POD	Peroxidases
PVA	Polyvinyl alcohol
PVP	Polyvinyl-pyrrolidone
PVPP	Polyvinylpolypyrrolidone
RH	Relative humidity
ROS	Reactive Oxygen Species
S. aureus	*Staphylococcus aureus*
SEM	Scanning Electron Microscope
SR	Swelling rate
SOD	Superoxide dismutase
TA	Titratable acid
TBA	Thiobarbituric acid
TCA	Trichloroacetic acid

TS	Tensile Strength
TSS	Total soluble solids
WCA	Water contact angle
WS	Water solubility
WVTR	Water vapor transmission rate
WVP	Water vapor permeability

CHAPTER 1

INTRODUCTION

1.1. Background

Fruits and vegetables are rich in essential vitamins, minerals, fibers and health-enhancing compounds. Consumption of fruits and vegetables has increased dramatically in recent years as a result of growing awareness of their nutritional value. Consumers rightfully demand high quality produce that is safe and nutritionally secure. As a result, there is a growing interest in the nutritional content, texture and flavor of fruits and vegetables (Sivakumar & Bautista-Baños, 2014). With rising living standards and changing consumer habits, the impact of the fruit industry on the global economy has grown significantly in recent decades, with many developing countries ranking among the world's top producers of fresh fruit annually, according to the most recent data from the Food and Agriculture Organization of the United Nations (FAO) (Chen *et al.,* 2021). However, severe quality deterioration and post-harvest losses are inevitable due to a variety of factors at the pre- and post-harvest stages, which are particularly prevalent in developing countries. Unfortunately, about one third of the fresh fruit produced in these regions never reaches the consumer's table. Chief among the many factors contributing to these losses are inherent physiological aging and susceptibility to infection by fungal pathogens (Tian *et al.,* 2016). While the use of synthetic chemicals remains a relatively convenient and economical way to manage post-harvest losses, the long-term reliance on chemical pesticides has raised public concerns about

environmental pollution and food safety. Therefore, there is an urgent need to modernize the traditional technologies used to effectively control fruit aging, enhance resistance, regulate oxidative senescence and extend the shelf life of fresh products (Ma, Zhang, Bhandari, & Gao, 2017).

Traditionally, coatings have served to protect foods from physiological disorders and microbial contamination. As early as the 12th and 13th centuries, the Chinese pioneered the use of wax coatings on lemons and oranges to prevent them from spoiling (Kumar, 2019). In recent years, consumer awareness of the importance of edible, biodegradable and environmentally friendly packaging materials has increased. As a result, films and coatings have grown rapidly in the food processing sector, providing freshness solutions for a wide range of foods, including fruits such as apples, pears, bananas, mangoes, kiwis and pineapples, vegetables such as carrots and potatoes, as well as dairy products and meats (Aitboulahsen *et al.,* 2018; Senturk Parreidt, Schmid, & Müller, 2018; Suhag, Kumar, Petkoska, & Upadhyay, 2020). Coatings or films are recognized as environmentally friendly alternatives to synthetic or plastic packaging materials and play a key role in reducing post-harvest losses of fruits and vegetables (Bashir, Jan, & Aggarwal, 2017; Moghadam *et al.,* 2020). These coatings are effective in protecting foods from various microbial contaminants (Bajpai, Chand, & Lodhi, 2013), extending shelf life (Hasan, Ferrentino, & Scampicchio, 2020), reducing lipid oxidation (Kazemian-Bazkiaee *et al.,* 2020) and moisture loss (De Pilli, 2020).

Coatings and films have different uses: coatings are applied directly to the surface of fruits, vegetables and other foods, while films are used as packaging materials (Aguirre-Joya *et al.,* 2018). These coatings are made from biodegradable, non-toxic materials derived from a variety of biopolymer matrices such as polysaccharides, proteins, lipids and composites (Zubair & Ullah,

2020). Biopolymer-based coatings are effective in blocking gas diffusion, moisture migration, aroma changes and solute exchange (Sabbah *et al.,* 2019). These coating materials can be sprayed or impregnated to form a thin protective layer on food products (Yousuf, Qadri, & Srivastava, 2018).

Chitosan (CS), a linear polysaccharide composed of glucosamine and N-acetylglucosamine units and is the only cationic pseudo-natural polymer. Chitin is the second most abundant biopolymer in nature and is mainly derived from the exoskeleton of crustaceans such as shrimp and lobster (Bellich *et al.,* 2016). In addition, CS has shown excellent properties as a film-forming material. CS films are selectively permeable to gases such as carbon dioxide and oxygen. However, CS films are highly permeable to water vapor, which severely limits their utility (Elsabee & Abdou, 2013). Effective control of moisture transfer is a key property sought after in most food products, especially those stored in humid environments. Consequently, a number of methods have been employed to enhance the physical properties of biopolymer films. These methods include the utilization of various chemical and physical methods that have proven to be effective in enhancing the mechanical properties of the films. Examples include the use of cross-linking agents, irradiation, ultrasonic treatments and blending techniques (Cieśla, Salmieri, & Lacroix, 2006).

Modification of CS by cross-linking has been widely used to prepare various CS-based materials. Cross-linking affects several key properties of CS, including its mechanical strength, stability, swelling behavior, permeability, solubility and other related properties (Saheed, Da Oh, & Suah, 2021). Various cross-linkers, which are able to effectively bind to the abundant amino and hydroxyl groups in CS, have been used to modify CS in various adsorption applications. This process typically involves the use of cross-linkers such as epichlorohydrin, tripolyphosphate and glutaraldehyde or other chemicals that have already been cross-linked combined with CS (Saheed

et al., 2021; Zhang *et al.,* 2018). Although cross-linking may reduce the adsorption capacity of CS, it has also been used to enhance the mechanical strength of CS (Kumar *et al.,* 2004).

Polymer blending provides a versatile platform for creating materials with improved properties, functionality and activity. Synthetic polymers typically have higher, customizable properties (Khosravi *et al.,* 2020; Zarrintaj *et al.,* 2020). CS blends with other polymers are widely used as solution blends or melt blends (Correlo *et al.,* 2005; Przybysz *et al.,* 2018).CS blends are primarily formulated by mixing CS with solutions of other polymers. Due to its adaptability and compatibility, CS can be combined with various types of blends to improve the mechanical, oxygen and moisture permeability, as well as the antimicrobial and antioxidant properties of the polymers.

CS co-polymers as well as essential oils (EOs) can also be more effective in prolonging the conditions of a willing product's post-harvest life, while maintaining the overall quality of the fruit's nutritional content. The main benefit of using EOs in polymer coatings is the ability to slow the rate of diffusion of antimicrobial agents. Incorporation of EOs into the coating effectively reduces the inoculum intensity of post-harvest pathogens on the fruit surface. In addition, the application of fruit coatings can help reduce weight loss during storage and transportation, largely due to the enhanced hydrophobicity of these coatings. In addition to this, blending with EOs also reduces the respiration rate of fruits, which may be attributed to the lipophilic nature of essential oils in controlling as well as dispersing in various matrices (Chen *et al.,* 2023).

Therefore, in this work, in order to maximize the effectiveness of the coating treatment, the development of three materials based on CS, polymers and EOs using both cross-linking and blending treatments on the post-harvest quality of fresh fruits and the metabolism of reactive oxygen species (ROS) has been proposed.

1.2. Objectives

Based on above-explained fact, therefore, the objectives of this study were to (1) develop composite coatings using chitosan, polymers (epoxidized polyethylene glycol or polyvinyl alcohol) and *trans*-cinnamaldehyde. (2) characterize the functional properties of the coating film. (3) apply the coating on fresh fruit and characterize the effects. The finding expected that it may facilitate the development of bio-active coating for agriculture products.

1.3. Thesis layout

- Chapter 1 presents the background, objectives, thesis layout, and list of publication and conferences.
- Chapter 2 exhibits cross-linked films based on chitosan/diepoxy-poly (ethylene glycol) incorporating *trans*-cinnamaldehyde essential oil: Preparation, properties, and application in banana storage
- Chapter 3 demonstrates the characterization and bio-functional performance of chitosan/poly (vinyl alcohol)/*trans*-cinnamaldehyde ternary biopolymeric films.
- Chapter 4 shows the water barrier coating of chitosan/poly (vinyl alcohol)/*trans*-cinnamaldehyde regulated postharvest quality and reactive oxygen species metabolism of 'Frutica' tomato (*Solanum lycopersicum L.*)
- Chapter 5 summarizes the contents of all chapters presented in this this paper and presents an outlook.

1.4. Publication and conferences

Peer-reviewed journal publications:

- Yan, X., Meng, F., Van, T. T., Wigati, L. P., Nkede, F. N., Hamayoon, W. M., ... & Tanaka, F. (2024). Water barrier coating of chitosan/poly (vinyl alcohol)/*trans*-cinnamaldehyde regulated postharvest quality and reactive oxygen species metabolism of 'Frutica'tomato (Solanum lycopersicum L.). Postharvest Biology and Technology, 212, 112910. Doi: https://doi.org/10.1016/j.postharvbio.2024.112910
- Yan, X., Meng, F., Wigati, L. P., Van, T. T., Phuong, N. T. H., Koga, A., ... & Tanaka, F. (2024). Improvement of cross-linked films based on chitosan/diepoxy-poly (ethylene glycol) incorporating *trans*-cinnamaldehyde essential oil: Preparation, properties, and application in banana storage. International Journal of Biological Macromolecules, 130299. Doi: https://doi.org/10.1016/j.ijbiomac.2024.130299
- Yan, X., Wardana, A. A., Wigati, L. P., Meng, F., Leonard, S., Nkede, F. N., ... & Tanaka, F. (2023). Characterization and bio-functional performance of chitosan/poly (vinyl alcohol)/*trans*-cinnamaldehyde ternary biopolymeric films. International Journal of Biological Macromolecules, 246, 125680. Doi: https://doi.org/10.1016/j.ijbiomac.2023.125680
- Yan, X., Dong, T., Yun, X., Tanaka, F., Tanaka, F., Wardana, A. A., & Meng, F. (2023). Improving 'Nanguo'pear fungal disease and storability by chitosan coating combined with diepoxy-poly (ethylene glycol). Food Bioscience, 53, 102842. Doi: https://doi.org/10.1016/j.fbio.2023.102842

Conference publications:

- Xirui Yan, Fanze Meng, Fumina Tanaka, Fumihiko Tanaka, Effect of the ternary bioactive water-barrier coating on storage quality and antioxidant of "Frutica" tomato (Solanum

lycopersicum L.), Poster at the The 77th Kyushu Society of Agricultural and Food Science and Technology Annual Meeting Research Presentation Program.

- Xirui Yan, Xueyan Yun, Tungalag Dong, Fumina Tanaka, Fumihiko Tanaka, Optimization of cross-linked chitosan coating formulations for improving postharvest quality of pear fruit, International Symposium on Machinery and Mechatronics for Agricultural and Biosystems Engineering 2022 (ISMAB2022), Kaohsiung Exhibition Center, Kaohsiung, Taiwan.
- Xirui Yan, Fumina Tanaka, Fumihiko Tanaka, Optimization of cross-linked chitosan coating formulations for improving the quality of pears during storage, Presented at the The 76th Kyushu Society of Agricultural and Food Science and Technology Annual Meeting Research Presentation Program.

1.5. References

Aguirre-Joya, J. A., De Leon-Zapata, M. A., Alvarez-Perez, O. B., Torres-León, C., Nieto-Oropeza, D. E., Ventura-Sobrevilla, J. M., . . . Ramos-Aguiñaga, M. E. (2018). *Basic and applied concepts of edible packaging for foods*. In *Food packaging and preservation* (pp. 1-61): Elsevier

Aitboulahsen, M., Zantar, S., Laglaoui, A., Chairi, H., Arakrak, A., Bakkali, M., & Hassani Zerrouk, M. (2018). Gelatin-based edible coating combined with Mentha pulegium essential oil as bioactive packaging for strawberries. *Journal of Food Quality,* 2018.

Bajpai, S., Chand, N., & Lodhi, R. (2013). Water sorption properties and antimicrobial action of zinc oxide nano particles loaded sago starch film. *Journal of microbiology, Biotechnology and food sciences,* 2(4), 2368-2387.

Bashir, K., Jan, K., & Aggarwal, M. (2017). Thermo-rheological and functional properties of gamma-irradiated wholewheat flour. *International Journal of Food Science & Technology,* 52(4), 927-935.

Bellich, B., D'Agostino, I., Semeraro, S., Gamini, A., & Cesàro, A. (2016). "The good, the bad and the ugly" of chitosans. *Marine drugs,* 14(5), 99.

Chen, S., Tian, H., Mao, J., Ma, F., Zhang, M., Chen, F., & Yang, P. (2023). Preparation and application of chitosan-based medical electrospun nanofibers. *International Journal of Biological Macromolecules,* 226, 410-422.

Chen, T., Ji, D., Zhang, Z., Li, B., Qin, G., & Tian, S. (2021). Advances and strategies for controlling the quality and safety of postharvest fruit. *Engineering,* 7(8), 1177-1184.

Cieśla, K., Salmieri, S., & Lacroix, M. (2006). Modification of the properties of milk protein films by gamma radiation and polysaccharide addition. *Journal of the Science of Food and Agriculture,* 86(6), 908-914.

Correlo, V. M., Boesel, L., Bhattacharya, M., Mano, J., Neves, N., & Reis, R. (2005). Properties of melt processed chitosan and aliphatic polyester blends. *Materials Science and Engineering: A,* 403(1-2), 57-68.

De Pilli, T. (2020). Development of a vegetable oil and egg proteins edible film to replace preservatives and primary packaging of sweet baked goods. *Food Control,* 114, 107273.

Elsabee, M. Z., & Abdou, E. S. (2013). Chitosan based edible films and coatings: A review. *Materials science and engineering: C,* 33(4), 1819-1841.

Hasan, S. K., Ferrentino, G., & Scampicchio, M. (2020). Nanoemulsion as advanced edible coatings to preserve the quality of fresh-cut fruits and vegetables: a review. *International Journal of Food Science & Technology,* 55(1), 1-10.

Kazemian-Bazkiaee, F., Ebrahimi, A., Hosseini, S. M., Shojaee-Aliabadi, S., Farhoodi, M., Rahmatzadeh, B., & Sheikhi, Z. (2020). Evaluating the protective effect of edible coatings on lipid oxidation, fatty acid composition, aflatoxins levels of roasted peanut kernels. *Journal of Food Measurement and Characterization,* 14, 1025-1038.

Khosravi, A., Fereidoon, A., Khorasani, M. M., Naderi, G., Ganjali, M. R., Zarrintaj, P., . . . Gutiérrez, T. J. (2020). Soft and hard sections from cellulose-reinforced poly (lactic acid)-based food packaging films: A critical review. *Food Packaging and Shelf Life,* 23, 100429.

Kumar, M. R., Muzzarelli, R. A., Muzzarelli, C., Sashiwa, H., & Domb, A. (2004). Chitosan chemistry and pharmaceutical perspectives. *Chemical reviews,* 104(12), 6017-6084.

Kumar, N. (2019). Polysaccharide-based component and their relevance in edible film/coating: A review. *Nutrition & Food Science,* 49(5), 793-823.

Ma, L., Zhang, M., Bhandari, B., & Gao, Z. (2017). Recent developments in novel shelf life extension technologies of fresh-cut fruits and vegetables. *Trends in Food Science & Technology,* 64, 23-38.

Moghadam, M., Salami, M., Mohammadian, M., Khodadadi, M., & Emam-Djomeh, Z. (2020). Development of antioxidant edible films based on mung bean protein enriched with pomegranate peel. *Food Hydrocolloids,* 104, 105735.

Przybysz, M., Zedler, Ł., Saeb, M. R., & Formela, K. (2018). Structure-property relationships in peroxide-assisted blends of poly (ε-caprolactone) and poly (3-hydroxybutyrate). *Reactive and Functional Polymers,* 127, 113-122.

Sabbah, M., Di Pierro, P., Dell'Olmo, E., Arciello, A., & Porta, R. (2019). Improved shelf-life of Nabulsi cheese wrapped with hydrocolloid films. *Food Hydrocolloids,* 96, 29-35.

Saheed, I. O., Da Oh, W., & Suah, F. B. M. (2021). Chitosan modifications for adsorption of

pollutants–A review. *Journal of hazardous materials,* 408, 124889.

Senturk Parreidt, T., Schmid, M., & Müller, K. (2018). Effect of dipping and vacuum impregnation coating techniques with alginate based coating on physical quality parameters of cantaloupe melon. *Journal of Food Science,* 83(4), 929-936.

Sivakumar, D., & Bautista-Baños, S. (2014). A review on the use of essential oils for postharvest decay control and maintenance of fruit quality during storage. *Crop protection,* 64, 27-37.

Suhag, R., Kumar, N., Petkoska, A. T., & Upadhyay, A. (2020). Film formation and deposition methods of edible coating on food products: A review. *Food Research International,* 136, 109582.

Tian, S., Torres, R., Ballester, A., Li, B., Vilanova, L., & González-Candelas, L. (2016). Molecular aspects in pathogen-fruit interactions: Virulence and resistance. *Postharvest Biology and Technology,* 122, 11-21.

Yousuf, B., Qadri, O. S., & Srivastava, A. K. (2018). Recent developments in shelf-life extension of fresh-cut fruits and vegetables by application of different edible coatings: A review. *Lwt,* 89, 198-209.

Zarrintaj, P., Ramsey, J. D., Samadi, A., Atoufi, Z., Yazdi, M. K., Ganjali, M. R., . . . Formela, K. (2020). Poloxamer: A versatile tri-block copolymer for biomedical applications. *Acta biomaterialia,* 110, 37-67.

Zhang, B., Hu, R., Sun, D., Wu, T., & Li, Y. (2018). Fabrication of chitosan/magnetite-graphene oxide composites as a novel bioadsorbent for adsorption and detoxification of Cr (VI) from aqueous solution. *Scientific reports,* 8(1), 15397.

Zubair, M., & Ullah, A. (2020). Recent advances in protein derived bionanocomposites for food packaging applications. *Critical reviews in food science and nutrition,* 60(3), 406-434.

CHAPTER 2

Improvement of cross-linked films based on chitosan/diepoxy-poly (ethylene glycol) incorporating *trans*-cinnamaldehyde essential oil: Preparation, properties, and application in banana storage

2.1. Introduction

The banana (*Musa acuminata* L. AAA group, cv. cavendish) is widely cultivated and cherished because of its nutritional richness, which includes starch, phenols, dietary fiber, carotenoids, minerals, and trace elements (Qamar & Shaikh, 2018). However, as a climatic fruit, bananas are highly susceptible to rotting within a short period postharvest. The exposure of the fruit to air, where the cells in the banana constantly absorb oxygen and release carbon dioxide, accelerates the respiration rate and color change (browning) and reduces the sugar content, thereby negatively affecting consumer and market acceptance (Xie *et al.,* 2022). Hence, it is crucial to employ innovative technologies that can prolong the shelf-life of bananas and other food products.

Many strategies have been used to retard banana ripening during storage, including low-temperature storage (Wang *et al.,* 2021), modified atmosphere packaging (MAP) (Li *et al.,* 2023), UV irradiation (Yang *et al.,* 2022), and coatings (Yang, Zhai, et al., 2022). Nevertheless, low-temperature treatment is highly prone to cold damage and accelerated decay (Sagu, Nso, Karmakar, & De, 2014), and MAP technology has been noted to create a humid environment within the packaging, which could increase the risk of spoilage growth (Brat, Bugaud, Guillermet, & Salmon, 2020). Furthermore, UV irradiation has been observed to induce discoloration and the loss of nutrients, such as vitamins and antioxidants, which diminish the desirability and nutritional value for customers (Chemat *et al.,* 2020). According to previous reports, the film and coating may form a barrier layer on the fruit to maintain gas permeability characteristics (O_2, CO_2, and ethylene), controlling the respiration rate and growth of microorganisms (Nguyen *et al.,* 2021). Moreover, fruit coatings may be composed of natural substances such as polysaccharides, lipids, and proteins.

Chitosan (CS) is a widely used biopolymer known for its nontoxic and biodegradable nature. CS can create semipermeable membranes, thereby enhancing the shelf life of postharvest products.

Wantat et al. reported that the CS coatings with high or medium molecular weights (540 kDa and 265 kDa) effectively decrease the respiration rate and malondialdehyde (MDA) content and maintain the 'Hom Thong' banana fruit qualities at room temperature during storage (Wantat, Rojsitthisak, & Seraypheap, 2021). However, the poor mechanical properties and low gas permeability of CS frequently necessitate the addition of other polymers or essential oils (EOs) for film modification (Sultan, Elsayed, & Taha, 2023; Tessaro, Lourenço, Martelli-Tosi, & do Amaral Sobral, 2021).

Polyethylene glycol (PEG) is a water-soluble biocompatible, non-immunogenic, and nontoxic biomaterial. Moreover, crosslinking with CS can form a hydrogel film with desirable expansion properties owing to its high gas permeability, making it a suitable environment for the tissues of postharvest products (Yan *et al.,* 2022). Ahmadi et al. reported that adding PEG to CS films improves the water solubility of the composite film (Ahmadi, Oveisi, Samani, & Amoozgar, 2015). Other studies have found that the mechanical properties of CS membranes are slightly improved by the addition of PEG. However, the improvement was not substantial, and excessive amounts of PEG had an adverse effect on these properties. Recently, it has been demonstrated that incorporating hydrophobic EOs into composite films strengthens the water barriers and other properties (Hao *et al.,* 2023; Oyom *et al.,* 2022). Cinnamaldehyde (CIN), the primary constituent of cinnamon EO derived from plants, has been extensively studied as a potent antimicrobial agent with remarkable efficacy against bacteria and fungi. Noshirvani et al. reported that applying CIN oil as a plasticizer for CS-carboxymethyl cellulose (CMC) films enhanced the moisture permeability and preserved the antifungal properties (Noshirvani *et al.,* 2017). Fasihi *et al.* developed a CMC/polyvinyl alcohol/CIN film with notable antioxidant activity and strong ability to inhibit UV radiation (Fasihi *et al.,* 2019). Studies have revealed that bananas stored in a

nanocomposite film made of polypropylene and halloysite nanotube-CIN had superior performance and retained their high nutritional value for over seven days (Kolgesiz *et al.,* 2023). Others discovered that using a soybean protein isolate/zinc oxide nanoparticle/CIN coating could prevent detrimental alterations in fruit firmness throughout storage (Li *et al.,* 2019).

In our previous report (Yan *et al.,* 2022), cross-linked CS-PEG films, which exhibited a marked enhancement in the mechanical and gas permeability characteristics of CS-PEG37 films (1.0% CS and 0.6% PEG), were prepared successfully. Nevertheless, there was no significant difference between the pure CS coating and the cross-linked coating in terms of antibacterial activity against *Escherichia coli* (*E. coli*) and *Staphylococcus aureus* (*S. aureus*).

In this study, we applied a polymeric composite coating comprising CIN as an antibacterial agent with a cross-linked CS/PEG37 film to prolong the shelf life of post-harvest bananas and then assessed the physicochemical and antibacterial characteristics of the active composite films before banana coating. Throughout the storage period, the banana appearance and biological changes were monitored.

2.2. Materials and methods

2.2.1. Coating and film preparation

In a recent effort to generate crosslinked films, CS/PEG37 was chosen to integrate CIN because of its excellent mechanical qualities and gas permeability (Yan *et al.,* 2022). In brief, CS (1.0 g) was dissolved in 100 mL of 1% acetic acid. PEG (0.6 g) was dissolved in 100 mL distilled water and added to the CS solution. The mixture was left to react at 80 ℃ for 6 h during magnetic stirring. After that, tween 80 (0.2%) and CIN (w/w) was added, and the solutions were again heated for 15 min at 45 ℃. Then, CIN at three different concentrations (0.5, 1.0, and 1.5% w/w) was added to the CS/PEG37 solutions, followed by homogenization at 13000 rpm for 5 min. Degassing

was then performed for 15 min using a vacuum pump to remove air bubbles. The solution (aliquots of 15 mL) was poured into polystyrene Petri dishes and dried in an oven at 40 °C for 48 h. The dry films were peeled off and stored for 48 h at 25 °C and 50 ± 4% RH before further analysis. CS/PEG37 served as a control.

Control: CS/PEG37: 1.0% CS (w/v) + 0.6% PEG(w/v);

CS/PEG/CIN0.5: 1.0% CS (w/v) + 0.6% PEG(w/v) + 0.5% CIN (v/v);

CS/PEG/CIN1.0: 1.0% CS (w/v) + 0.6% PEG(w/v) + 1.0% CIN (v/v);

CS/PEG/CIN1.5: 1.0% CS (w/v) + 0.6% PEG(w/v) + 1.5% CIN (v/v).

2.2.2. Thickness

A digital micrometer (SK MITUTOYO Co., Ltd., Japan) was used to measure the thickness of the samples. This thickness was utilized for mechanical and opacity calculations.

2.2.3. Mechanical properties

The mechanical properties were assessed using an electrodynamic test bench (FGS-50E-L; Nidec-Shimpo, Japan). Slender samples (60 mm × 10 mm) were clamped between two grippers on the test platform at a speed of 60 mm/min. Each treatment was performed in triplicate.

2.2.4. Moisture content

The moisture content method was based off of that of Yan et al. (Yan *et al.,* 2023). First, an empty stainless-steel plate was weighed. A 2 cm × 2 cm film sample was placed on the same stainless-steel plate and weighed. The samples were then dried in an oven at 105 °C for one night, and the MC of the samples was determined by

$$\text{Moisture content (\%)} = \frac{W_{before} - W_{after}}{W_{before}} \times 100$$

where W_{before} represents before-dry sample weight (g), W_{after} represents after-dry sample weight (g)

2.2.5. Film swelling

Film swelling was measured using the Hosseini method (Hosseini, Rezaei, Zandi, & Farahmandghavi, 2015). The films were immersed in 25 mL distilled water at 80 rpm for 24 h, and the surface was wiped with filter paper until equilibrium was attained after 24 h. The SR was calculated by

$$Swelling\ rate\ = \frac{W_{swollen} - W_{dry}}{W_{dry}} \times 100$$

where W_{swollen} represents the weight of swollen samples (g), W_{dry} represents dry sample weight (g)

2.2.6. Water solubility

The film sample was initially stirred in 25 ml of distilled water at room temperature for 24 h and then the wiped films were placed in an oven at 105 °C for 24 h. The solubility was calculated by

$$\text{Water solubility (\%)} = \frac{W_{initial} - W_{final}}{W_{final}} \times 100$$

where W_{initial} is the weight of the film sample before immersion, W_{final} is the weight of the final dried film sample.

2.2.7. Water vapor permeability

The Water vapor permeability (WVP) was calculated gravimetrically in triplicate using ASTM E96-05 (ASTM, 2005). Films without faults were sealed on top of 28-cm glass test cups with 15 g of anhydrous calcium chloride as a desiccant at 0% RH. After weighing the cup, it was

placed in a 25 °C, 85% RH constant temperature and humidity chamber. The readings were recorded hourly for 12 h. Eq. shows how the water vapor transmission rate (WVTR) and WVP were determined by

$$\text{WVTR} = \frac{\triangle m}{\triangle t \times A}$$

$$\text{WVP} = \frac{WVTR \times L}{\triangle P}$$

where Δm/Δt is the moisture gain in weight per time (g s^{-1}), A is the exposed surface area (m^2), L is the thickness (mm), and ΔP is per unit difference in vapor pressure between the two sides (kPa)

2.2.8. Color

A color difference meter (CR-20; Konica Minolta Inc., Japan) was used to measure the film. A white standard color plate (L^* = 94.2, a^* = 0, b^* = 0) was used to calibrate the device before the measurement. The total color difference (ΔE) was determined by

$$\Delta E = \sqrt{(\Delta L^*)^2 + (\Delta a^*)^2 + (\Delta b^*)^2}$$

where L^*, a^*, and b^* are the color parameter values of the film sample.

2.2.9. Light transmission and opacity

The light transmission of the film samples (1 × 4 cm) was measured using a UV-Vis spectrophotometer (V-530; Jasco, Japan) at wavelengths ranging from 200 to 800 nm. Each treatment was repeated three times. The opacity of the films was calculated by

$$\text{Opacity} = \frac{Abs_{600}}{thickness}$$

where Abs_{600} is the value of absorbance at 600 nm

2.2.10. Scanning electron microscopy

The samples were appropriately sliced and affixed to an aluminum stub using conductive double-sided tape. Subsequently, the film samples were coated under vacuum conditions using an osmium coater before imaging. The surface morphology and cross section of the films were observed using SEM (SU3500; Hitachi, Japan) with an accelerating voltage of 15 kV.

2.2.11. Atomic force microscopy

AFM (5200S; Hitachi, Tokyo, Japan) was utilized to examine the surface morphology of the film with a 30 μm × 30 μm scan size. Two statistical parameters associated with the roughness of the samples were determined: the average roughness (Ra) and root-mean-square roughness (Rq).

2.2.12. In vitro activity

We evaluated the effect of the films on the growth of *E. coli* and *S. aureus* using the disk diffusion method employed by Zhou and Chiu with slight modification (Chiu & Lai, 2010; Zhou *et al.,* 2020). *E. coli* (NBRC 15034) and *S. aureus* (NBRC12732) obtained from the National Institute of Technology and Evaluation of the Biological Resource Center, Tokyo, Japan, were first cultured and then transferred using a sterile inoculation loop to a sterilized test tube containing 15 mL of TSB medium and incubated for 24 h at 37 °C. Subsequently, the bacterial concentration was diluted to 1×10^7 CFU/mL.

15 mL of sterilized TSA solution were poured into 90 mm diameter plastic dishes. After the medium had solidified, 100 μL of bacterial suspension of the test microorganism (1×10^7 CFU/mL) was inoculated onto the solidified agar. The prepared sterilized paper disc with a diameter of 10 mm, which had been sterilized by UV irradiation for 0.5 h, was placed in the center of the plate. A 200 μL of distilled water (control) or coating solution (CS/PEG; CS/PEG/CIN0.5; CS/PEG/CIN1;

CS/PEG/CIN1.5) was added to the paper disc using a pipette, and then incubated at 37 °C for 24h. The inhibition zone was measured using ImageJ software.

2.2.13. Application of bioactive films in banana preservation

Green bananas (Cavendish, Philippines) were purchased from the Nanguoku store eight weeks after harvesting (40–50% maturity). Bananas with uniform shape, weight, and no apparent damage were selected and immediately transferred to the laboratory. The coating was prepared according to the method described in Section 2.2.1, and the green bananas were divided into five groups with different treatments: control (not coated), CS/PEG, CS/PEG/CIN0.5, CS/PEG/CIN1, and CS/PEG/CIN1.5, respectively. The bananas were wiped and evenly coated for spread coating using a brush and dried with a fan for 2-3 h until a layer formed on the surface of the fruits. Then the products were stored in a refrigerator at 25 ˚C and 75% humidity for 24 days. Samples were randomly selected from each treatment for testing, and the physical and chemical parameters of the bananas were measured and photographed every four days.

2.2.14. Sensory evaluation and quality score

Sensory evaluation was performed based on previous methods (Yang *et al.,* 2022) with some modifications. The sensory characteristics of bananas were evaluated by 10 specially trained and voluntary professional doctoral students from food program of Kyushu University. All treatment groups were assessed within 1 h to prevent the loss of nutritional indicators. Sensory evaluation was performed based on five essential sensory aspects: color, flavor, texture, senescent spotting, and taste. These characteristics were rated on a 5-point scale; where 5.0 - 4.1 scale means that: the color is emerald green, the flavor is strong grassy, the texture is strong film, no spots and taste is complex and astringent to swallow; where 4.0 - 3.1 scale means that: the color is chartreuse, the

flavor is slight grassy, the texture is slight film, 1-25% spots and taste is slightly astringent with bitter, where 3.0 - 2.1 scale means that: the color is bright yellow, the flavor is pronounced banana flavor with a slight sweetness, the texture is softer with slight mushiness, 26 - 50% spots and taste is slightly sweet and slightly tangy; where 2.0 - 1.1 scale means that: the color is tawny, the flavor is intense banana flavor with a slight a nutty undertone, the texture is soft and mushy, 51-75% spots and taste is Very sweet with a subtle musky flavor; where 1.0 - 0 scale means that: the color is brown, the flavor is overripe banana flavor with an intense sweetness, the texture is very soft and squishy, 76 -100% spots and the taste is overly sweet and slightly fermented. A score of less than 2.0 was considered a loss of business value.

2.2.15. Weight loss of banana

An additional 15 bananas (five replicates per treatment group) were selected, stored at 25 ˚C for 24 days, and accurately weighed after 4, 8, 12, 16, 20, and 24 days of whole storage.

$$Weight\ loss = \frac{\text{initial weight} - daily\ \text{weight}}{\text{initial weight}} \times 100\%$$

where initial weight is the weight of the first day, (g); daily weight is the weight of the test day, (g).

2.2.16. Firmness of banana

Firmness was measured using a texturometer (GY-1) with 3 mm-deep holes pierced into the tested banana samples. The firmness of the bananas was measured in newtons (N).

2.2.17. Total soluble solids

Total soluble solid (TSS) content was analyzed using the Brix-Acidity Meter method (ATAGO PAL-BX|ACID121, Co., Ltd., Japan). Three grams of bananas were ground in 6 mL of distilled water and centrifuged at 2500 × g for 5 min, with three replicates for each storage day.

2.2.18. Respiration rate

An autosampler extracted a 0.5 mL gas sample and automatically injected it into a gas chromatograph (GC-2014; GL Science Inc., Japan). The headspace volume of the desiccator was determined by measuring the headspace of intact single bananas deposited for 2 h in a sealed, fixed-volume desiccator (240G2, 245 mm inside diameter; ASOEN Co., Ltd.). The helium carrier discharge rate was 33 mL/min. The oven, injector, and thermal conductivity detector temperature settings were set to 50, 80, and 100 °C, respectively. A calibration curve for the quantitative analysis was created using the absolute calibration method. The respiratory rate was measured in CO_2 (mg/kg/h).

2.2.19. Titratable acid

The titratable acid (TA) of the fruits was determined using a modified titration method (Nguyen *et al.,* 2021). Briefly, 10 g of the pulp sample was ground and transferred to a 100 mL volumetric flask. The mortar was then cleaned with distilled water and filtered. After adding 2 drops of 1% phenolphthalein indicator to 20 mL of filtrate, 0.1 mol/L sodium hydroxide solution was titrated until the solution appeared pink and did not fade within 0.5 min.

$$Titratable\ acid\ (\%) = \frac{V_{NaOH}(mL) \times C_{NaOH}(N) \times 0.067 \times 100}{10g}$$

where V_{NaOH} is the volume of NaOH solution consumed by the titrant, mL; C_{NaOH} is the molarity of NaOH solution, N; 0.064 is the conversion factor for maleic acid.

2.2.20. Reducing sugar

The reducing sugar content was determined using the 3,5-dinitrosalicylic acid (DNS) method by (Xie *et al.,* 2022) with modifications. A 25 mL test tube was filled with 1 g of banana mashed with distilled water. Leach lowering sugars at 80 °C for 30 minutes. After removal and chilling, the leachate was filtered, placed in a 100 mL volumetric flask, and set aside as a reducing sugar extraction solution. The color was developed by boiling 1 mL of the centrifugal supernatant and 1.5 mL DNS reagent for five min, then diluting it to 25 mL. Absorbance was measured at 540 nm. Distilled water served as a control, and the standard glucose curve was used to calculate reducing sugar in mg/g.

2.2.21. Statistical analysis

The experiments were repeated thrice for each method, except for thickness. One-way analysis of variance (ANOVA) using IBM SPSS software (version 26.0) was used to analyze the experimental data. To identify significant differences between treatments, the Least Significant Difference (LSD) and Duncan's multiple range tests were employed at a significance level of $p < 0.05$. Principal Component Analysis (PCA) was performed using GraphPad Prism 9 software to explore the relationship between the quality of the coated fruits and their physicochemical properties in each treatment group.

2.3. Results and discussion

2.3.1. Film thickness and mechanical properties

The film thickness of all the treated samples is shown in Table 2.1. The interaction of the EOs with the polymer matrix, causing swelling or altering the arrangement of the aggregated substance chains, caused the bioactive film to thicken to a maximum of 0.041 mm, a significant increase of

70.81% compared to the composite coating group (CS/PEG). The film thickness increasing may be due to increasing oil content of film (Sultan *et al.,* 2021). The thickness behavior was based on previous reports on CS-incorporated tea seed oil films.

The TS of the control film was 41.59 MPa and increased substantially after the addition of CIN. CS/PEG/CIN1 exhibited a significant increase in the TS value, with a maximum of 60.96 MPa. This may be due to the fact that CIN functions as a compatibilizer between CS and PEG, interacts with the polymer chains, promotes stronger intermolecular bonds, and enhances interfacial adhesion, thereby increasing the TS of the film. However, the TS decreased with further increase in CIN content. In this case, CIN has a plasticizing effect and reducing film stiffens (Arman Alim *et al.,* 2022; Kadirkhan *et al.,* 2022).

Table 2.1 shows that the minimum EAB of CS/PEG was only 17%. As the concentration of CIN increased, the EAB levels first increased and then decreased. Initially, at lower concentrations, CIN acted as a plasticizer in the complex solution, breaking the intermolecular forces between the polymer chains, thereby allowing them to move freely and increasing the overall flexibility of the film. However, at higher concentrations, CIN produced localized regions with increased stiffness, which led to partial aggregation and increased film brittleness. Yu *et al.* also observed a similar phenomenon when adding CIN EOs to hydroxypropyl starch nanocomposite films (Yu et al.,2023).

Table 2.1. Thickness, tensile strength (TS), elongation-at-break (EAB) of control CS/PEG and incorporated with different amounts of CIN.

CIN (%w/v)	Thickness (mm)	Tensile Strength (MPa)	Elongation at break (%)	Young's modulus (MPa)
0.0	0.024 ± 0.005^{c}	41.59 ± 1.51^{c}	17.04 ± 2.61^{d}	1431.02 ± 15.66^{d}
0.5	0.030 ± 0.004^{bc}	59.16 ± 4.48^{b}	27.93 ± 1.03^{b}	1801.61 ± 27.38^{a}
1.0	0.032 ± 0.002^{b}	60.96 ± 3.15^{a}	29.96 ± 4.00^{a}	1592.31 ± 45.96^{c}
1.5	0.041 ± 0.009^{a}	55.31 ± 2.41^{b}	20.49 ± 5.12^{c}	1698.61 ± 36.21^{b}

2.3.2. Moisture content

A high MC can have detrimental effects on the antibacterial properties of the film because it creates a more favorable environment for the growth and survival of microorganisms. Consequently, films or packaging materials with lower moisture levels are preferred (Zhou *et al.,* 2020). The MC values of the films with and without CIN are listed in Table 2.2. The high MC (16.81 ± 2.50%) observed in CS/PEG films can be attributed to their inherent characteristics. CS and PEG are hydrophilic polymers with high moisture affinity. However, as CIN was added to the composite coated film, the MC content slowly decreased from 9.92% to 9.88%, probably because of the hydrophobic nature of CIN, which implied that it repelled water. When CIN was added to the CS/PEG matrix, a barrier was formed that restricted the movement of water molecules through the film. This prevents the formation of channels that promote water vapor transport and maintains the integrity of the film (Li *et al.,* 2023).

2.3.3. Film swelling

Predicting the stability and quality variations of bio-based films during packaging and food storage requires knowledge of water sorption (Yang *et al.,* 2022). The film swelling values of all samples are shown in Table 2.2. According to the result, the control (CS/PEG) film confirmed a high value of swelling rate was 40.12%, which may be attributed to the hydrophilic properties of CS and PEG. However, the incorporation of CIN reduced the swelling of the films; that of CS/PEG/CIN0.5, CS/PEG/CIN1, and CS/PEG/CIN1.5 were 32.01, 25.66, and 25.57%, respectively. The swelling rate may be lower because CIN decreases the propensity of the CS/PEG composite matrix to bind water, limiting the number of groups in the network that can form hydrogen bonds with water molecules. Meanwhile, there was no significant difference between

1% and 1.5% of CIN. Similar results were obtained in the GS/gum Arabic/PEG composite films incorporated with black pepper and ginger EOs by (Amalraj et al., 2020).

2.3.4. Water solubility

The solubility of a film can be used to determine its stability and water resistance. The solubilities of the control and CIN composite bioactive films in distilled water at ambient temperature were investigated (Table 2.2). In the case of the CS/PEG37 film, the solubility content was higher than 35.74% that of the CIN-coated composite film. In addition, the bioactive film decreased significantly ($p < 0.05$) than CS/PEG films and the values from 25.29% (0.5%) to 18.73% (1.5%) due to the effective reaction with the composite matrix and the reduction of hydrophilic groups.

2.3.5. WVTR and WVP

Table 2.2 showed the WVTR and WVP values for each treatment group. Notably, the incorporation of CIN demonstrated a reduction in the WVTR value, particularly when 1.5% CIN was added to the CS/PEG composite film. In comparison to the control group (CS/PEG), the WVTR value decreased by 76.87%. This observation is consistent with the anticipated outcome and may be ascribed to the hydrophobic properties of CIN, which improve the water barrier characteristics of the polymer-based films. In addition, the distance water molecules traverse the film is increased when an oil phase is introduced. As a result, the induced polymer aggregation state changes disrupt the hydrogen bonds between CS and water in the matrix (Sánchez-González et al., 2009). Consequently, a lower WVTR is achieved.

As shown in Table 2.2, the WVP value of the CS/PEG film was significantly higher ($p < 0.05$) than that of the other treatment groups, with a value of $10.22 \pm 0.77 \times 10^{-10}$ ($g \cdot m^{-1}s^{-1}m^{2} \cdot Pa^{-1}$) that

was three times that of the other groups containing EOs, probably due to numerous hydrophilic groups, which is similar to previous results (Yan *et al.,* 2023). As CIN concentration increased, the value of WVP decreased from 3.56 ± 0.41×10^{-10} (g·$m^{-1}s^{-1}m^2$·Pa^{-1}) to 1.67 ± 0.72×10^{-10} (g·$m^{-1}s^{-1}m^2$·Pa^{-1}), indicating that CIN improved the water-resistance properties of composite films. In contrast, the introduction of the oil phase altered the aggregation state of the polymer and severed the water hydrogen bonds formed by the cross-linking of CS and PEG in the matrix.

Table 2.2. Moisture content (MC), swelling rate (SR), water solubility (WS), water vapor transmission rate (WVTR), water vapor permeability (WVP) of control CS/PEG and incorporated with different amounts of CIN

CIN (% w/v)	MC (%)	SR (%)	WS (%)	WVTR ×10^{-2} (g/s^{-1}·m^{-2})	WVP ×10^{-10} (g/$m^{-1}s^{-1}m^2$·Pa^{-1})
0.0	16.81±2.50^{a}	40.12±5.76^{a}	35.74±5.87^{a}	2.94±0.53^{b}	10.22±0.77^{a}
0.5	9.92±1.17^{c}	32.01±3.84^{b}	25.29±3.20^{b}	2.35±0.61^{a}	3.56±0.41^{b}
1.0	9.93±0.88^{c}	25.66±2.24^{c}	21.32±2.14^{bc}	0.76±0.17^{c}	2.14±0.26^{c}
1.5	9.88±0.63^{c}	25.57±1.48^{c}	18.73±1.13^{cd}	0.68±0.18^{d}	1.67±0.72^{d}

2.3.6. Color and opacity

The color and opacity of all treatment groups are shown in Table 2.3. Visually, the CS/PEG film appeared colorless, whereas the CIN-loaded films changed from slightly yellow to deep yellow, as inferred from the *b* values (yellowness/blueness). In addition, the apparent color of the bioactive film was influenced by the CIN concentration. For example, the Δ*E** value gradually increased with CIN-added films from 11.65 ± 0.27 to 22.67 ± 1.57, illustrating the color change.

The opacities of the control and CINs films are listed in Table 2.3. The values of CS/PEG, CS/PEG/CIN0.5, CS/PEG/CIN1, and CS/PEG/CIN1.5 were 1.67, 2.17, 2.20, and 2.48 AU/ mm, respectively. As the concentration of CIN increased, there was a gradual increase in opacity,

probably due to the addition of the yellow CIN agent and good dispersion, resulting in enhanced light absorption and reflection. Similar color and opacity variations have been reported for gellan gum-CS polyelectrolytes with thyme EO nano-emulsion (Zhang *et al.,* 2021).

Table 2.3. The color and opacity of control CS/PEG and incorporated with different amounts of CIN

CIN (%w/v)	*L**	*a**	*b**	*ΔE*	Opacity (AU/ mm)
0.0	95.48±0.39^{a}	-0.15±0.04^{d}	10.18±0.8^{c}	10.26±0.46^{c}	1.67±0.12^{c}
0.5	95.34±0.32^{a}	-0.67±0.22^{c}	11.58±0.85^{b}	11.65±0.27^{c}	2.17±0.21^{b}
1.0	94.93±0.60^{b}	-1.34±0.44^{b}	13.43±0.48^{b}	13.51±0.93^{b}	2.20±0.15^{b}
1.5	94.10±0.67^{b}	-2.63±0.44^{a}	22.51±3.87^{a}	22.67±1.57^{a}	2.48±0.10^{a}

2.3.7. Light transmittance

It is also crucial to focus on lipid oxidation by UV light (Rincón et al., 2019). The UV transmission spectra of the CS/PEG and CS/PEG/CIN films are shown in Figure 2.1. At 200–350 nm, the control group was significantly higher ($p < 0.05$) than the other treatment groups by approximately 76% (350 nm), which may be attributed to the specific properties of CS and PEG. It has been reported that CS and PEG can also have good optical properties and contribute to the high transmittance of the composite in specific wavelength ranges (Ahmed & Ikram, 2016). However, all CIN-containing films have an extremely low UV transmission at 200-300 nm (<0.05%) (Hosseini, Ghaderi, & Gómez-Guillén, 2021). As the CIN increases, the transmittance of the film decreased from 50% to 30% at 400 nm. This decrease in transmittance can be attributed to the introduction of additional components within the film that can absorb or scatter light across the visible and UV wavelength ranges, suggesting that the developed bioactive films have the potential to protect food products by mitigating the harmful effects of UV light, such as lipid oxidation, nutrient loss, discoloration, and the development of off-flavors (Sharma, Barkauskaite, Duffy, Jaiswal, & Jaiswal, 2020).

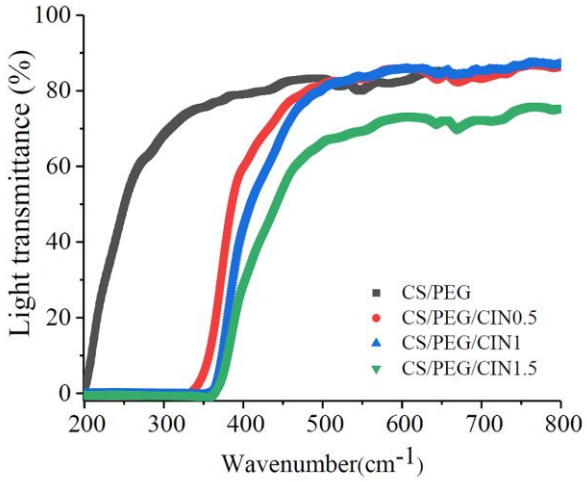

Figure 2.1. Light transmittance of control CS/PEG and incorporated with different amounts of CIN

2.3.8. Scanning electron microscope

Figure 2.2 showed the 2000 × SEM surface and cross-sectional images of the composite film and the films containing different concentrations of CIN. It can be seen that the surface of CS/PEG (Fig. 2A) was uniform, smooth, and compact and no bubbles, which confirmed the excellent compatibility of polymers at the interface. However, after the addition of CIN (Fig. 2.2 B–D), the surface became rougher with pores, most likely due to the pores created at the hydrophobic CIN oil and the polymer of hydrophilic nature, leading to matrix disruption, surface irregularity, and no surface integrality. Furthermore, it was observed that the introduction of CIN films increased the roughness of the cross-section (Fig. 2.2 b–d), which may result from aggregation or localized agglomeration of CIN on the film surface during solvent evaporation. Similar results were previously reported for starch with CS nanoparticles encapsulated in CIN films (Yu *et al.,* 2023).

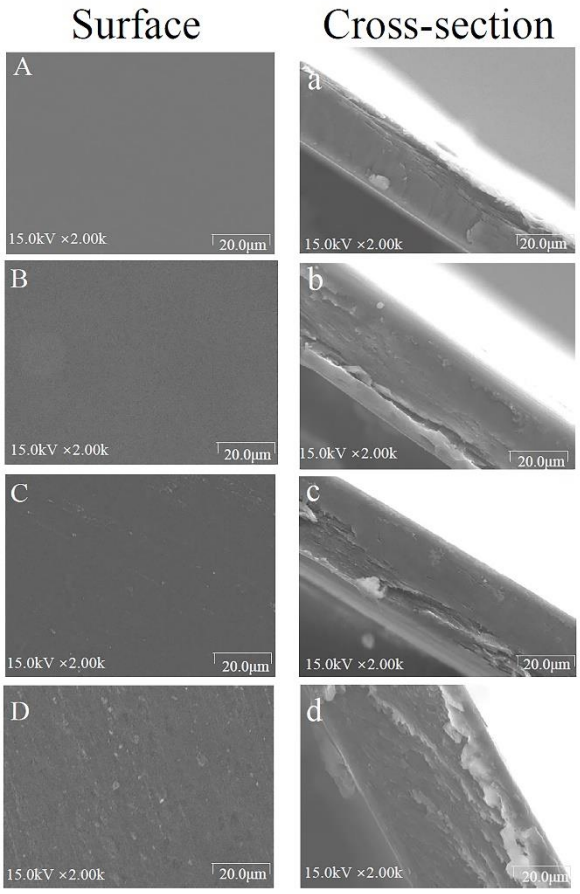

Figure 2.2. SEM micrographs of the surface and cross-section of CS/PEG (A; a) CS/PEG /CIN0.5 (B; b), CS/PEG /CIN1 (C; c), CS/PEG /CIN1.5 (D; d) films.

2.3.9. Atomic force microscopy

AFM is another potent imaging technique used to investigate the nanoscale surface topography of materials (Chen *et al.,* 2020). Figure 2.3 depicted images (2D and 3D) of the surface topographies of the biopolymer-based films with and without CIN agents, as well as Ra (nm) and Rq (nm). The CS/PEG composite film exhibited a relatively smooth surface. This can be attributed to the formation of an organized phase and uniform network structures between the biopolymers. The compatibility between CS and PEG resulted in smoother surfaces in the AFM images. However, the addition of CIN increased the roughness of the bioactive films, resulting in the loss

of their flat surface (2D and 3D) characteristics. Then, the maximal surface roughness for the CS/PEG/CIN1.5 film with Ra = 6.56 nm and Rq = 4.96 nm. CIN is a volatile compound, and the likelihood that CIN molecules aggregate or form colonies on the surface of a sample increases with increasing CIN concentration. In the 2D and 3D images, these clusters appear as rough features, which disrupt the observed uniformity of the CS/PEG samples. Consequently, an increase in CIN concentration resulted in an increase in the surface roughness of the bioactive film, which is consistent with the SEM results (Fig. 2.2).

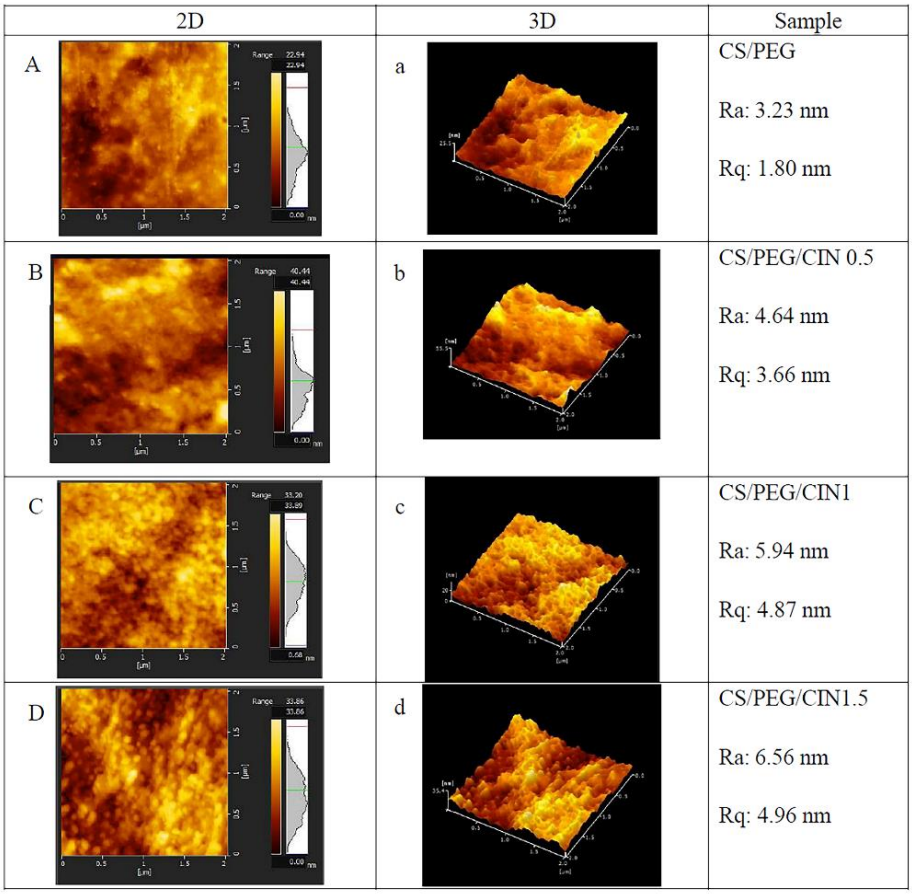

Figure 2.3. 2D and 3D surface morphology and roughness of control and incorporated with CIN (A-D; a-d).

2.3.10. In vitro activity

Antibacterial activity is a crucial property for food packaging applications (Seydim, Sarikus-Tutal, & Sogut, 2020). As shown in Figure 2.4, the inhibitory effects of the films against *E. coli* and *S. aureus* were evaluated by measuring the inhibition zone diameter. As shown in Figure 4, neither the control nor the CS/PEG showed an obvious antibacterial effect, as observed by the absence of an inhibition area around the samples. In contrast, film formulations containing CIN and CS/PEG demonstrated remarkable antibacterial activity against *E. coli* and *S. aureus*. As concentrations of CIN increased, the diameter of inhibitory zone increased as well. This may be because the carbonyl group near the double bond of CIN disrupts the cell wall structure and alters membrane permeability (Chen *et al.,* 2020). Because of their hydrophobicity, it has been postulated that EO and their derivatives may disrupt bacterial cytoplasmic leakage, cell lysis, and eventually bacterial viability (Xu *et al.,* 2019). Moreover, Gram-negative bacteria exhibit slightly larger inhibition zone diameters than Gram-positive bacteria, which may be due to the fact that *S. aureus* is usually more resistant to antimicrobials and it is more difficult for antimicrobials to disrupt their cell membranes (Zhou *et al.,* 2020.)

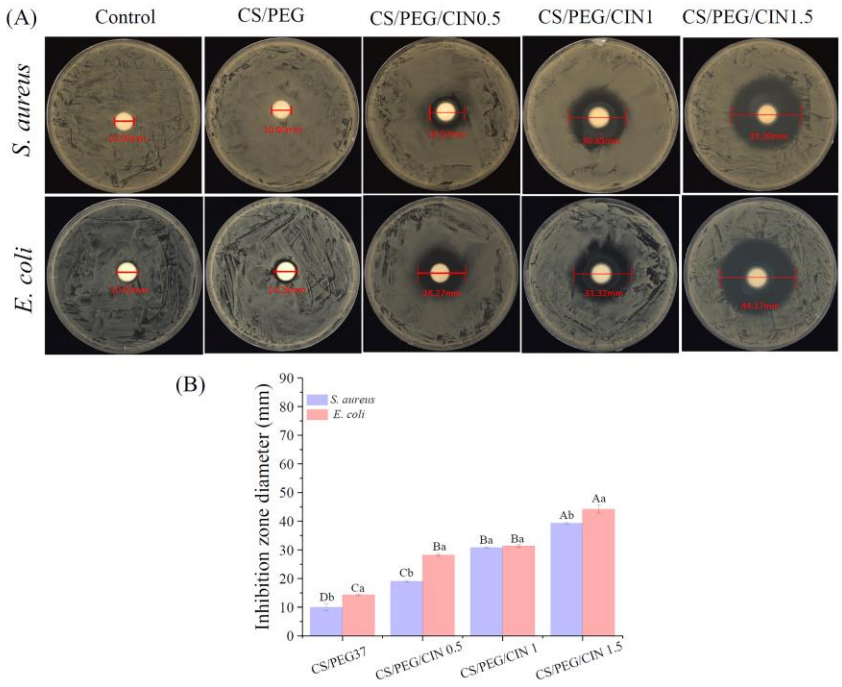

Figure 2.4. Different coating solutions on *E. coli* and *S. aureus* (A) Visual image of inhibition zone diameter (B) Statistical analysis after incubation.

2.3.11. Banana presentation: sensory evaluation and quality score

As shown in Figure 2.5 and Table S1, all treatment groups had the same level of ripeness at the initial stage, with a greenish color and score of 5. The uncoated bananas began to appear slightly yellow on the roots by day four, with the skin gradually turning yellow by day eight, when the respiration rate reached its maximum (Fig. 2.6 D). By day 20, the enzymatic browning of phenolic chemicals caused quinone deposition in the banana peel, resulting in dark brown patches (Huang et al., 2017). At end-of-storage scores below 0.5, the fruit loses its food value and is considered unacceptable to consumers and the market. In addition, For the CS/PEG group, the skin turned yellow with spots after 12 days, indicating that the bananas were gradually ripening, which was delayed by four days compared to the control group. However, the effect could be more favorable, as the score fell below 2.0 and could not be consumed on day 24.

However, the CIN-coated treatment groups exhibited green skin for the initial eight days. For the CS/PEG/CIN0.5 and CS/PEG/CIN1 groups, slight spotting occurred after 12 days. The texture of the bananas was better preserved until the end of storage, and the quality score was approximately 3, which was significantly higher ($p < 0.05$) than that of the other treatment groups, indicating delayed senescence, which was prolonged by approximately eight days compared to the control group. Notably, at the later stage of storage, the CS/PEG. CIN 1.5 samples showed browning of the roots and softening of hardness, which could be due to excessive CIN addition resulting into decreasing TS (Tab.1) of the film and the lack of permeability (Tab.2). Both in sensory evaluation and quality score, there was no significant difference between CS/PEG/CIN0.5 and CS/PEG/CIN1.

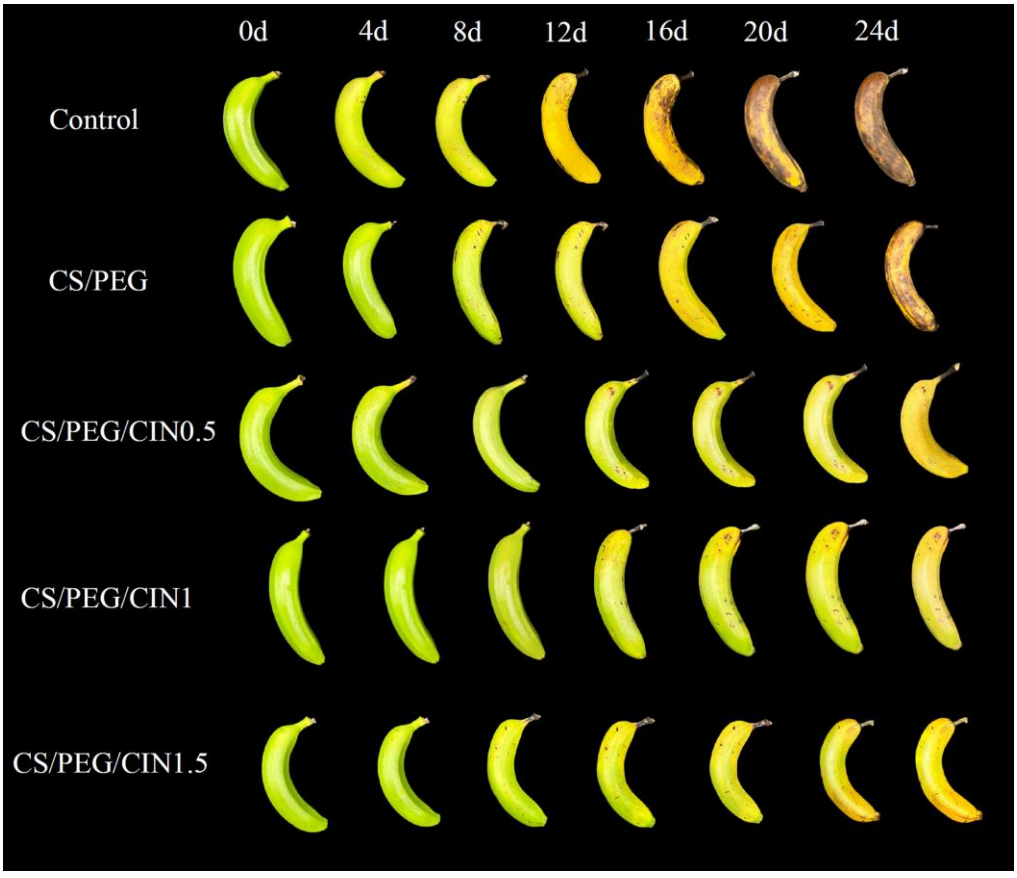

Figure 2.5. Appearance of banana during the storage.

2.3.12. Weight loss of banana

Weight loss is a critical indicator of postharvest production deterioration (Nguyen *et al.,* 2021). As shown in Figure 2.6A and Table S2, weight loss showed an upward trend throughout the storage period. In the control treatment group, there was a rapid increase to 7.55% by day 12, followed by a sustained increase to 22.31% by the end of the storage, probably due to the uncoated fruit being exposed to the environment directly, which accelerated water loss. Compared with the CS/PEG treatment group, significantly ($p < 0.05$) lower weight loss percentages were found in the CS/PEG/CIN0.5, CS/PEG/CIN1, and CS/PEG/CIN1.5 coated bananas (5.39 ± 0.26, 5.43 ± 0.21, and 6.29 ± 0.23%, respectively) after day 16. These results may be attributed to the fact that bioactive coatings enriched with CIN significantly improve water barrier properties, thereby reducing water loss from the banana surface. Meanwhile, CS/PEG/CIN0.5 (11.04 ± 0.24) and CS/PEG/CIN1 (11.01 ± 0.33) treatment groups had a lower weight loss than CS/PEG/CIN1.5 (12.54 ± 1.09) at the end of storage, but there was no significant difference between CS/PEG/CIN0.5 and CS/PEG/CIN1. Similar results have been observed in previous studies on the mandarin fruits coated with CS-enriched CIN, where it was reported that the use of 0.5% and 1.0% CIN reduced weight loss. In comparison, the 1.5% treatment group was less effective than other groups. This is probably because excessive CIN affects the ability of fruits to self-regulate (Gao *et al.,* 2018).

2.3.13. Firmness of banana

As shown in Figure 2.6B and Table S3, the firmness of all treatment groups showed a decreasing trend during the storage period, with the decrease rate of the control groups being the greatest, decreasing from 46.50 N (on the first day) to 11.87 N (day 16). The CS/PEG-coated group observed a sharp decline, from 46.57 N to 21.15 N (day 16) and then to 5.67 N on the final day of

the storage period. However, the firmness of the CIN-coated samples decreased gradually ($p < 0.05$). After 16 days, the firmness of bananas coated with CIN bioactive groups about 30.07 N, indicating that the bioactive coating was effective in maintaining the hardness of the bananas, probably due to the fact that the coating reduced the physiological activity of the cells and delayed fruit ripening. Among them, CS/PEG/CIN1.5 was the most effective. This was also consistent with the results reported by Das et al., who used caraway oil coated with CS to maintain the firmness of the banana at around 29 N (Das, Vishakha, Das, & Ganguli, 2023).

2.3.14. Total soluble solids content

As shown in Figure 2.6C and Table S4, the TSS content of all coated and uncoated groups showed an increasing trend, which may be the result of the hydrolysis of starch into sugars and carbohydrates, such as glucose, sucrose, and fructose (Nguyen *et al.,* 2021). Initially, the %TSS of all banana samples was insignificant ($p < 0.05$), and the value was 0.50–1.30%. The control group increased rapidly from 1.87% (day 8) to 7.17% (day 12), then continuously increased to 14% at the end of storage. This may be because fruits lack a protective coating and, when exposed to air, respiration increases, thereby accelerating the rate of starch hydrolysis. At the later stage of storage, the %TSS content of CS/PEG-coated film increased from 6.50% (day 12) to 12% (day 24), whereas the groups with CIN-coated film increased from 2.00% (day 12; CS/PEG/CIN0.5) to 9.50% (day 24; CS/PEG/CIN1.5). This result was due to the addition of EO with hydrophobic properties which reduced the rate of water loss and respiration and delayed ripening, indicating that the CIN bioactive coating provided the most efficient protection to harvested bananas during the entire storage period.

2.3.15. Respiration rate

The climacteric fruits were assessed based on CO_2 production (mg/kg/h), as shown in Figure 2.6D and Table S5. There was no significant difference in the first four days for all treatment groups at approximately 63 mg CO_2 (kg/h). However, because the control group was wholly exposed to the air without a protective layer, the respiration rate peaked on day eight (92.87 mg CO_2 kg/h), indicating that the fruit had become maturational. For the CS/PEG group, the peak was delayed by four days compared to the control group, reached its peak on day 12, and then dropped rapidly to 68.33 mg CO_2 kg/h. Compared to the other treatment groups, the bioactive film samples increased gradually during the initial storage period, peaked on day 16, and then decreased, indicating that the film with CIN can substantially delay the ripening and senescence of bananas. This may be because the CIN ternary film generated a gas barrier that protected the bananas from oxidative damage, thereby reducing respiration. Similar findings have been reported for fruits such as early crisp pear (Oyom *et al.,* 2022) and apple (Sapper, Palou, Pérez-Gago, & Chiralt, 2019) after the incorporation of EO into the CS coating treatment.

2.3.16. Titratable acid

The variation in the malic acid content, which is the predominant organic acid in bananas, functions as an additional indicator for determining whether a coating is effective in extending the shelf life of bananas. Organic acids, such as malic acid, are utilized as part of the respiration process, influencing acidity levels and, consequently, the maturation process of fruits (La *et al.,* 2021). Changes in the TA of bananas with and without coating during the entire storage period are shown in Figure 2.6E. The TA values of all treatments showed a declining trend owing to respiration during ripening and consumption of organic acids. The TA decline rates of control, CS/PEG, CS/PEG/CIN0.5, CS/PEG/CIN1, and CS/PEG/CIN1.5 were 33.3, 20.8, 9.4, 15.9, and

15.0%, respectively, after day eight, and then the TA value of the blank group was only 0.028 mg/g, which was significantly higher than other coating groups by the end of the storage. For the CS/PEG groups, the decrease rate of titratable acid was from 23.8% to 30.5% after day 8, which was significantly higher than that of the bio-active coated treatments. However, adding CIN to the CS/PEG coating increased the acidity, as the TA values after 12 days of storage remained between 0.14 mg/g and 0.17 mg/g when the CIN concentration ranged from 0.5% to 1.50%, respectively. At 0.5% and 1% CIN concentrations, the highest TA value measured after 20 days of storage was approximately 0.09 mg/g, which is consistent with the weight loss findings.

2.3.17. Reducing sugar

During post-ripening, the breakdown of starch in banana flesh into reducing sugars is promoted because the concentration of reducing sugars indicates the quality and ripeness of the banana (Li *et al.,* 2019). As shown in Figure 2.6F, with and without the coating, an increasing trend was observed with increasing storage time. For the control group, the rapid increase continued from day 4, reaching a maximum value of 109.27 mg/g on day 24, which was significantly higher than the other treatment groups and indicative of the banana pulp senescence rate. On day 24, the reducing sugar of bananas treated with CS/PEG, CS/PEG/CIN0.5, CS/PEG/CIN1, and CS/PEG/CIN1.5 coating were 90.79, 71.18, 70.19, and 74.96 mg/g respectively, revealing that the CIN-coated treatment group effectively decreased amylase activity, inhibited glycogen decomposition, and delayed banana maturation (Xie *et al.,* 2022).

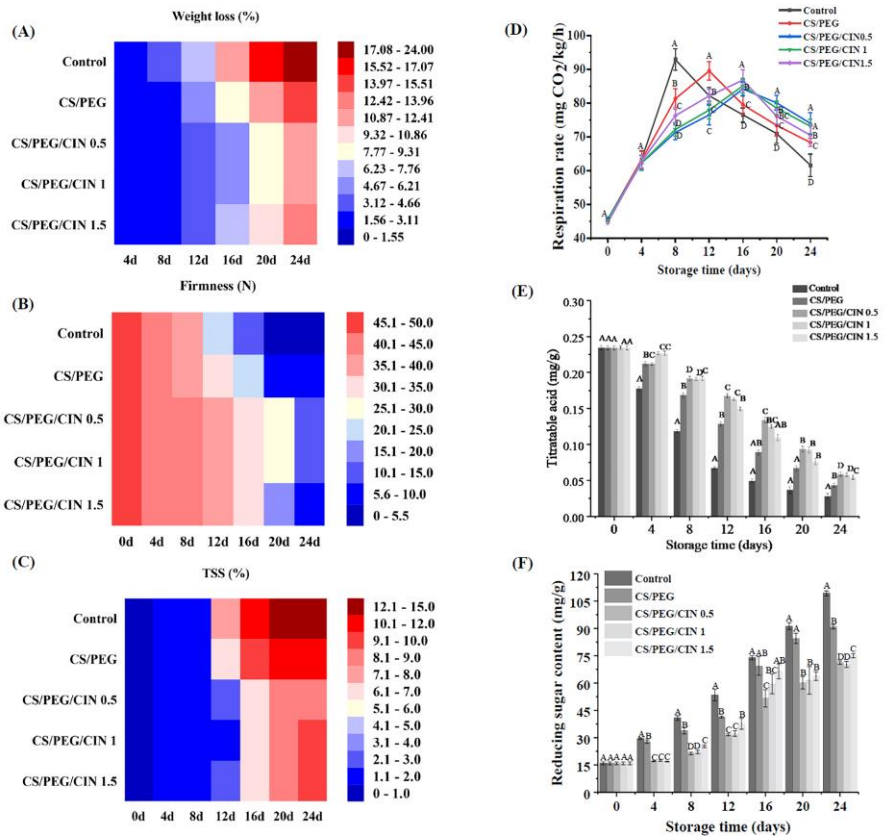

Figure 2.6. (A) Weight loss, (B) Firmness, (C) TSS, (D) Respiration rate, (E) Titratable acid, (F) Reducing sugar of banana during the storage

2.3.18. Principal component analysis

Principal component analysis was performed to evaluate the effects of the coating films on the freshness of bananas at room temperature under different treatments. Multivariate analysis of the sample data supported the reduction of these variables to two principal components, which accounted for 97.5% of the total variance, with PC1 contributing 85.24% and PC2 contributing 12.26%. As depicted in Figure 2.7A, the loadings of each indicator on the principal components were further investigated to determine which indicator had the most significant influence on banana characteristics. Weight loss, TSS, and reducing sugar content increased with storage time and were positively correlated with PC1, whereas TA content, sensory score, and firmness were

negatively correlated. Consistent with the previous analysis, the results indicated that the weight loss rate, TSS, and reducing sugar were negative performance evaluation parameters.

The contribution of the variables to the separation of the samples was determined by their projection on PC1 and PC2; the more significant the effect, the more prominent the projection (Jiang *et al.,* 2020). As illustrated in Figure 2.7, the variable line of the respiration rate was the longest, had the most prominent projection, and had the most significant impact on the freshness of bananas. Meanwhile, combined with the PC scores, the aggregates for each treatment group at 4-day intervals were primarily concentrated in the fourth quadrant (respiration rate). The respiration rate correlated with weight loss and TSS, indicating that an increase in weight loss and decrease in TSS significantly impacted the ripeness of bananas during storage. Weight loss was significantly positively correlated with reducing sugar content and negatively associated with firmness, TSS, and TA. The CIN bioactive coating created a semi-permeable barrier on the surface of the bananas, delaying the rate of respiration and weight loss, thereby extending the shelf life of the banana.

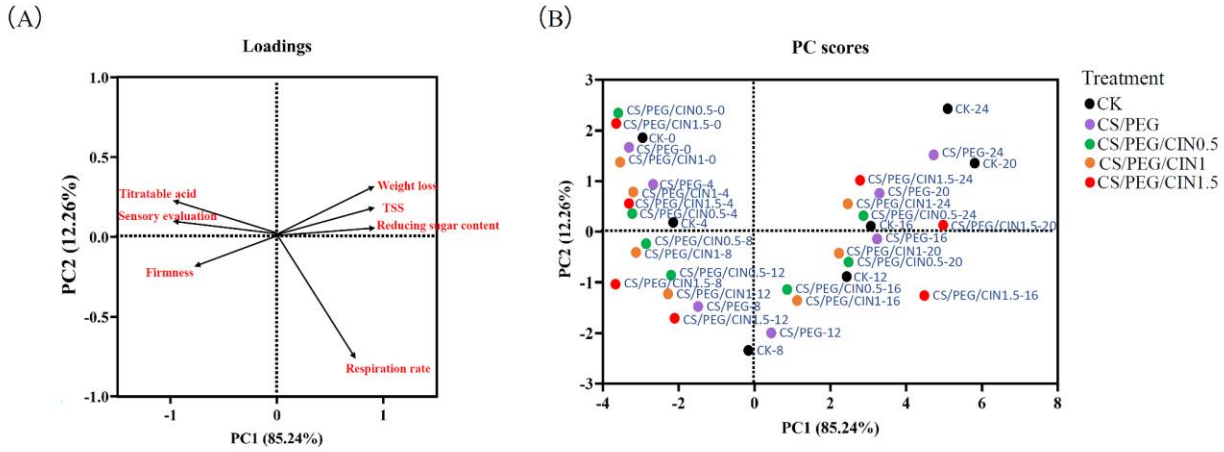

Figure 2.7. (A) Loading plots of sensory tests by PCA, (B) PCA scores of sensory tests of different treatment groups

2.4. Reference

Ahmadi, F., Oveisi, Z., Samani, S. M., & Amoozgar, Z. (2015). Chitosan based hydrogels: characteristics and pharmaceutical applications. *Research in pharmaceutical sciences,* 10(1), 1.

Ahmed, S., & Ikram, S. (2016). Chitosan and gelatin based biodegradable packaging films with UV-light protection. *Journal of Photochemistry and Photobiology B: Biology,* 163, 115-124.

Amalraj, A., Raj, K. J., Haponiuk, J. T., Thomas, S., & Gopi, S. (2020). Preparation, characterization, and antimicrobial activity of chitosan/gum arabic/polyethylene glycol composite films incorporated with black pepper essential oil and ginger essential oil as potential packaging and wound dressing materials. *Advanced Composites and Hybrid Materials,* 3, 485-497.

Arman Alim, A. A., Mohammad Shirajuddin, S. S., & Anuar, F. H. (2022). A review of nonbiodegradable and biodegradable composites for food packaging application. *Journal of Chemistry,* 2022.

Brat, P., Bugaud, C., Guillermet, C., & Salmon, F. (2020). Review of banana green life throughout the food chain: From auto-catalytic induction to the optimisation of shipping and storage conditions. *Scientia Horticulturae,* 262, 109054.

Chemat, F., Vian, M. A., Fabiano-Tixier, A.-S., Nutrizio, M., Jambrak, A. R., Munekata, P. E., . . . Cravotto, G. (2020). A review of sustainable and intensified techniques for extraction of food and natural products. *Green Chemistry,* 22(8), 2325-2353.

Chen, S., Wu, M., Lu, P., Gao, L., Yan, S., & Wang, S. (2020). Development of pH indicator and antimicrobial cellulose nanofibre packaging film based on purple sweet potato anthocyanin

and oregano essential oil. *International Journal of Biological Macromolecules,* 149, 271-280.

Chiu, P.-E., & Lai, L.-S. (2010). Antimicrobial activities of tapioca starch/decolorized hsian-tsao leaf gum coatings containing green tea extracts in fruit-based salads, romaine hearts and pork slices. *International journal of food microbiology,* 139(1-2), 23-30.

Das, S. K., Vishakha, K., Das, S., & Ganguli, A. (2023). Antibacterial and antibiofilm activities of nanoemulsion coating prepared by using caraway oil and chitosan prolongs the shelf life and quality of bananas. *Applied Food Research,* 3(1), 100300.

Fasihi, H., Noshirvani, N., Hashemi, M., Fazilati, M., Salavati, H., & Coma, V. (2019). Antioxidant and antimicrobial properties of carbohydrate-based films enriched with cinnamon essential oil by Pickering emulsion method. *Food Packaging and Shelf Life,* 19, 147-154.

Gao, Y., Kan, C., Chen, M., Chen, C., Chen, Y., Fu, Y., . . . Chen, J. (2018). Effects of chitosan-based coatings enriched with cinnamaldehyde on Mandarin fruit cv. Ponkan during room-temperature storage. *Coatings,* 8(10), 372.

Hao, Y., Kang, J., Guo, X., Sun, M., Li, H., Bai, H., . . . Shi, L. (2023). pH-responsive chitosan-based film containing oregano essential oil and black rice bran anthocyanin for preserving pork and monitoring freshness. *Food Chemistry,* 403, 134393.

Hosseini, S. F., Ghaderi, J., & Gómez-Guillén, M. C. (2021). trans-Cinnamaldehyde-doped quadripartite biopolymeric films: Rheological behavior of film-forming solutions and biofunctional performance of films. *Food Hydrocolloids,* 112, 106339.

Hosseini, S. F., Rezaei, M., Zandi, M., & Farahmandghavi, F. (2015). Bio-based composite edible films containing Origanum vulgare L. essential oil. *Industrial Crops and products,* 67, 403-413.

Huang, H., Ge, Z., Limwachiranon, J., Li, L., Li, W., & Luo, Z. (2017). UV-C treatment affects browning and starch metabolism of minimally processed lily bulb. *Postharvest Biology and Technology,* 128, 105-111.

Jiang, Y., Yu, L., Hu, Y., Zhu, Z., Zhuang, C., Zhao, Y., & Zhong, Y. (2020). The preservation performance of chitosan coating with different molecular weight on strawberry using electrostatic spraying technique. *International Journal of Biological Macromolecules,* 151, 278-285.

Kadirkhan, F., Goh, P. S., Ismail, A. F., Wan Mustapa, W. N. F., Halim, M. H. M., Soh, W. K., & Yeo, S. Y. (2022). Recent advances of polymeric membranes in tackling plasticization and aging for practical industrial CO2/CH4 applications—a review. *Membranes,* 12(1), 71.

Kim, J., Choi, J.-Y., Kim, J., & Moon, K.-D. (2022). Effect of edible coating with Morus alba root extract and carboxymethyl cellulose for enhancing the quality and preventing the browning of banana (Musa acuminata Cavendish) during storage. *Food Packaging and Shelf Life,* 31, 100809.

Kingwascharapong, P., Tanaka, F., & Tanaka, F. (2021). Effect of edible coatings developed from chitosan incorporated with tea seed oil on Japanese pear. *Scientia Horticulturae,* 288, 110314.

Kolgesiz, S., Tas, C. E., Koken, D., Genc, M. H., Yalcin, I., Kalender, K., . . . Unal, H. (2023). Extending the Shelf Life of Bananas with Cinnamaldehyde-Impregnated Halloysite/Polypropylene Nanocomposite Films. *ACS Food Science & Technology*.

La, D. D., Nguyen-Tri, P., Le, K. H., Nguyen, P. T., Nguyen, M. D.-B., Vo, A. T., . . . Chung, W. J. (2021). Effects of antibacterial ZnO nanoparticles on the performance of a chitosan/gum arabic edible coating for post-harvest banana preservation. *Progress in Organic Coatings,*

151, 106057.

Li, J., Sun, Q., Sun, Y., Chen, B., Wu, X., & Le, T. (2019). Improvement of banana postharvest quality using a novel soybean protein isolate/cinnamaldehyde/zinc oxide bionanocomposite coating strategy. *Scientia Horticulturae,* 258, 108786.

Li, S., Diao, X., Mao, X., Liu, H., Shan, K., Zhao, D., . . . Li, C. (2023). The red, firm, non-exudative and pale, soft, exudative pork have different in vitro digestive properties of protein. *Meat Science*, 109110.

Li, X., Xiong, T., Zhu, Q., Zhou, Y., Lei, Q., Lu, H., . . . Zhu, X. (2023). Combination of 1-MCP and modified atmosphere packaging (MAP) maintains banana fruit quality under high temperature storage by improving antioxidant system and cell wall structure. *Postharvest Biology and Technology,* 198, 112265.

Nguyen, T. T., Nguyen, T.-T. H., Pham, B.-T. T., Van Tran, T., Bach, L. G., Thi, P. Q. B., & Thuc, C. H. (2021). Development of poly (vinyl alcohol)/agar/maltodextrin coating containing silver nanoparticles for banana (Musa acuminate) preservation. *Food Packaging and Shelf Life,* 29, 100740.

Noshirvani, N., Ghanbarzadeh, B., Gardrat, C., Rezaei, M. R., Hashemi, M., Le Coz, C., & Coma, V. (2017). Cinnamon and ginger essential oils to improve antifungal, physical and mechanical properties of chitosan-carboxymethyl cellulose films. *Food Hydrocolloids,* 70, 36-45.

Oyom, W., Xu, H., Liu, Z., Long, H., Li, Y., Zhang, Z., . . . Prusky, D. (2022). Effects of modified sweet potato starch edible coating incorporated with cumin essential oil on storage quality of ‘early crisp’. *Lwt,* 153, 112475.

Qamar, S., & Shaikh, A. (2018). Therapeutic potentials and compositional changes of valuable

compounds from banana-A review. *Trends in Food Science & Technology,* 79, 1-9.

Rincón, E., Serrano, L., Balu, A. M., Aguilar, J. J., Luque, R., & García, A. (2019). Effect of bay leaves essential oil concentration on the properties of biodegradable carboxymethyl cellulose-based edible films. *Materials,* 12(15), 2356.

Sagu, S. T., Nso, E. J., Karmakar, S., & De, S. (2014). Optimisation of low temperature extraction of banana juice using commercial pectinase. *Food Chemistry,* 151, 182-190.

Sánchez-González, L., Vargas, M., González-Martínez, C., Chiralt, A., & Cháfer, M. (2009). Characterization of edible films based on hydroxypropylmethylcellulose and tea tree essential oil. *Food Hydrocolloids,* 23(8), 2102-2109.

Sapper, M., Palou, L., Pérez-Gago, M. B., & Chiralt, A. (2019). Antifungal starch–gellan edible coatings with thyme essential oil for the postharvest preservation of apple and persimmon. *Coatings,* 9(5), 333.

Seydim, A. C., Sarikus-Tutal, G., & Sogut, E. (2020). Effect of whey protein edible films containing plant essential oils on microbial inactivation of sliced Kasar cheese. *Food Packaging and Shelf Life,* 26, 100567.

Sharma, S., Barkauskaite, S., Duffy, B., Jaiswal, A. K., & Jaiswal, S. (2020). Characterization and antimicrobial activity of biodegradable active packaging enriched with clove and thyme essential oil for food packaging application. *Foods,* 9(8), 1117.

Sultan, M., Elsayed, H., & Taha, G. (2023). Potential effect of citrate nanocellulose on barrier, sorption, thermal and mechanical properties of chitosan/Arabic gum packaging film. *Food Bioscience,* 56, 103246.

Sultan, M., Hafez, O. M., Saleh, M. A., & Youssef, A. M. (2021). Smart edible coating films based on chitosan and beeswax–pollen grains for the postharvest preservation of Le Conte pear.

RSC Advances, 11(16), 9572-9585.

Tessaro, L., Lourenço, R. V., Martelli-Tosi, M., & do Amaral Sobral, P. J. (2021). Gelatin/chitosan based films loaded with nanocellulose from soybean straw and activated with "Pitanga"(Eugenia uniflora L.) leaf hydroethanolic extract in W/O/W emulsion. *International Journal of Biological Macromolecules,* 186, 328-340.

Wang, L., Liu, F., Jiang, Y., Chai, Z., Li, P., Cheng, Y., . . . Leng, X. (2011). Synergistic antimicrobial activities of natural essential oils with chitosan films. *Journal of Agricultural and Food Chemistry,* 59(23), 12411-12419.

Wang, Z., Pu, H., Shan, S., Zhang, P., Li, J., Song, H., & Xu, X. (2021). Melatonin enhanced chilling tolerance and alleviated peel browning of banana fruit under low temperature storage. *Postharvest Biology and Technology,* 179, 111571.

Wantat, A., Rojsitthisak, P., & Seraypheap, K. (2021). Inhibitory effects of high molecular weight chitosan coating on 'Hom Thong'banana fruit softening. *Food Packaging and Shelf Life,* 29, 100731.

Xie, J., Wang, R., Li, Y., Ni, Z., Situ, W., Ye, S., & Song, X. (2022). A novel Ag2O-TiO2-Bi2WO6/polyvinyl alcohol composite film with ethylene photocatalytic degradation performance towards banana preservation. *Food Chemistry,* 375, 131708.

Xu, T., Gao, C., Feng, X., Huang, M., Yang, Y., Shen, X., & Tang, X. (2019). Cinnamon and clove essential oils to improve physical, thermal and antimicrobial properties of chitosan-gum arabic polyelectrolyte complexed films. *Carbohydrate Polymers,* 217, 116-125.

Yan, X., Dong, T., Yun, X., Liu, B., & Meng, J. (2022). Enhancing the functionality of cross-linked chitosan coating on vibration damaged Nanguo pears. *Lwt*, 113454.

Yan, X., Dong, T., Yun, X., Tanaka, F., Tanaka, F., Wardana, A. A., & Meng, F. (2023). Improving

‘Nanguo’pear fungal disease and storability by chitosan coating combined with diepoxy-poly (ethylene glycol). *Food Bioscience*, 102842.

Yang, Z., Li, M., Zhai, X., Zhao, L., Tahir, H. E., Shi, J., . . . Xiao, J. (2022). Development and characterization of sodium alginate/tea tree essential oil nanoemulsion active film containing TiO2 nanoparticles for banana packaging. *International Journal of Biological Macromolecules,* 213, 145-154.

Yang, Z., Zhai, X., Zhang, C., Shi, J., Huang, X., Li, Z., . . . Povey, M. (2022). Agar/TiO2/radish anthocyanin/neem essential oil bionanocomposite bilayer films with improved bioactive capability and electrochemical writing property for banana preservation. *Food Hydrocolloids,* 123, 107187.

Yu, X., Yang, Y., Liu, Q., Jin, Z., & Jiao, A. (2023). A hydroxypropyl methylcellulose/hydroxypropyl starch nanocomposite film reinforced with chitosan nanoparticles encapsulating cinnamon essential oil: Preparation and characterization. *International Journal of Biological Macromolecules,* 242, 124605.

Zhang, X., Liu, D., Jin, T. Z., Chen, W., He, Q., Zou, Z., . . . Guo, M. (2021). Preparation and characterization of gellan gum-chitosan polyelectrolyte complex films with the incorporation of thyme essential oil nanoemulsion. *Food Hydrocolloids,* 114, 106570.

Zhou, Y., Zhu, X., Zhang, C., Chai, W. S., Chew, K. W., Du, A., & Show, P. L. (2020). Characterization of whey protein isolate and pectin composite film catalyzed by small laccase from Streptomyces coelicolor. *Environmental Technology & Innovation,* 19, 100999.

Zhou, Z., Liu, Y., Liu, Z., Fan, L., Dong, T., Jin, Y., . . . Sun, W. (2020). Sustained-release antibacterial pads based on nonwovens polyethylene terephthalate modified by β-

cyclodextrin embedded with cinnamaldehyde for cold fresh pork preservation. *Food Packaging and Shelf Life,* 26, 100554.

CHAPTER 3

Characterization and Bio-functional Performance of Chitosan/Poly (vinyl alcohol)/*trans*-Cinnamaldehyde Ternary Biopolymeric Films

3.1. Introduction

The today's usage of non-renewable fossil-based raw materials for packaging is a critical issue, due to the finite amount of fossil fuel resources and the shortcomings of the non-biodegradable plastic materials produced. Consequently, there is a remarkable increase interest and research of new antimicrobial/antioxidant bio-packaging from rapidly renewable sources to meet the growth in food demand and consumption trends (Yildirim *et al*., 2018). In addition, active packaging protects against external hazardous factors to improve food preservation and quality. Currently, various natural polymeric substances are available as viable packaging film alternatives with good film-forming properties (Fan, Yang, Duan, & Li, 2021). CS is one such biopolymer, comprised of β-1,4-linked glucosamine and N-acetylglucosamine. It is attractive for its non-toxicity, biodegradability, biocompatibility, and film-forming ability. (Kong, Chen, Xing, & Park, 2010). Previous investigations have demonstrated that CS innately inhibits microbial growth due to positively charged amino groups. However, this antibacterial ability is only demonstrated in aqueous media. Both degree of acetylation and molecular weight are associated with CS antibacterial activities. (Sharma, Barman, & Siddiqui, 2016). Moreover, CS-based films exhibit poor moisture barrier performance and weak mechanical properties due to their hydrophilic characteristics (Ojagh, Rezaei, Razavi, & Hosseini, 2010). One approach to overcoming these constraints is combining the CS with other polymers and EOs (Lee, Kim, & Park, 2018).

Blending natural and synthetic polymers is an emerging novel strategy to enhance film production cost-effectiveness. Poly (vinyl alcohol) (PVA) is a water-soluble, non-toxic, biocompatible, and synthetic biodegradable polymer with excellent mechanical properties, and has the capacity to form films, essential for food packaging applications (Chen & Huang, 2016). Composite CS/PVA films are also reported to have interesting characteristics. Hajji *et al*. reported

that PVA-incorporating CS improves mechanical strength and miscibility (Hajji *et al*., 2016). Bonilla *et al*. also revealed that CS/PVA films have a stronger tensile strength, especially for a 3:1 weight ratio of PVA to CS. Despite the improved functional characteristics of CS/PVA films, there are also reports that PVA-added films exhibited poor moisture absorption rates and low blended-film thermal stability, which increases with the degree of hydrogen bonding (-OH) (Bonilla, Fortunati, Atarés, Chiralt, & Kenny, 2014; Lewandowska, 2009). Due to the water barrier permeability issues and thermal stability limitations, CS/PVA films are not fully used in industrial applications. Therefore, research efforts are focused on modifying the CS/PVA film characteristics to enable use as food packaging materials. To improve CS/PVA films, various natural/bioactive substances/EOs are incorporated, significantly impacting film mechanical, antibacterial and physicochemical characteristics.

A recent approach to improve the antibacterial or antioxidant activity of films is to impregnating the biopolymers with various EOs (Kuai et al., 2020). *trans*-Cinnamaldehyde (CIN), 3-phenyl-2-propenal, is a hydrophobic aromatic aldehyde found in the EO of cinnamon (Cinnamomum verum). It is classed as a safe food flavoring agent by the Expert Committee on Food Additives. (Chen *et al.,* 2016). Additionally, CIN is a widely acknowledged antimicrobial, with demonstrated efficacy against different microorganisms in several studies (Xing *et al.,* 2016). Coating combinations of CS and CIN are demonstrated to improve the stability and antimicrobial properties of coated particles (Hosseini, Kaveh, & Schmid, 2022). Wang *et al*. compared the antifungal activity edible CS films incorporating clove bud EO or CIN. They reported that the CIN-CS film exhibited higher antifungal activity with respect to the CB-CS film (Wang *et al.,* 2011). Mold is also noted to exhibit greater does sensitivity towards CIN than to carvacrol. Moreover, a CS (0.5 %)-CIN coating was observed to be most effective in limiting green mold

spoilage (Sun *et al.,* 2014). It is also reported that CIN/CS/nanoparticles and CS/PVA/fish gelatin ternary matrices exhibited enhanced antioxidant capacity and antibacterial activity (Hosseini, Ghaderi, & Gómez-Guillén, 2022). In recent years, numerous studies have focused on the behavior of film-forming solutions, as they can influence the thickness, uniformity, and mechanical properties of the resulting film. CS, PVA, and CIN are commonly used as packaging materials, resulting in considerable reference data. However, no investigations combining these three polymers are published. Considering that CIN may have concentration-dependent effects on the physicochemical and antifungal properties of the film.

Therefore, this study assessed the structure-property relationships in CS/PVA/CIN coating films by varying the CIN content, evaluating changes in the structural, mechanical, physicochemical, microscopic (surface and cross-section), antifungal, and antioxidant properties.

3.2. Materials and methods

3.2.1. Coating and film preparation

CS/PVA blends with CIN were formed via the following steps: 1) CS solution (1.5% w/v) was prepared by dissolving 1.5 g CS in 100 mL of a 1 % glacial acetic acid (w/v), agitated over 4 h at 40 °C and filtered overnight. Meanwhile, PVA solution (2% w/v) was prepared by dissolving 2 g PVA in 100 mL distilled water were heated and stirred for 3 h at 85 °C. 2) The CS and PVA solutions were combined and mixed well. Then, while stirring the mixed solution, glycerol (0.3 g/g) and Tween 80 (0.2 % w/w CIN) were added. The solution was heated at 40 °C for 30 min. 3) Three different concentrations (0.5, 1.0, and 1.5 % of per total solution volume) of CIN were added to the CS/PVA solution, followed by homogenization. 4) Degassing was carried out for 15 min to remove air bubbles, then dried in an oven for 48 h, removed and stored at 25 °C for one week prior to further analysis. The CIN samples are abbreviated as CS/PVA/CIN0.5, CS/PVA/CIN1, and

CS/PVA/CIN1.5, respectively. For simplicity and visualization, the table 3.1 – 3.5 may refer to the CIN-containing films as 0.5 %, 1.0 % and 1.5 %, respectively.

3.2.2. Zeta potential

The Zeta potential was measured by using a Zeta potential analyzer (Zetasizer Nano ZS3600, Malvern Instruments Inc. UK). All of the treatment solutions were tenfold diluted with distilled water, with the exception of CIN, which was tenfold diluted with ethanol. The capillary cell was filled with diluted emulsion using a 1 mL syringe with an equilibrium time of 120 s and repeated three times at room temperature (25 ˚C).

3.2.3. ATR/FT-IR spectroscopy

Before analysis, to ensure complete film dehydration, film samples were stored in a silica gel desiccator over two weeks. Infrared spectra for each film were obtained using an ATR-FTIR spectrometer (FT-IR 4700, JASCO Inc., Japan). Spectra were collected with a resolution of 4 cm^{-1} and 16 scans over a range of 4000–400 cm^{-1} and with a horizontal viewing range of 4000-500 cm^{-1} for analysis purposes.

3.2.4. Film thickness

Film thickness was evaluated with a precision of 0.001 mm using an auto digital micrometer (micrometer-707, Mitutoyo Corporation, Japan) at ten random positions on each film of ten films for each treatment.

3.2.5. Mechanical property

Mechanical properties were measured using a motorized force test stand (FGS-50E-L, Nidec-Shimpo, Japan). Samples were cut into an elongated shape (50×10 mm) and clamped between the

grip pair of the test stand with an initial pitch of 25 mm and speed of 65 mm/min. Results were collected at room temperature and in an air environment.

3.2.6. Moisture content

The moisture content evaluation method used is described by Laras *et al*. (Wigati, Wardana, Tanaka, & Tanaka, 2022b). Separate weighing of small stainless-steel plates with and without (2 × 2 cm) film samples was performed. Samples were then dried at 105 °C in an oven for 24 h, with moisture content calculated as follows Eq:

$$\text{Moisture content (\%)} = \frac{W_1 - W_2}{W_1} \times 100$$

Where W_1 represents pre-dry sample weight (g), W_2 represents after-dry sample weight (g)

3.2.7. Swelling rate

The swelling rate was evaluated using the method reported by Hosseini (2016). Dry weight films (2 × 2 cm) (W_d) were placed in 25 mL centrifuge tubes with distilled water and shaken overnight at 80 rpm. Films were weighed (W_s) after gently wiping the surface with filter paper. The swelling rate (SR %) was computed using the following Eq:

$$\text{Swelling rate} = \frac{W_s - W_d}{W_d} \times 100$$

Where W_s is the weight of swollen samples (g); W_d is the weight of dry samples (g)

3.2.8. Water solubility

After the swelling test, the film sample was then wiped of surface moisture and placed in an oven overnight at 105 °C (W_i). The resulting film weight after drying as W_f. The solubility was calculated using the following Eq:

$$\text{Water solubility (\%)} = \frac{W_i - W_f}{W_f} \times 100$$

Where W_i is the weight of initial dry film samples (g); W_f is the weight of final dry film samples (g)

3.2.9. Water activity

The water activity was determined using a water activity meter (Rotronic HygroPalm-2, Process Sensing Technologies, Japan). Each film of 3 cm^2 diameter was placed into the center of circular test cup of 16 cm^2 diameter. Results were collected and recorded three times in replicate at room temperature (20 ± 1°C).

3.2.10. Water contact angle measurement

The Smart Contact Mobile Entry 2 (Exima Yokohama Lab Co., Ltd. Japan) analyzer was used to determine the hydrophilic/hydrophobic properties of the film. Distilled water (about 2 μL) was dropped onto the film. This process was recorded, screenshots taken, and steps repeated after 30 s. Each measurement was performed in triplicate.

3.2.11. WVP

Water vapor permeability of the films was evaluated by placing 15 g of calcium chloride (anhydrous) in a unique circular test cup of 28 cm^2 diameter. This was then sealed with an unbroken and unblemished film (0 % RH environment). After weighing the cups for the 0 h measurement, they were then placed in a temperature and humidity-controlled chamber at 25 °C and 85 % RH. The weight was recorded each hour over 12 h.

3.2.12. Oxygen permeability

The deoxidizer method by (Zhang *et al.,* 2020) was used to assess film oxygen permeability, with slight modification. Circular test cups with a diameter of 28 cm^2 were tightly covered in films, then filled with a 15 g deoxidizer (the main components are activated iron powder, toner, sodium salts). The cups were weighed then placed in a constant temperature and humidity chamber at 25 °C and 85 % RH for 24 h with weight recorded each hour. The deoxygenation main reactions and OP were obtained using the following Eq:

$$\text{OTR} = \frac{\triangle m}{\triangle t \times A}$$

$$\text{OP} = \frac{OTR \times L}{\triangle P}$$

Where oxygen transmission rate (OTR) is expressed as the volume of oxygen that passes through a unit area of the films per unit of time, Δm is the gas quality through the film (g); Δt is the time (s); A is the effective area of the film (m^2); L is the average film thickness (mm); ΔP is per unit difference in vapor pressure between the two sides (kPa).

3.2.13. Film color

A color difference meter (CR-20, Konica Minolta Inc., Japan) was used to measure the color of the film at ambient temperature. Before the measurement was conducted, a white standard color plate (L^* = 94.2) was used for calibration. Subsequently, the color parameter L^* (light) and chromaticity parameters, a^* (red/green) and b^* (yellow/ blue), were recorded by taking multiple measurements at various locations on the film.

3.2.14. Light transmission and opacity

Film samples (1 × 4 cm) were measured with a UV–Vis spectrophotometer (Jasco, V-530,

Japan) at wavelengths ranging from 200 to 800 nm. In addition, the thickness and Abs_{600} of each film were measured. Each measurement was performed in triplicate

3.2.15. Scanning electron microscopy

Before analysis, the film was immersed in liquid nitrogen for 5 min and then broken immediately after being removed. And the samples were mounted on double-sided conductive adhesive tabs, and sputter-coated with a thin layer of gold. The ternary film surface and cross-sectional morphology was observed using an SEM (SU3500, Hitachi, Japan) with an acceleration voltage of 15 kV at 500 × and 1000 × magnifications.

3.2.16. Atomic force microscopy

The surface morphology was assessed using an AFM (Hitachi 5200S, Tokyo, Japan) with 5 μm × 5 μm a scan size at 0.7-0.84 Hz for 24 h in a natural setting. Two statistical parameters related to the roughness were calculated: the average roughness (Ra) and the root-mean-square roughness (Rq).

3.2.17. In vitro antifungal activity assay

The films' influence on fungi growth (*P. italicum* & *B. cinerea*) was evaluated using the solid medium method of Ata with slight modifications (Wardana, Koga, Tanaka, & Tanaka, 2021). Fungi were first cultivated for 7 days on potato dextrose agar (PDA) (Nissui Pharmaceutical Co., Ltd., Japan). Then, 10 mL of each coating solution (CS, PVA, CS/PVA and CS/PVA/CINs) were mixed with 10 mL of PDA and put in Petri plates (90 mm diameter). Once the dish had solidified, an 8 mm diameter disk of mycelium from a 7-day-old culture of *P. italicum* and *B. cinerea* was placed in the center of each Petri dish and incubated at 25 °C. The diameter of the colonies was measured after 5 days using ImageJ software. Each coating was repeated three times with the following

formula for percentage inhibition (PI) using Eq

$$PI(\%) = \frac{d_c - d_t}{d_c} \times 100$$

where d_c (mm) and d_t (mm) refer to the diameters of the colonies for the control and each treated group.

3.2.18. Spore germination assay

Sequentially, to a small Petri dish, were added 1 mL of sample (CS; PVA; CS/PVA; CS/PVA/CINs) solution, 1 mL of potato dextrose broth (PDB) (Difco™, USA), and 1 mL of spore solution (*P. italicum* & *B. cinerea*) containing 2×10^5 CFU/mL. The mixture was agitated at 100 rpm over 24 h, centrifuged for 10 min and washed using buffer solution standard (pH 6.86) at room temperature. Using a 50 × objective lens, the spore germination was observed through confocal laser scanning microscopy (CLSM) (Olympus IX71, Japan)

To evaluate changes in membrane permeability of *P. italicum* and *B. cinerea*, they were stained with 50 (mg/L^{-1}) propidium iodide (Sigma Aldrich, USA) for 15 min. The samples were then observed using a CLSM with 543 nm and 585 nm excitation and emission wavelengths, respectively.

3.2.19. DPPH radical scavenging

Film DPPH antioxidant ability was evaluated using the method of Hosseini *et al*. (Hosseini, Ghaderi, & Gómez-Guillén, 2021). Briefly, a 1 mg film sample was added to a centrifuge tube with 10 mL of methanol, then mixed by stirring at 100 rpm for 4 hours. Afterward, 200 µL of the supernatant of the film was extracted and mixed with 2 mL of 1 mM methanolic DPPH solution. After storing in the dark for 30 min at room temperature, the absorbance of the mixture was measured at 517 nm. Each measurement was taken in triplicate. The DPPH radical-scavenging

activity (%) was calculated using Eq:

$$\text{DPPH radical scavenging activity (\%)} = \frac{Abs_{blank} - Abs_{sample}}{Abs_{blank}} \times 100$$

3.2.20. Ferric reducing antioxidant power assay

The FRAP value was determined using a modified method according to Abdelhedi *et al*. (Abdelhedi *et al*., 2018). A 1 mg film sample in phosphate buffer with a pH of 6.6, and potassium ferricyanide were stirred together in a water bath at 45 °C for 30 min. Then, 250 µL of 10 % trichloroacetic acid was added, followed by centrifugation at 5000 g for 5 min. From this, 1.25 mL of supernatant was collected and mixed with 1.25 mL of distilled water and 0.25 mL 0.1 % ferric chloride. The resulting mixture was allowed to stand for 15 min and absorbance measured at 700 nm at room temperature. Each test was conducted in triplicates.

3.2.21. Statistical analysis

All data were analyzed using SPSS (Version 26.0, SPSS Inc., Chicago, Illinois, USA). Statistical differences between the different variables were analyzed using a one-way analysis of variance (ANOVA) followed by a least significant difference (LSD) and Duncan's new multiple range test to determine the significant difference ($p < 0.05$). All Figures were drawn by Origin 2017.

3.3. Result and discussion

3.3.1. Zeta potential

The zeta potential values indicate the stability of the colloidal dispersion system by representing the electrostatic repulsion forces among the particles (Luo, Zhang, Whent, Yu, & Wang, 2011). The zeta potential values of all the film-forming solutions are shown in Table 3.1. For the pure PVA solution, zeta potential was negatively charged (-0.188 ± 0.02 mV) due to the

presence of hydroxyl groups (-OH) on their polymer molecules (Clogston & Patri, 2011). These hydroxyl groups can ionize in an aqueous environment producing a net negative charge on the PVA surface (Dominguez-Martinez *et al*., 2017). The zeta potential value of the CS solution exhibited a positively charged (37.20 ± 7.5 mV), indicating that the system contains protonated amino groups. For CS/PVA blend solution, electrostatic repulsion between the particles was generated, yielding the stable systems, which was consistent with the reported result of the potential of CS/PVA composites (Dominguez-Martinez *et al*., 2017).

An absolute zeta potential above 30 mV is generally considered to be a sufficiently strong electrostatic repulsive force to maintain the physical stability of the particles (Xinhui Zhang *et al*., 2021). As shown in Table 3.1, the zeta potential of CIN-loaded particles increased to values between 46.90 and 47.80 mV, which can be attributed to the hydrogen bonding and hydrophobic interactions at the oil-water interface as a result of the reaction of CIN with CS via Schiff bases, and the presence of an electron-donating group (phenolic hydroxyl) on CIN provided electrons that the surface positive charges on the N atom (Huang *et al*., 2021). Notably, the zeta potential increased slightly but did not change significantly with increasing CIN concentration, most likely due to the complete reaction of CS/PVA at the oil-water interface with CIN in the oil phase, indicating excellent dispersion and homogeneity.

Table 3.1. Zeta potential of pure CS, PVA, CIN, CS/PVA, CS/PVA/CIN0.5, CS/PVA/CIN1 and CS/PVA/CIN1.5 films

Sample	Zeta potential (mV)
PVA	-0.188±0.02^{e}
CS	37.20±7.5^{b}
CIN	5.64±0.81^{d}
CS/PVA	31.21±5.00^{c}
0.5%	46.90±2.14^{a}
1%	47.10±2.05^{a}
1.5%	47.80±1.59^{a}

3.3.2. ATR/FT-IR spectroscopy

The FTIR spectra of pure CS, PVA, CIN, CS/PVA and CIN-added films are shown in Figure 3.1. In the spectrum of pure PVA, a wide band at 3263 cm^{-1} is attributed to -OH stretching vibrations of inter- and intramolecular hydrogen bonds (Abdelghany, Menazea, & Ismail, 2019). The stretching vibration of the methylene group (CH_2) is observed at 2941 cm^{-1} (Abdelghany *et al*., 2019). At 1416 cm^{-1}, the vibration is assigned to the C=O groups of the residual vinyl acetate groups in the PVA backbone (Ghaderi, Hosseini, Keyvani, & Gómez-Guillén, 2019). The band at 1327 cm^{-1} is assigned to C-O-H bending vibrations. The bands observed at 1234 and 833 cm^{-1} correspond to the C-C stretching and C-H motions of PVA (Narasagoudr, Hegde, Vanjeri, Chougale, & Masti, 2020). In addition, the strong absorption at 1084 cm^{-1} is assigned to the C-O stretching vibration (Lević *et al*., 2014).

The stretching vibrations of -OH and -NH in CS are identifiable as the broad peaked at 3349 and 2881 cm^{-1}, respectively (Osugi, Dong, Hexig, & Inoue, 2010). At 1639 and 1543 cm^{-1} occur the C=O stretching (amide band I) and asymmetric stretching -NH bending (amide band II) vibrations, respectively (Kaur, Jindal, Maiti, & Mahajan, 2019; Narasagoudr, Hegde, Vanjeri, *et al*., 2020). The bands at a 1151 cm^{-1} are likely due to the asymmetric stretching of the bridge C-O-C, with the band at 1019 cm^{-1} possibly due to C-O stretching (Queiroz, Teodosio Melo, Sabry, Sassaki, & Rocha, 2014; Tomadoni, Ponce, Pereda, & Ansorena, 2019). The saccharide group is represented by the bands that appeared at 889 cm^{-1} (Jin, Wang, & Bai, 2009).

The spectra of the CS/PVA films showed slight shifts in the CS and PVA characteristic peaks. Peaks associated with the C=O and C-O-H stretching vibrations of PVA shifted from 1416 to 1411 cm^{-1}, and 1327 to 1376 cm^{-1}, respectively. The -NH stretching vibrations of CS shifted to higher energies, from 1543 to 1557 cm^{-1}. Compared to free CS and PVA, the PVA/CS film exhibited a

decrease in the characteristic absorption peak of the -OH from 3349 to 3286 cm-1, indicating a strong intermolecular interaction between CS and PVA owing to the presence of electrostatic interactions between composite films (Yi *et al*., 2022).

The FTIR spectrum of pure CIN showed a C=O absorption vibration peak at 1670 cm^{-1} probably due to the presence of an aldehyde group and another peak at 1616 cm^{-1} due to aromatic benzene ring in conjugation with alkene. These data are similar to the results of Gadkari *et al.* (Gadkari *et al*., 2019). After the addition of CIN, the tensile vibration peaks of C=O in CIN at 1670 cm^{-1} disappeared, and the characteristic peak of imine bond (-C=N) appeared at 1633 cm^{-1}, suggesting the formation of a Schiff base (C=N), between the aldehyde group of CIN and the amino group of CS, which may be responsible for the improved tensile properties (Narasagoudr, Hegde, Vanjeri, *et al*., 2020). In addition, the decrease in intensity of the characteristic absorption peak at 1543/1557 cm^{-1}, indicating the conversion of the amino group into the imine/enamine functionality and the formation of the Schiff base. The diminution of the -NH absorption peak and the appearance of a new peak at a higher frequency are additional indications of the formation of the Schiff base. Furthermore, with increasing CIN content, the peak at 1319 cm^{-1} slightly shifts to 1308/1304 cm^{-1}, and may be attributed to a CIN aromatic ring C-H stretching vibration, indicating a blue shift caused by the electrostatic interaction between the aromatic ring in CIN and the hydroxyl group in PVA. Based on the ATR/FT-IR observations above, CIN addition is hypothesized to affect film intermolecular and intramolecular ordering, hence altering their mechanical and physicochemical properties (Xu *et al*., 2019).

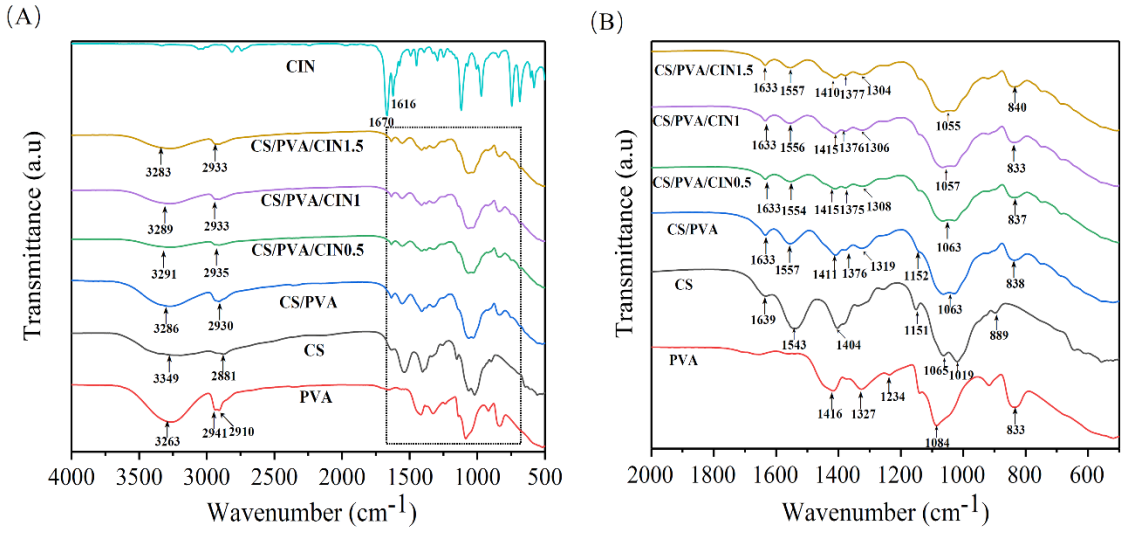

Figure 3.1. ATR/FT-IR spectra of pure CS, PVA, CIN, CS/PVA, CS/PVA/CIN0.5, CS/PVA/CIN1 and CS/PVA/CIN1.5 films.

3.3.3. Thickness and mechanical property

Mechanical strength is a key factor for food packaging integrity and in withstanding external stresses. Film thickness, Young's modulus, tensile strength (TS) and elongation at break (EAB) were measured and are listed in Table 3.2.

CIN inclusion increased film thickness from 0.031 ± 0.011 mm (0.5 %) to 0.052 ± 0.009 (1.5 %). This is suggested to arise from the increased non-solvent content of the film-forming solution. The PVA films were thicker with film thickness affected by degree of hydrolysis, surface tension and molecular weight. In general, PVA with a high average Mw has very long polymer chains. When dissolved in water, formed a highly viscous solution with increased water retention capacity, making the film thicker (Ortuño *et al*., 2003). This conclusion reflects findings reported by Bonilla *et al*. (Bonilla *et al*., 2014).

Table 3.2 showed that the tensile strength of the CS film was 79.51 MPa and its elongation at break was 8.73 %. This implies a lack of flexibility in the CS film (Yan, Dong, Yun, Liu, & Meng,

2022). Pure PVA films exhibit higher EAB values, about 131.91 % with a lower TS value at 53.04 MPa. Generally, PVA films with high EAB values lack tensile strength, an observation generally supported by other reports (Bonilla *et al*., 2014). For the CS/PVA films, the TS value was higher than the pure PVA film, at around 63.70 MPa and an EAB of 31.29 %. The ATR-FT/IR spectra indicated bond formation between polymer chains in the blends. This is demonstrated by the improved TS of the blend films, likely due to the interactions between PVA -OH groups and the -NH_2 groups of CS.

The TS gradually increased while EAB greatly decreased for the bioactive films with increasing CIN content. This suggests that hydrophobic substance addition altered film structure, supported by SEM and AFM analysis. The compositional changes lead to variations in intermolecular interactions between CS, PVA, and CIN, as reflected in the ATR-FT/IR spectra. These interactions improved the TS of blended films. The TS enhancement may be attributed to Schiff base (C=N) formation between the CIN hydroxyl group and the CS amino group. This additional bonding occupies polymer interspaces, reducing water absorption and improving tensile strength. (Zhang, Liu, Sun, Wang, & Li, 2020). Ojagh *et al*. observed a decrease in film elongation for CS-CIN blended films due to strong interactions between the carbohydrate polymer and EOs. According to the report, the decrease in the elongation at break (EAB) parameter of the polysaccharide-based films was consistent with expectations. This behavior is attributed to the structural disruptions present in the film network, which resulted from the dispersed lipid phase. (Ojagh *et al*., 2010).

Meanwhile, Young's modulus values ranged from the 815.31 MPa (PVA) to the 2060.90 MPa (CS). The higher the Young's modulus, the more rigid and less elastic the material is. (Wigati, Wardana, Tanaka, & Tanaka, 2022a). CS films have a high Young's modulus due to their semi-

crystalline structure and strong intermolecular hydrogen bonds between the polymer chains (Yan *et al*., 2022). However, the presence of hydroxyl groups in PVA reduced interchain bonding, resulting in lower Young's modulus values (Narasagoudr, Hegde, Chougale, *et al*., 2020). Furthermore, the addition of CIN to the CS/PVA composite films, the Young's modulus values from 1772 MPa to the 1924 MPa. That may be due to the strong interaction between CIN and CS/PVA in the film matrix and the increased number of bonds, which enhanced Young's modulus, making the bio-active films much stronger but less elastic (Bangar *et al.,* 2022).

Table 3.2. Thickness, tensile strength (TS), elongation-at-break (EAB) and Young's modulus of pure CS, PVA, CS/PVA, CS/PVA/CIN0.5, CS/PVA/CIN1 and CS/PVA/CIN1.5 films.

Sample	Thickness (mm)	Tensile Strength (MPa)	Elongation at break (%)	Young's modulus (MPa)
CS	0.030 ± 0.006^{d}	79.51 ± 2.70^{a}	8.73 ± 2.11^{e}	2060.90 ± 34.58^{a}
PVA	0.048 ± 0.023^{b}	53.04 ± 3.06^{d}	131.91 ± 5.94^{a}	815.31 ± 17.67^{e}
CS/PVA	0.030 ± 0.005^{d}	63.70 ± 1.38^{c}	31.29 ± 1.25^{d}	1215.30 ± 29.21^{d}
0.5%	0.031 ± 0.011^{d}	68.52 ± 1.70^{b}	73.10 ± 2.34^{b}	1772.00 ± 33.09^{b}
1%	0.040 ± 0.012^{c}	74.28 ± 1.31^{ab}	48.13 ± 3.68^{c}	1659.00 ± 15.31^{c}
1.5%	0.052 ± 0.009^{a}	76.95 ± 2.78^{a}	45.84 ± 2.20^{c}	1924.00 ± 16.72^{a}

3.3.4. Moisture content

The moisture content in a film is a measure of the amount of free water it contains. A high MC can negatively impact a film's antibacterial properties by creating a more hospitable environment for microorganisms. Thus, food packaging with less moisture is preferred (Zhou *et al*., 2020). The MC of CS, PVA, and CS/PVA composite films treated with varying concentrations of CIN is listed in Table 3.3. The MC of the PVA film, composed of both hydrophilic and

hydrophobic groups, was around 11 %. After CIN addition, the MC value decreased to 10.25 % and remained constant with CIN1.5 %. The hydrogen bonding interactions between the phenolic components of CIN and the amino and hydroxyl groups of the CS molecules enhanced film hydrophobicity and water resistance, in addition to the putative preservation effect of CIN, which diminishes the rate of water loss. (Yi *et al*., 2022).

3.3.5. Swelling rate

Understanding swelling is crucial as it affects packaging stability changes in quality. As summarized in Table 3.3, the swelling rate of the pure CS film was 572 %, which may be explained by the presence of hydrophilic and polar peptides. Moreover, the hydrophilic (-OH) pure PVA (100.52 %) and CS/PVA (82.00 %) composite films also exhibited significant SRs. Upon the addition of the hydrophobic EO, a greatly reduced film SR was observed, from a concentration of 0.5 % (54.47 % SR) to 1.5% (32.53 % SR). This indicates that CIN addition reduced water absorption, presumably by filling internal voids between CS/PVA films and by associating with free polymer hydroxyl groups, reducing interactions with water and making the film less water absorbent. This conclusion is consistent with the findings reported by Hosseini *et al*. (Hosseini *et al*., 2021).

3.3.6. Water solubility

As noted in Table 3.3, water solubility decreased gradually. The results show that the WS of the bioactive film containing CIN was lower than that of the control CS (58.89 %) and PVA (95.50 %). This may be due to strong interactions of the CIN with the CS/PVA matrix, limiting polymer chain mobility by hydrogen and Schiff bonds (C=N). This behavior is known to reduce the binding of free hydroxyl groups to water (Sajjan *et al*., 2020). Thus, these bioactive films

provide excellent stability in low-solubility settings.

3.3.7. Water activity

For food packaging materials, the water activity is a crucial factor that influence the susceptibility to microbial growth (Espíndola Sobczyk *et al.,* 2021). Lund *et al*., reported the pathogenic bacteria growth is optimized at a_w levels of 0.98. The majority of bacteria are unable to proliferate at a_w values below 0.85, while fungi cannot grow below as 0.61 (Lund, Baird-Parker, & Gould, 2000; Perumal *et al*., 2022). The a_w values of films prepared by CS and/or PVA mixed with CIN are displayed in Table 3.3. All the values of the films were in the range of 0.43-0.60. The a_w of pure PVA film was 0.60 due to its high hydrophilicity (Figure. 3.2). Subsequently, no significant differences were observed between the a_w of CS (0.54) and CS/PVA (0.57) films. However. with the addition of the hydrophobic of CIN, the a_w values decreased from 0.5% (0.47) to 1.5% (0.43). This may be a result of the hydrophobic CIN forming a barrier that inhibited the growth of fungus by reducing a_w. This is also consistent with results of antifungal activity in in vitro assay. Notably, the difference between 1% and 1.5% was not significant, and similar findings was reported by (de Espíndola Sobczyk *et al*., 2021).

Table 3.3. Moisture content (MC), swelling rate (SR), water solubility (WS), water activity(a_w) and water contact angle (WCA) of pure CS, PVA, CS/PVA, CS/PVA/CIN0.5, CS/PVA/C IN1, CS/PVA/CIN1.5 films.

Sample	MC (%)	SR (%)	WS (%)	a_w	WCA (°)	
					t = 0 s	t = 30 s
CS	16.66±0.89^{a}	572.20±18.32^{a}	58.89±1.68^{b}	0.54±0.02^{b}	85.02±2.31^{b}	72.32±2.13^{b}
PVA	11.73±0.97^{c}	100.52±6.72^{b}	95.50±2.02^{a}	0.60±0.04^{a}	47.13±3.20^{c}	38.27±1.44^{c}
CS/PVA	11.91±1.91^{c}	82.00±4.73^{c}	47.19±2.78^{c}	0.57±0.02^{ab}	77.66±1.01^{b}	66.82±1.48^{b}
0.5%	11.89±2.92^{c}	54.47±4.30^{d}	32.98±4.36^{d}	0.47±0.01^{c}	103.99±1.31^{ab}	104.50±1.11^{a}
1%	10.25±1.55^{c}	42.18±3.60^{e}	27.51±4.31^{e}	0.43±0.04^{d}	106.45±2.83^{ab}	106.72±2.54^{a}
1.5%	10.60±1.09^{c}	32.53±2.82^{e}	25.60±4.74^{f}	0.43±0.02^{d}	107.83±1.08^{a}	103.99±1.12^{a}

3.3.8. Water contact angle analysis

WCA is an essential indicator for determining package structural integrity in a moist environment. WCA values of $0^{\circ} < \theta < 50^{\circ}$ indicate 'Superhydrophilic' (rough with r > 1); $50^{\circ} < \theta < 90^{\circ}$ indicate 'hydrophilic'; $90^{\circ} < \theta < 150^{\circ}$ indicate 'hydrophobic' and $\theta > 150^{\circ}$ indicate 'superhydrophobic' (Drelich, Chibowski, Meng, & Terpilowski, 2011). WCA values of each treatment were evaluated over time, at the initial contact ($\theta_t = 0$) and after 30 s ($\theta_t = 30$) of water contact as shown in table 3.3 and figure 3.2. The lowest values for $\theta_t = 0$ (47.13°) and $\theta_t = 30$ (38.27°) were found in the PVA film, indicating its superhydrophilic properties. Meanwhile, for the CS and CS/PVA composite films, the WCA at $\theta_t = 0$ reached 85.02° and 77.66° respectively, while the contact angle rapidly decreased to 72.32° and 66.82° after 30 s. This demonstrated that they are all hydrophilic substances ($\theta < 90^{\circ}$).These results were slightly little lower than those for CS/PVA films previously reported (69 ± 1°) (Narasagoudr, Hegde, Vanjeri, *et al*., 2020). Discrepancies between investigations may be due to differences in the substance's quality and the film-making procedure.

Due to the extremely hydrophobic nature of the bioactive agent, the ternary film containing CIN demonstrated excellent hydrophobic qualities, and the solubility values remained at a high level even after 30 s. As can be seen in Table 3.3 and figure 3.2, the highest value reached was 107.83° ($\theta_t = 0$; 1.5%), which is about 56 % higher than the lowest value ($\theta_t = 0$; PVA). This is likely due to the hydrophobic nature of CIN-added CS/PVA film to form a denser and more water-resistant structure.

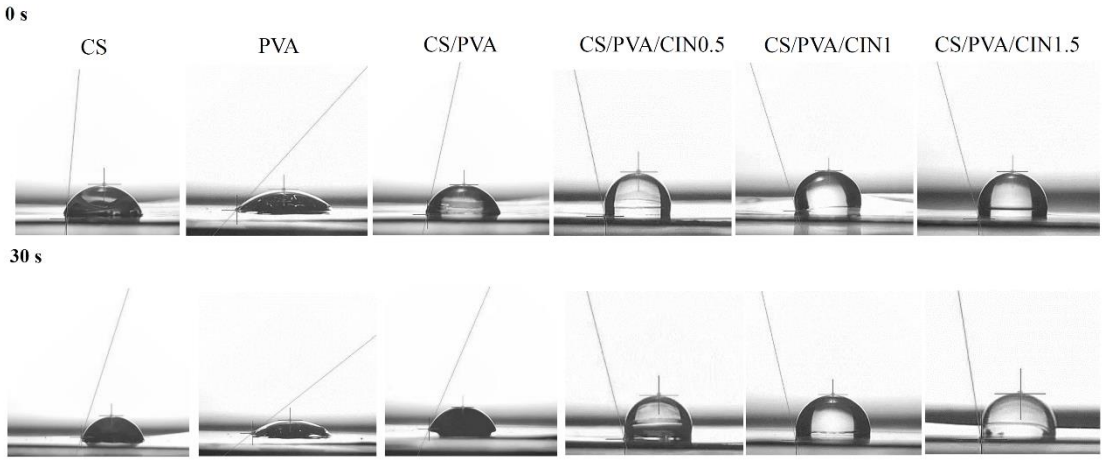

Figure 3.2. Water contact angle (WCA) photos of CS, PVA, CS/PVA, CS/PVA/CIN0.5, CS/PVA/CIN1, CS/PVA/CIN1.5 films

3.3.9. WVTR and WVP

The WVTR and WVP values for each treatment group are listed in Table 3.4. It was discovered that the inclusion of CIN decreased the WVTR film values. Adding 0.5% CIN (1.22×10^{-2} $g/s^{-1}\cdot m^{-2}$), for instance, decreased the WVTR value by 47% compared to pure CS films (2.32×10^{-2} $g/s^{-1}\cdot m^{-2}$). Bioactive films containing 1.5% CIN demonstrated a lower WVTR (0.98×10^{-2} $g/s^{-1}\cdot m^{-2}$). This is consistent with expectations and may be attributable to the higher concentration of CIN phase aggregating and increasing the distance of channels in the membrane, thereby resulting in the lower WVTR.

The CS film exhibited the highest WVP value of 17.76×10^{-11} ($g\cdot m^{-1}s^{-1}m^2\cdot Pa^{-1}$). This was followed closely by the PVA and CS/PVA films with WVP values of 13.53 and 13.15×10^{-11} ($g\cdot m^{-1}s^{-1}m^2\cdot Pa^{-1}$), respectively, with no significant difference ($P > 0.05$) between them. This variation can be attributed to the change in film thickness. By incorporating CIN into the polymer matrix, the WVP value decreased gradually from 10.08×10^{-11} ($g\cdot m^{-1}s^{-1}m^2\cdot Pa^{-1}$) to 6.73×10^{-11} ($g\cdot m^{-1}s^{-1}m^2\cdot Pa^{-1}$). This behavior may also be attributed to CIN's hydrophobic properties enhancing the

polymer-based films' water barrier characteristics. In addition, the introduction of an oil phase increases the distance water molecules travel through the film. The induced polymer aggregation state changes thus interrupts the CS-water hydrogen bonding in the matrix, leading to decreased WVP (Sánchez-González *et al*., 2009). In any case, the WVP values of 1.5 % found in the previous study are lower than those reported for CS-based thyme/cinnamon EO films, i.e., $8.43 \pm 0.53 \times 10^{-11}$ ($g \cdot m^{-1}s^{-1}m^2 \cdot Pa^{-1}$) (Peng & Li, 2014). The variation between investigations may be attributed to differences in polymer content and film-making techniques.

3.3.10. Oxygen permeability

As noted in table 3.4, the PVA film had a low oxygen transmission rate (OTR) of 13.36 $cm^3/(m^2 \cdot 24\ h)$ and 2.31×10^{-14} ($cm^3 \cdot m/m^2 \cdot s \cdot Pa$). As PVA is dense and non-porous, the number of pores allowing oxygen molecules to pass through are minimized. In addition, the polymer chains in the PVA are tightly packed, also hindering oxygen diffusion. Likewise, the OTR and OP of CS were relatively low, at around 14.99 $cm^3/(m^2 \cdot 24\ h)$ and 3.43×10^{-14} ($cm^3 \cdot m/m^2 \cdot s \cdot Pa$), respectively. Compared with the CS and PVA film, the OP of the CIN-containing bioactive films increased by 13.99 %, 19.88 % and 30.32 %, respectively. This increase may be explained by improved CIN distribution in the CS/PVA matrix. Particularly, the CS/PVA composite film with 1.5% CIN yielded an OTR and OP of 17.93 $cm^3/(m^2 \cdot 24\ h)$ and 4.47×10^{-14} ($cm^3 \cdot m/m^2 \cdot s \cdot Pa$). This is 1.94 times higher than that of the pure PVA film. It is well known that good polymer OP values are necessary for packaging postharvest fruit and vegetables. This experiment highlighted improvements in the OP of films, supporting it as a promising packaging film.

Table 3.4. Water vapor transmission rate (WVTR), Water vapor permeability (WVP), oxygen transmission rate (OTR) and oxygen permeability (OP) of CS, PVA, CS/PVA, CS/PVA/CIN0.5, CS/PVA/CIN1, CS/PVA/CIN1.5 films.

Sample	WVTR $\times10^{-2}$ ($g/s^{-1}\cdot m^{-2}$)	WVP $\times10^{-11}$ ($g/m^{-1}s^{-1}m^{2}\cdot Pa^{-1}$)	OTR ($cm^3/m^2\cdot24h$)	OP $\times10^{-14}$ ($cm^3\cdot m/m^2\cdot s\cdot Pa$)
CS	2.32 ± 0.21^{a}	17.76 ± 1.31^{a}	14.99 ± 1.24^{d}	3.43 ± 0.24^{d}
PVA	1.28 ± 0.28^{c}	13.53 ± 2.48^{b}	13.36 ± 2.11^{e}	2.31 ± 0.91^{e}
CS/PVA	1.43 ± 0.23^{b}	13.15 ± 1.80^{b}	16.31 ± 1.09^{c}	3.71 ± 0.22^{c}
0.5%	1.22 ± 0.11^{c}	10.08 ± 1.25^{c}	16.90 ± 2.01^{bc}	3.91 ± 0.34^{bc}
1%	1.21 ± 0.05^{c}	8.60 ± 0.40^{d}	17.33 ± 2.77^{ab}	4.11 ± 0.11^{ab}
1.5%	0.98 ± 0.08^{d}	6.73 ± 0.59^{e}	17.93 ± 1.83^{a}	4.47 ± 0.09^{a}

3.3.11. Color and opacity

Color and transparency levels of packaging materials are crucial to safeguard food from the harmful effects of UV light. The color values and the opacity of each treatment group is listed in table 3.5. The neat CS and PVA films have a high transparency. Correspondingly, their L^* and ΔE^* values are higher than those of the other groups (L^* = 87.67, 92.50; ΔE^*=8.50, 3.42) due to the transparency of materials. The color value of the CS/PVA composite film is close to that of the CS film, and after neutralizing the color of the PVA, the ΔE^* value is around 9.75. However, the steady increase in the film's ΔE^* value (from 13.00 to 23.70) following the addition of CIN (0.5 % to 1.5 %) is primarily attributed to the increased b^* value. As seen in table 3.5, the b-values (yellowness/blueness) showed a significant difference ($p < 0.05$), primarily attributable to the intrinsic yellow color of the CIN agent and the microstructure resulting from its interaction with polymer molecules in the film matrix. Similar color variations are reported for cinnamaldehyde-loaded CS nanoparticles (Hosseini, Ghaderi, *et al*., 2022) and poly(lactic acid)-based active bilayer films (Hosseini, Kaveh, *et al*., 2022).

Regarding opacity, as noted in table 3.5, the obtained values for the CS, PVA and CS/PVA

film are 1.59, 1.24, and 1.63 AU/mm, respectively. The incorporation of CIN increases the ternary film's opacity, reaching 2.27 AU/mm at the maximum concentration (i.e., CS/PVACIN1.5), an increase of 45.37 % compared to pure PVA. The reduction in biofilm transparency is due to the added yellow CIN and film matrix shrinkage, from the reduction in polymer inter-chain spacing. As a result, light absorption and reflection are enhanced, with transmission reduced (Xue *et al*., 2019).

Table 3.5. The color and opacity of pure CS, PVA, CS/PVA, CS/PVA/CIN0.5, CS/PVA/CIN1, CS/PVA/CIN1.5 films.

Sample	*L**	*a**	*b**	*ΔE*	Opacity (AU/ mm)
CS	87.67±2.80^{b}	-0.69±0.13^{d}	3.57±0.38^{d}	8.50±2.28^{d}	1.59±0.18^{bc}
PVA	92.50±1.57^{a}	1.59±0.09^{a}	-1.1±1.28^{e}	3.42±0.82^{e}	1.24±0.19^{d}
CS/PVA	85.80±2.29^{b}	-1.18±0.29^{c}	4.2±0.08^{d}	9.75±2.20^{d}	1.63±0.09^{c}
0.5%	83.73±0.98^{bc}	-2.37±0.40^{b}	7.53±0.46^{c}	13.00±1.45^{c}	1.64±0.04^{bc}
1%	80.43±2.56^{c}	-2.47±0.45^{b}	9.40±1.22^{b}	16.40±0.39^{b}	1.87±0.14^{b}
1.5%	80.20±0.70^{c}	-2.09±0.78^{b}	14.43±2.94^{a}	23.70±0.68^{a}	2.27±0.12^{a}

3.3.12. Light transmittance

A major cause of food oxidation includes UV light, while lipid oxidation also strongly impacts bioactive film physicochemical properties. Figure 3.3 illustrated the light transmittance between 300-800 nm for the films. The PVA film transmitted the maximum UV and visible light at 300 nm (about 20 %), while the other films transmitted less UV light between 300−350 nm. Upon CIN content increase from 0.5 % to 1.5 %, the ternary bioactive film light transmittance gradually decreased. This is likely due to light scattering and reflection at the interface of the polymer matrix oil droplets after the addition of CIN. This result is consistent with those observed for colored films (Hosseini, Rezaei, Zandi, & Farahmandghavi, 2015). Additionally, a comparable phenomenon was observed when CIN was added to a CS nanoparticle solution, investigated by Hosseini *et al*.,

(Hosseini, Ghaderi, *et al*., 2022). Thus, confirming the ability of the bioactive films to protect food against UV-induced deterioration and oxidative discoloration. According to Fig 3.3, increased CIN content caused a gradual transition from transparent to yellow, similar to the increased opacity listed in table 3.5. Although the bioactive film has a diminished transmittance, it nonetheless possesses good optical characteristics. Thus, ternary films are quite suitable food packaging materials.

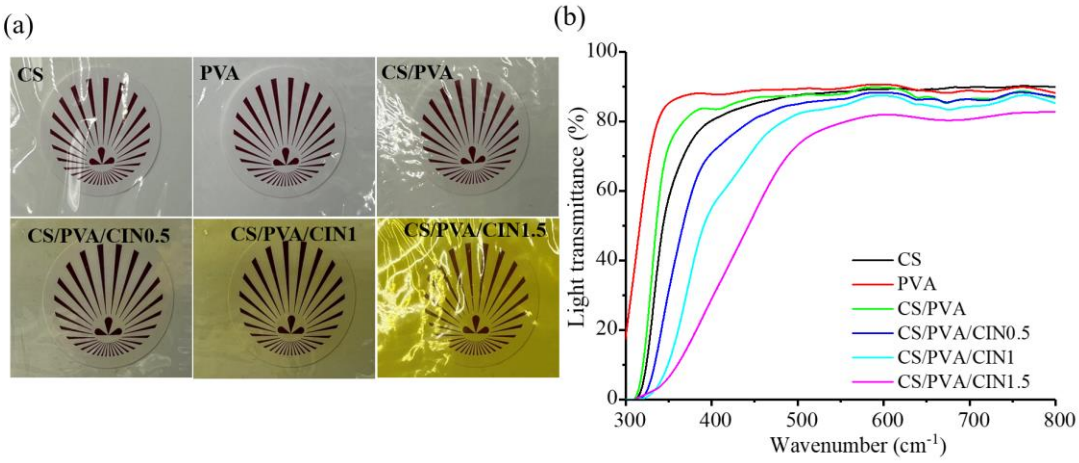

Figure 3.3. The visual appearance of each treatment films (a), light transmittance of CS, PVA, CS/PVA, CS/PVA/CIN0.5, CS/PVA/CIN1, CS/PVA/CIN1.5 films (b).

3.3.13. Scanning electron microscope

To evaluate the surface and internal structure of the pure CS, CS/PVA, and CS/PVA/CIN films, they were analyzed by SEM at magnifications of 500 and 1000 ×, as depicted in Figure 3.4. The film surface is visually similar between pure CS and PVA films, being relatively smooth, flat and uniform without pores or cracks, indicating that PVA dissolves well in water and CS in a slightly acidic environment. In the case of the CS/PVA films, although tiny particles were observed on the surface of the film, the surface was continuous, indicating good compatibility characteristics. These findings were comparable to those reported by Ghaderi *et al*. (Ghaderi *et al*., 2019). When

the content of CIN was increased to 0.5 %, the biopolymer surface remained uniform, despite some pore formation. However, this did not affect the overall surface morphology, indicating that the CIN is well dispersed in the membrane matrix. Upon increasing CIN content, variously sized oil droplet-like holes appeared on the surface of the films. This may be due to the hydrophobic nature of CIN, leading to agglomeration within the film during drying. Fortunately, CIN incorporation leads to a more dense composite film, an observation supported by earlier studies *(Dashipour et al*., 2015; Shen & Kamdem, 2015).

A cross-sectional image of the composite film was obtained by SEM to evaluate biopolymeric film uniformity, density, coating process efficacy, and CIN thickness within the CS/PVA substrate. Both the CS and PVA films exhibited compact and smoother morphological structures than other films. However, the PVA films are thicker than CS films, reflecting the superior tensile capabilities inherent to PVA materials. The CS/PVA composite film presented a continuous morphology, free of imperfections, air bubbles, or pores and without any evidence of phase separation, in accordance with the observation in Fig 3.4 (C). With the addition of CIN, films become rougher and denser (Figure 4 d ~f). No bubbles and no indications of phase separation are observed, as expected for a relatively homogenous material. This may be a result of strong interactions between the CIN and polymer chains. Previous studies have suggested that this is due an increased density of the intermolecular polymers through Schiff base (C=N) formation and hydrogen bonding (Hosseini *et al*., 2021). The increased surface coarseness of CIN EO composite films is reported previously (Hosseini, Ghaderi, *et al*., 2022).

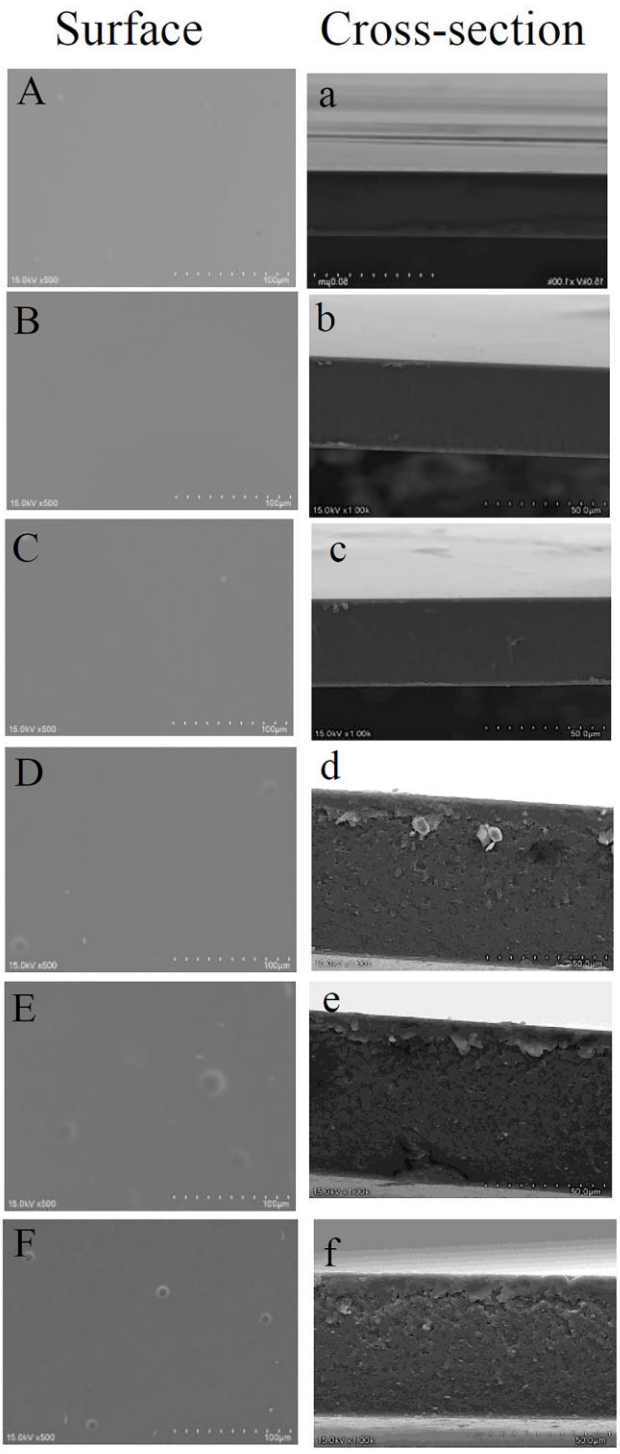

Figure 3.4. SEM micrographs of the surface and cross-section of CS (A; a), PVA (B; b), CS/PVA (C; c) CS/PVA/CIN0.5 (D; d), CS/PVA/CIN1 (E; e), CS/PVA/CIN1.5 (F; f) films.

3.3.14. Surface AFM analysis

For further explore surface morphology and roughness variation between pure CS, PVA, CS/PVA composite and ternary biopolymeric films. Typical roughness values for the 2D surface and 3D valley-morphology of films scanned over an area of 5 × 5 μm^2 as shown in Figure 3.5. For the pure PVA films, a smooth superficial surface and a high flatness distribution is observed. Also, the roughness is the lowest compared to the other groups (Ra = 4.39 nm, Rq = 4.86 nm), consistent with the SEM results. Meanwhile, the CS and CS/PVA composite film topographies were relatively homogeneous, as indicated by the relatively low Ra and Rq values (5.30, 5.89 nm, and 6.19, 7.43 nm, respectively), suggesting good compatibility between chitosan and PVA films. However, CIN addition to the bio-composite film resulted in a roughening with higher hill-valley images, as indicated by the higher Ra, Rq values (7.65, 6.59 nm). Moreover, the difference in surface voltage is represented by white colors. The 2D images clearly exhibited the appearance of white spots, representing the formation of small droplets or agglomerations of the EOs on the film surface, which can create a rougher appearance. As the CIN content increases from 0.5% to 1.5%, it can be seen that slight agglomeration and migration lead to a change in the surface roughness of the film. This state may be attributed to the extension of creamed droplets on the film surface after drying, filling the relative irregularities of the film substrate surface. A slight decrease in roughness parameters was observed. This result is in agreement with that obtained by cross-section SEM analysis. A similar behavior was also reported by Zhang *et al*. (Xinhui Zhang *et al*., 2021).

2D	3D	
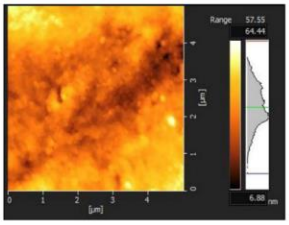	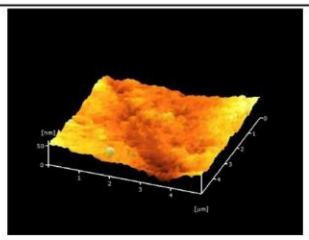	CS Ra: 5.30 nm Rq: 5.89 nm
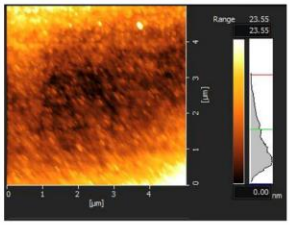	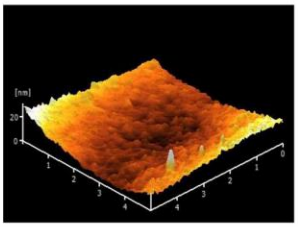	PVA Ra: 4.39 nm Rq: 4.86 nm
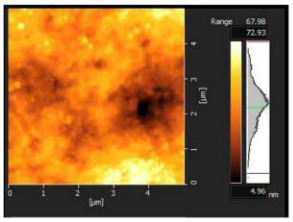	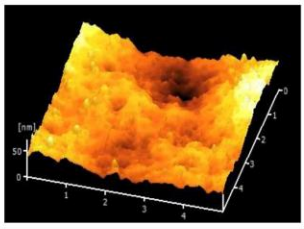	CS/PVA Ra: 6.19 nm Rq: 7.43 nm
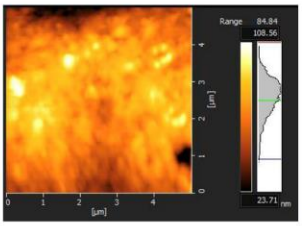	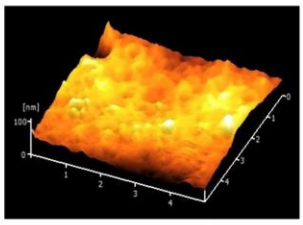	CS/PVA/CIN0.5 Ra: 7.65 nm Rq: 6.59 nm
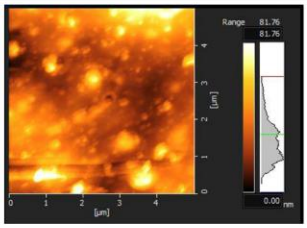	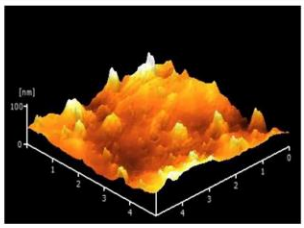	CS/PVA/CIN1 Ra: 6.25 nm Rq: 6.45 nm
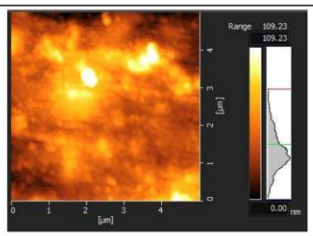	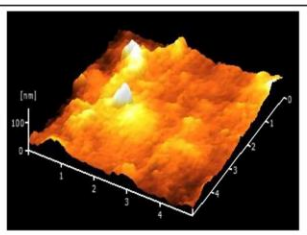	CS/PVA/CIN1.5 Ra: 4.51 nm Rq: 4.03 nm

Figure 3.5. 2D and 3D of surface morphology with the respective roughness of CS, PVA, CS/PVA, CS/PVA/CIN0.5, CS/PVA/CIN1, CS/PVA/CIN1.5 films.

3.3.15. In vitro antifungal activity assay

The in vitro activity assay and mycelium growth results are presented in Figure 3.6. In the control group, both *P. italicum* and *B. cinerea* extensively covered the inoculated agar by the 6th day. Notably, the results for PVA were similar to the control, indicating that PVA does not inhibit mold growth. This observation is supported in the literature (Haghighi *et al*., 2019). However, *B. cinerea* was strongly inhibited by CS and CS/PVA groups. This is likely due to its CS amino groups, which can confer broad-spectrum antibacterial activities (Yan *et al*., 2022). No difference was observed between CS, PVA and CS/PVA in *P. italicum* inhibition, as *P. italicum* is unaffected by PVA inhibition. For all CIN-containing films, clear inhibition zones ($P < 0.05$) against *P. italicum* and *B. cinerea* were observed. The bioactive film with the maximum amount of CIN (1.5 %) effectively suppressed microorganism expansion. This suppression may be a consequence of the high electrophilicity of the carbonyl group near the CIN double bond, which activates compounds that combine with nucleophilic reagents to exhibit potent antibacterial activities (H. Chen *et al*., 2016). It is also noted that EO hydrophobicity aids in microbial cell plasma membrane destabilization, leading to cell rupture and disintegration (Xu *et al*., 2019). CIN antifungal activity is attributed to its ability to disrupt fungal cells' membranes, releasing cellular components, and leading to cell death. When CIN is added to CS or PVA films, it forms a physical barrier that prevents the attachment and growth of fungal cells on the film surface. Similar effects have been observed in basil. (Wigati, Wardana, Tanaka, & Tanaka, 2023) and cajuput (Wardana, Tanaka, & Tanaka, 2021) as well as tea seed EOs (Kingwascharapong, Tanaka, & Tanaka, 2021).

The inhibition zone diameter surrounding the sample on the inoculated agar and the PI value is displayed in Figure 3.6 (B). The stronger the inhibition, the greater the PI. According to figure 3.6 (B), the diameter of both molds for the control group ranged from 85 to 90 mm, with an

inhibition of nearly zero. Consistent with the in vitro antifungal activity assay result. Yet, the PI values for all bioactive films containing CIN were much greater than for the other treatment groups, with a sustained inhibition rate of about 90 %. No significant difference was observed between CIN concentrations (Fig 3.6B). This suggests that CIN efficiently inhibited mold growth, and was capable of releasing its antibacterial characteristics in both the film and the solution, making the packaging material antibacterial.

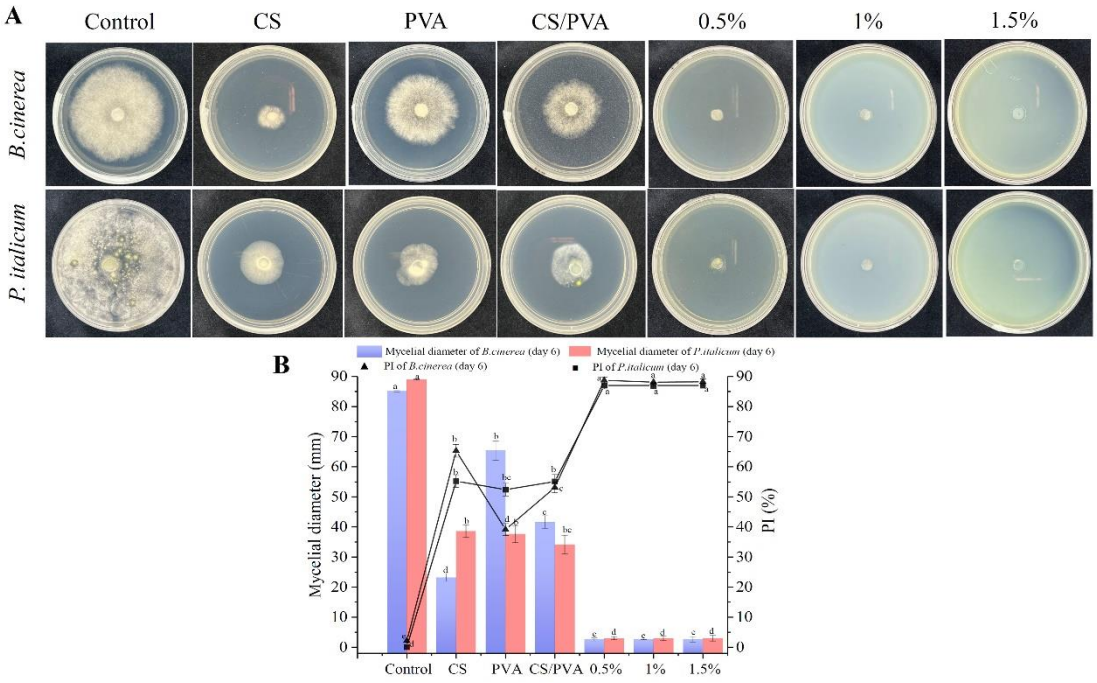

Figure 3.6. Different coating solutions on *P. italicum* and *B. cinerea* (A) Visual image of mycelium diameter at the incubation's end. (B) Statistical analysis after 6 days incubation.

Note: 0.5%: CS/PVA/CIN0.5, 1%: CS/PVA/CIN1 and 1.5%: CS/PVA/CIN1.5.

3.3.16. Spore germination assay

To further evaluate the impact of each coating solution on *P. italicum* and *B. cinerea,* spore germination and membrane integrity were examined. Spore germination of each sample is shown in figure 3.7 (A). For the control and PVA groups, well-formed spores were observed, which

germinated promptly, and were not restricted in either form, confirming the previous findings. The control and PVA solutions possessed no discernible inhibition. In the solution containing CS, spore germination was inhibited, but germinated spores were still present, demonstrating that while CS was inhibitive, it was not particularly effective. Upon CIN addition, spore inhibition was observed, which may be due to the carbonyl group near the CIN double bond.

To evaluate the changes of each treatment, *P. italicum* spore cell membrane integrity was investigated using propidium iodide staining. Propidium iodide is a unique fluorescent molecule that intercalates with cell DNA, and is commonly used to indicate dead or damaged cells. However, when cell membranes are compromised, it can enter the cell, fluorescing red when appropriately excited. (Wardana, Kingwascharapong, Wigati, Tanaka, & Tanaka, 2022). Therefore, redder areas indicate a greater number of disrupted spores, and thus greater inhibition. Conversely, the greater the number of healthy spores, the lower the inhibition. As shown in Figure 3.7 (A) and 3.7 (B), spores in the control group were not stained, indicating intact cell membranes. However, spores exposed to CS/PVA/CIN showed significantly increased red fluorescence compared to the other coating solutions. Furthermore, upon CIN addition, the red area and intensity increased, with the highest observed for the 1.5 % CIN (Fig.3.7 C). This demonstrates the excellent antifungal properties for the CIN-added ternary films with the red fluorescence of dead spores demonstrating this phenomenon (Fig.3.7A). This data shows that the CIN-containing coating compromises spore membranes, disturbing metabolic processes and leading to spore death (Suzuki, Fujikura, Higashiyama, & Takata, 1997).

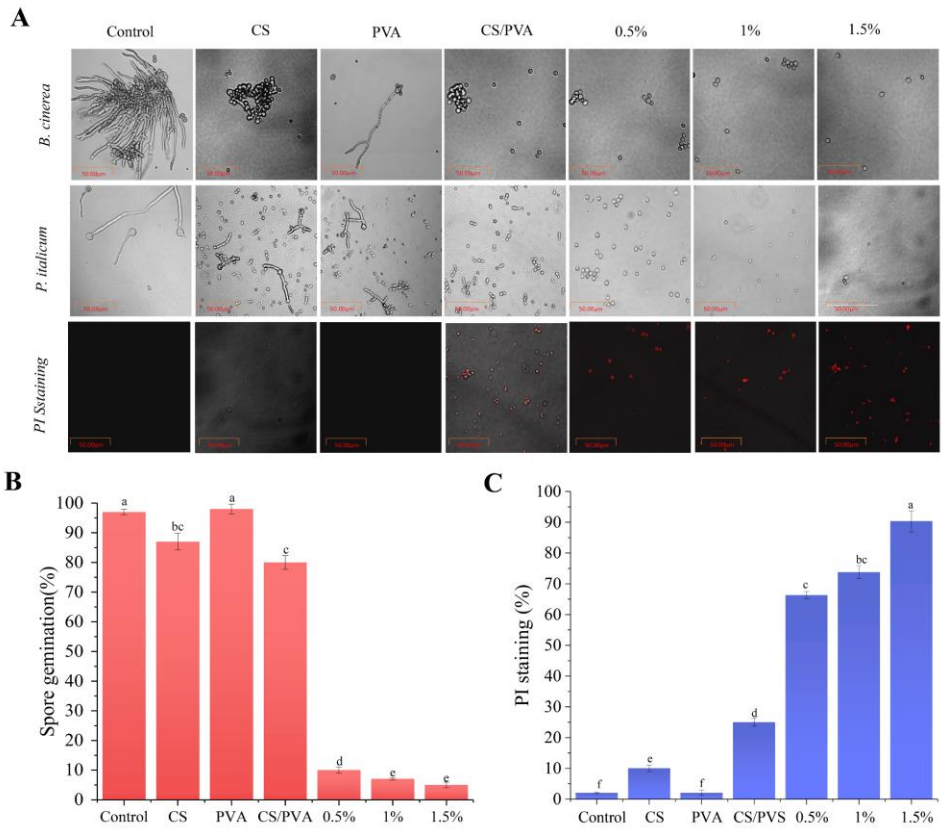

Figure 3.7. Inhibitory effects of coating solutions on spore germination of *P. italicum* and *B. cinerea* (A) optical and CLSM image of the cell membrane. (B) and (C) statistical effects of coating solutions on spore germination and PI staining of *P. italicum*

3.3.17. DPPH radical scavenging assay

Figure 3.8 (A) displays the DPPH radical scavenging absorption value at 517 nm. The CS film has a DDPH scavenging activity rate of 11.51 % compared to only 2.84 % for the PVA film. This behavior may be attributed to the presence of amino ($-NH_2^+$) and hydroxyl (-OH) groups in CS, which have radical scavenging capacity. Thus, the free radical scavenging ability of pure CS films and CS/PVA composite films is about 5 times stronger than of pure PVA films. Sun *et al*. reported that medium molecular weight CS exhibited modest antioxidant activity related to its M_w (Sun, Zhou, Mao, & Zhu, 2007). Previous evaluations of DPPH radical scavenging inhibition for

pure CS varied around 9.8 to 11 %, reflecting our observations (Martins, Cerqueira, & Vicente, 2012).

Furthermore, increasing CIN from 0.5 % to 1.5 %, resulted in an increase in DPPH radical scavenging rate from 19.22 % to 31.43 %. With the maximum scavenging rate three-fold that of pure chitosan. The excellent antioxidant properties of the bioactive film containing CIN can be attributed to the CIN aromatic structures, which increase its ability to scavenge free radicals and improve anti-inflammatory properties, which may also contribute to its capacity to protect cells from oxidative stress and damage. (Kuai *et al*., 2020). In addition, it is reported that hydroxyl groups on EOs and/or benzene rings, function as hydrogen donors to DPPH, and are responsible for the stability and improved antioxidant effects (Ksouda *et al*., 2019). This is similar to reports of other antioxidant-rich films containing EOs like curcuma oil (Fernández-Marín, Fernandes, Sánchez, & Labidi, 2022), apricot kernel EOs (Priyadarshi *et al*., 2018), and thyme oil (Zhao *et al*., 2023). From these results, it is important to highlight the potential bioactivity of CIN as it provides ternary membranes with improved antioxidant properties.

3.3.18. FRAP assay analysis

Due to variability in oxidation capacity, it is necessary to combine multiple techniques in determining the antioxidation properties of films. It is well-established that metal ions play a role as precursors in lipid peroxidation (Chentir *et al*., 2019). Figure 3.8 (B) illustrated the reduction of ferrous ions (Fe^{3+}) to blue ferrous iron (Fe^{2+}) levels for each treatment group at 700 nm. In the case of the pure PVA, only a modest of reducing power activity ($OD_{700\ nm}$ = 0.036) was imparted. For the CS and CS/PVA film, the Fe^{3+} reducing power was ($OD_{700\ nm}$ = 0.116; $OD_{700\ nm}$ = 0.105), respectively. This may have occurred because of the amide band of CS. However, increasing CIN from 0.5 % to 1.5% resulted in the reducing power of CS/PVA/CIN 1.5 reaching a maximum value

of $OD_{700\ nm}$ =0.172. Both the DPPH radical scavenging capacity and the FRAP assay of the film with CIN indicate strong antioxidant activity. This finding demonstrates that CIN-containing substances react well with free radical products.

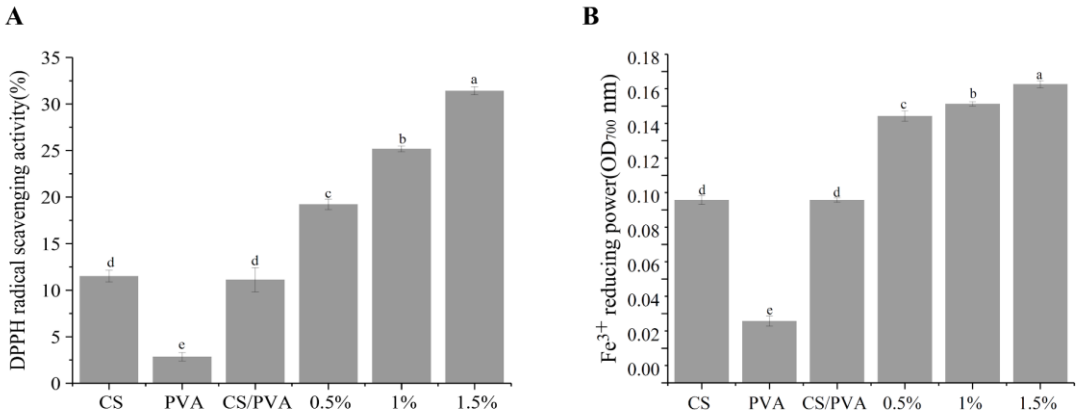

Figure 3.8. Antioxidant activity of DPPH radical scavenging assay (A) and FRAP assay (B) of pure CS, PVA, CS/PVA, CS/PVA/CIN0.5, CS/PVA/CIN1 and CS/PVA/CIN1.5 films.

3.4. Reference

Abdelghany, A., Menazea, A., & Ismail, A. (2019). Synthesis, characterization and antimicrobial activity of Chitosan/Polyvinyl Alcohol blend doped with Hibiscus Sabdariffa L. extract. Journal of Molecular Structure, 1197, 603-609.

Abdelhedi, O., Nasri, R., Jridi, M., Kchaou, H., Nasreddine, B., Karbowiak, T., . . . Nasri, M. (2018). Composite bioactive films based on smooth-hound viscera proteins and gelatin: Physicochemical characterization and antioxidant properties. Food Hydrocolloids, 74, 176-186.

Bangar, S. P., Whiteside, W. S., Dunno, K. D., Cavender, G. A., & Dawson, P. (2022). Pearl millet starch-based nanocomposite films reinforced with Kudzu cellulose nanocrystals and essential oil: Effect on functionality and biodegradability. *Food Research International,* 157,

111384.

Bonilla, J., Fortunati, E., Atarés, L., Chiralt, A., & Kenny, J. M. (2014). Physical, structural and antimicrobial properties of poly vinyl alcohol–chitosan biodegradable films. Food Hydrocolloids, 35, 463-470.

Chen, C.-K., & Huang, S.-C. (2016). Preparation of reductant–responsive N-maleoyl-functional chitosan/poly (vinyl alcohol) nanofibers for drug delivery. Molecular Pharmaceutics, 13(12), 4152-4167.

Chen, H., Hu, X., Chen, E., Wu, S., McClements, D. J., Liu, S., . . . Li, Y. (2016). Preparation, characterization, and properties of chitosan films with cinnamaldehyde nanoemulsions. Food Hydrocolloids, 61, 662-671.

Chentir, I., Kchaou, H., Hamdi, M., Jridi, M., Li, S., Doumandji, A., & Nasri, M. (2019). Biofunctional gelatin-based films incorporated with food grade phycocyanin extracted from the Saharian cyanobacterium Arthrospira sp. Food Hydrocolloids, 89, 715-725.

Clogston, J. D., & Patri, A. K. (2011). Zeta potential measurement. Characterization of nanoparticles intended for drug delivery, 63-70.

Dashipour, A., Razavilar, V., Hosseini, H., Shojaee-Aliabadi, S., German, J. B., Ghanati, K., . . . Khaksar, R. (2015). Antioxidant and antimicrobial carboxymethyl cellulose films containing Zataria multiflora essential oil. International Journal of Biological Macromolecules, 72, 606-613.

De Espíndola Sobczyk, A., Luchese, C. L., Faccin, D. J. L., & Tessaro, I. C. (2021). Influence of replacing oregano essential oil by ground oregano leaves on chitosan/alginate-based dressings properties. International Journal of Biological Macromolecules, 181, 51-59.

Dominguez-Martinez, B. M., Martínez-Flores, H. E., Berrios, J. D. J., Otoni, C. G., Wood, D. F., & Velazquez, G. (2017). Physical characterization of biodegradable films based on chitosan, polyvinyl alcohol and opuntia mucilage. Journal of Polymers and the Environment, 25, 683-691.

Drelich, J., Chibowski, E., Meng, D. D., & Terpilowski, K. (2011). Hydrophilic and superhydrophilic surfaces and materials. Soft Matter, 7(21), 9804-9828.

Fan, Y., Yang, J., Duan, A., & Li, X. (2021). Pectin/sodium alginate/xanthan gum edible composite films as the fresh-cut package. International Journal of Biological Macromolecules, 181, 1003-1009.

Fernández-Marín, R., Fernandes, S. C., Sánchez, M. Á. A., & Labidi, J. (2022). Halochromic and antioxidant capacity of smart films of chitosan/chitin nanocrystals with curcuma oil and anthocyanins. Food Hydrocolloids, 123, 107119.

Gadkari, R. R., Suwalka, S., Yogi, M. R., Ali, W., Das, A., & Alagirusamy, R. (2019). Green synthesis of chitosan-cinnamaldehyde cross-linked nanoparticles: Characterization and antibacterial activity. Carbohydrate Polymers, 226, 115298.

Ghaderi, J., Hosseini, S. F., Keyvani, N., & Gómez-Guillén, M. C. (2019). Polymer blending effects on the physicochemical and structural features of the chitosan/poly (vinyl alcohol)/fish gelatin ternary biodegradable films. Food Hydrocolloids, 95, 122-132.

Haghighi, H., Biard, S., Bigi, F., De Leo, R., Bedin, E., Pfeifer, F., . . . Pulvirenti, A. (2019). Comprehensive characterization of active chitosan-gelatin blend films enriched with different essential oils. Food Hydrocolloids, 95, 33-42.

Hajji, S., Chaker, A., Jridi, M., Maalej, H., Jellouli, K., Boufi, S., & Nasri, M. (2016). Structural analysis, and antioxidant and antibacterial properties of chitosan-poly (vinyl alcohol) biodegradable films. Environmental Science and Pollution Research, 23(15), 15310-15320.

Hosseini, S. F., Ghaderi, J., & Gómez-Guillén, M. C. (2021). trans-Cinnamaldehyde-doped quadripartite biopolymeric films: Rheological behavior of film-forming solutions and biofunctional performance of films. Food Hydrocolloids, 112, 106339.

Hosseini, S. F., Ghaderi, J., & Gómez-Guillén, M. C. (2022). Tailoring physico-mechanical and antimicrobial/antioxidant properties of biopolymeric films by cinnamaldehyde-loaded chitosan nanoparticles and their application in packaging of fresh rainbow trout fillets. Food Hydrocolloids, 124, 107249.

Hosseini, S. F., Kaveh, F., & Schmid, M. (2022). Facile fabrication of transparent high-barrier poly (lactic acid)-based bilayer films with antioxidant/antimicrobial performances. Food Chemistry, 384, 132540.

Hosseini, S. F., Rezaei, M., Zandi, M., & Farahmandghavi, F. (2015). Bio-based composite edible films containing Origanum vulgare L. essential oil. Industrial Crops and products, 67, 403-413.

Huang, C., Liao, H., Ma, X., Xiao, M., Liu, X., Gong, S., . . . Zhou, X. (2021). Adsorption performance of chitosan Schiff base towards anionic dyes: Electrostatic interaction effects. Chemical Physics Letters, 780, 138958.

Jin, X., Wang, J., & Bai, J. (2009). Synthesis and antimicrobial activity of the Schiff base from chitosan and citral. Carbohydrate Research, 344(6), 825-829.

Kaur, K., Jindal, R., Maiti, M., & Mahajan, S. (2019). Studies on the properties and biodegradability of PVA/Trapa natans starch (N-st) composite films and PVA/N-st-g-poly (EMA) composite films. International Journal of Biological Macromolecules, 123, 826-836.

Tran, V. T., Kingwascharapong, P., Tanaka, F., & Tanaka, F. (2021). Effect of edible coatings developed from chitosan incorporated with tea seed oil on Japanese pear. Scientia Horticulturae, 288, 110314.

Kong, M., Chen, X. G., Xing, K., & Park, H. J. (2010). Antimicrobial properties of chitosan and mode of action: a state of the art review. International journal of food microbiology, 144(1), 51-63.

Ksouda, G., Sellimi, S., Merlier, F., Falcimaigne-Cordin, A., Thomasset, B., Nasri, M., & Hajji, M. (2019). Composition, antibacterial and antioxidant activities of Pimpinella saxifraga essential oil and application to cheese preservation as coating additive. Food Chemistry, 288, 47-56.

Kuai, L., Liu, F., Ma, Y., Goff, H. D., & Zhong, F. (2020). Regulation of nano-encapsulated tea polyphenol release from gelatin films with different Bloom values. Food Hydrocolloids, 108, 106045.

Lee, M. H., Kim, S. Y., & Park, H. J. (2018). Effect of halloysite nanoclay on the physical, mechanical, and antioxidant properties of chitosan films incorporated with clove essential oil. Food Hydrocolloids, 84, 58-67.

Lević, S., Obradović, N., Pavlović, V., Isailović, B., Kostić, I., Mitrić, M., . . . Nedović, V. (2014). Thermal, morphological, and mechanical properties of ethyl vanillin immobilized in polyvinyl alcohol by electrospinning process. Journal of Thermal Analysis and Calorimetry, 118, 661-668.

Lewandowska, K. (2009). Miscibility and thermal stability of poly (vinyl alcohol)/chitosan mixtures. Thermochimica Acta, 493(1-2), 42-48.

Lund, B. M., Baird-Parker, T. C., & Gould, G. W. (2000). The microbiological safety and quality of food: Springer.

Luo, Y., Zhang, B., Whent, M., Yu, L. L., & Wang, Q. (2011). Preparation and characterization of zein/chitosan complex for encapsulation of α-tocopherol, and its in vitro controlled release study. Colloids and Surfaces B: Biointerfaces, 85(2), 145-152.

Martins, J. T., Cerqueira, M. A., & Vicente, A. A. (2012). Influence of α-tocopherol on physicochemical properties of chitosan-based films. Food Hydrocolloids, 27(1), 220-227.

Mohammadi, A., Hashemi, M., & Hosseini, S. M. (2015). Nanoencapsulation of Zataria multiflora essential oil preparation and characterization with enhanced antifungal activity for controlling Botrytis cinerea, the causal agent of gray mould disease. Innovative food science & emerging technologies, 28, 73-80.

Narasagoudr, S. S., Hegde, V. G., Chougale, R. B., Masti, S. P., Vootla, S., & Malabadi, R. B. (2020). Physico-chemical and functional properties of rutin induced chitosan/poly (vinyl alcohol) bioactive films for food packaging applications. Food Hydrocolloids, 109, 106096.

Narasagoudr, S. S., Hegde, V. G., Vanjeri, V. N., Chougale, R. B., & Masti, S. P. (2020). Ethyl vanillin incorporated chitosan/poly (vinyl alcohol) active films for food packaging applications. Carbohydrate Polymers, 236, 116049.

Ojagh, S. M., Rezaei, M., Razavi, S. H., & Hosseini, S. M. H. (2010). Development and evaluation of a novel biodegradable film made from chitosan and cinnamon essential oil with low affinity toward water. Food Chemistry, 122(1), 161-166.

Osugi, N., Dong, T., Hexig, B., & Inoue, Y. (2010). Generation and characterization of compositional gradient structure in the biodegradable chitosan/poly (ethylene oxide) blend. Journal of Applied Polymer Science, 104(5), 2939-2946.

Peng, Y., & Li, Y. (2014). Combined effects of two kinds of essential oils on physical, mechanical and structural properties of chitosan films. Food Hydrocolloids, 36, 287-293.

Perumal, A. B., Huang, L., Nambiar, R. B., He, Y., Li, X., & Sellamuthu, P. S. (2022). Application of essential oils in packaging films for the preservation of fruits and vegetables: A review. Food Chemistry, 375, 131810.

Priyadarshi, R., Kumar, B., Deeba, F., Kulshreshtha, A., & Negi, Y. S. (2018). Chitosan films incorporated with Apricot (Prunus armeniaca) kernel essential oil as active food packaging material. Food Hydrocolloids, 85, 158-166.

Queiroz, M. F., Teodosio Melo, K. R., Sabry, D. A., Sassaki, G. L., & Rocha, H. A. O. (2014). Does the use of chitosan contribute to oxalate kidney stone formation? Marine drugs, 13(1), 141-158.

Sajjan, A. M., Naik, M. L., Kulkarni, A. S., Rudgi, U. F.-E.-H., Ashwini, M., Shirnalli, G. G., . . . Kalahal, P. B. (2020). Preparation and characterization of PVA-Ge/PEG-400 biodegradable plastic blend films for packaging applications. Chemical Data Collections, 26, 100338.

Sánchez-González, L., Vargas, M., González-Martínez, C., Chiralt, A., & Cháfer, M. (2009). Characterization of edible films based on hydroxypropylmethylcellulose and tea tree essential oil. Food Hydrocolloids, 23(8), 2102-2109.

Sharma, S., Barman, K., & Siddiqui, M. W. (2016). Chitosan: Properties and roles in postharvest quality preservation of horticultural crops. In Eco-friendly technology for postharvest produce quality, 269-296.

Shen, Z., & Kamdem, D. P. (2015). Development and characterization of biodegradable chitosan films containing two essential oils. International Journal of Biological Macromolecules, 74, 289-296.

Shojaee-Aliabadi, S., Hosseini, H., Mohammadifar, M. A., Mohammadi, A., Ghasemlou, M., Ojagh, S. M., . . . Khaksar, R. (2013). Characterization of antioxidant-antimicrobial κ-carrageenan films containing Satureja hortensis essential oil. International Journal of Biological Macromolecules, 52, 116-124.

Sun, T., Zhou, D., Mao, F., & Zhu, Y. (2007). Preparation of low-molecular-weight carboxymethyl chitosan and their superoxide anion scavenging activity. European polymer journal, 43(2), 652-656.

Sun, X., Narciso, J., Wang, Z., Ference, C., Bai, J., & Zhou, K. (2014). Effects of chitosan-essential oil coatings on safety and quality of fresh blueberries. Journal of Food Science, 79(5), M955-M960.

Suzuki, T., Fujikura, K., Higashiyama, T., & Takata, K. (1997). DNA staining for fluorescence and laser confocal microscopy. Journal of Histochemistry & Cytochemistry, 45(1), 49-53.

Tomadoni, B., Ponce, A., Pereda, M., & Ansorena, M. R. (2019). Vanillin as a natural cross-linking agent in chitosan-based films: Optimizing formulation by response surface methodology. Polymer Testing, 78, 105935.

Wang, L., Liu, F., Jiang, Y., Chai, Z., Li, P., Cheng, Y., . . . Leng, X. (2011). Synergistic antimicrobial activities of natural essential oils with chitosan films. Journal of Agricultural and Food Chemistry, 59(23), 12411-12419.

Wardana, A. A., Kingwascharapong, P., Wigati, L. P., Tanaka, F., & Tanaka, F. (2022). The antifungal effect against Penicillium italicum and characterization of fruit coating from

chitosan/ZnO nanoparticle/Indonesian sandalwood essential oil composites. Food Packaging and Shelf Life, 32, 100849.

Wardana, A. A., Koga, A., Tanaka, F., & Tanaka, F. (2021). Antifungal features and properties of chitosan/sandalwood oil Pickering emulsion coating stabilized by appropriate cellulose nanofiber dosage for fresh fruit application. Scientific reports, 11(1), 1-15.

Wardana, A. A., Tanaka, F., & Tanaka, F. (2021). Inhibition of Botrytis cinerea by alginate/cajuput essential oil and the composite's surface properties as potential antifungal coating. Materials Today: Proceedings, 45, 5263-5268.

Wigati, L. P., Wardana, A. A., Tanaka, F., & Tanaka, F. (2022). Edible film of native jicama starch, agarwood Aetoxylon Bouya essential oil and calcium propionate: Processing, mechanical, thermal properties and structure. International Journal of Biological Macromolecules.

Wigati, L. P., Wardana, A. A., Tanaka, F., & Tanaka, F. (2023). Application of pregelatinized corn starch and basil essential oil edible coating with cellulose nanofiber as Pickering emulsion agent to prevent quality-quantity loss of mandarin orange. Food Packaging and Shelf Life, 35, 101010.

Xing, Y., Xu, Q., Yang, S. X., Chen, C., Tang, Y., Sun, S., . . . Li, X. (2016). Preservation mechanism of chitosan-based coating with cinnamon oil for fruits storage based on sensor data. Sensors, 16(7), 1111.

Xu, T., Gao, C., Feng, X., Huang, M., Yang, Y., Shen, X., & Tang, X. (2019). Cinnamon and clove essential oils to improve physical, thermal and antimicrobial properties of chitosan-gum arabic polyelectrolyte complexed films. Carbohydrate Polymers, 217, 116-125.

Xue, F., Gu, Y., Wang, Y., Li, C., & Adhikari, B. (2019). Encapsulation of essential oil in emulsion based edible films prepared by soy protein isolate-gum acacia conjugates. Food Hydrocolloids, 96, 178-189.

Yan, X., Dong, T., Yun, X., Liu, B., & Meng, J. (2022). Enhancing the functionality of cross-linked chitosan coating on vibration damaged Nanguo pears. Lwt, 162, 113454.

Yi, G., Yin, C., Lao, Y., Shi, Z., He, X., Wu, J., . . . Gong, L. (2022). Antibacterial and antitumor activities of chitosan/polyvinyl alcohol films containing microemulsion of papaya seed essential oil. Materials Today Communications, 31, 103475.

Yildirim, S., Röcker, B., Pettersen, M. K., Nilsen-Nygaard, J., Ayhan, Z., Rutkaite, R., . . . Coma, V. (2018). Active packaging applications for food. Comprehensive Reviews in Food Science and Food Safety, 17(1), 165-199.

Zhang, L., Liu, Z., Sun, Y., Wang, X., & Li, L. (2020). Effect of α-tocopherol antioxidant on rheological and physicochemical properties of chitosan/zein edible films. Lwt, 118, 108799.

Zhang, X., Lian, H., Shi, J., Meng, W., & Peng, Y. (2020). Plant extracts such as pine nut shell, peanut shell and jujube leaf improved the antioxidant ability and gas permeability of chitosan films. International Journal of Biological Macromolecules, 148, 1242-1250.

Zhang, X., Liu, D., Jin, T. Z., Chen, W., He, Q., Zou, Z., . . . Guo, M. (2021). Preparation and characterization of gellan gum-chitosan polyelectrolyte complex films with the incorporation of thyme essential oil nanoemulsion. Food Hydrocolloids, 114, 106570.

Zhao, R., Chen, J., Yu, S., Niu, R., Yang, Z., Wang, H., . . . Wang, W. (2023). Active chitosan/gum Arabic-based emulsion films reinforced with thyme oil encapsulating blood orange anthocyanins: Improving multi-functionality. Food Hydrocolloids, 134, 108094.

Zhou, Y., Zhu, X., Zhang, C., Chai, W. S., Chew, K. W., Du, A., & Show, P. L. (2020). Characterization of whey protein isolate and pectin composite film catalyzed by small laccase from Streptomyces coelicolor. Environmental Technology & Innovation, 19, 100999.

CHAPTER 4

Water barrier coating of chitosan/poly (vinyl alcohol)/*trans*-cinnamaldehyde regulated postharvest quality and reactive oxygen species metabolism of 'Frutica' tomato (*Solanum lycopersicum L.*)

4.1. Introduction

'Frutica' tomato (*Solanum lycopersicum L.*) is an important source of vitamin C, lycopene, and β-carotene, and possesses a high antioxidant capacity, thereby providing numerous health benefits. However, the fruit is susceptible to tissue injury owing to excessive vibration during transportation and distribution (Wu & Wang, 2014). Mechanical damage caused by external forces can expose postharvest fruit to up to 400 times the risk of microbial infection compared to undamaged. (Fadiji *et al.,* 2016). Furthermore, mechanical injuries result in detrimental structural characteristics of fresh produce, leading to weight loss, increased respiration rate, wrinkled skin, metabolism, excessive accumulation of ROS, and eventual senescence and rot (Al-Dairi *et al.,* 2022). Thus, there is an urgent need for a preservation technology to delay deterioration and extend the storage period of postharvest products.

ROS are generated through the process of aerobic respiration and play a significant role in causing oxidative harm to macromolecules; these include superoxide anion radicals (O_2^-) and hydrogen peroxide (H_2O_2) (Piechowiak et al., 2020). ROS-scavenging systems can be divided into enzymatic and non-enzymatic components. In the enzymatic system, superoxide dismutase (SOD), catalase (CAT), and peroxidase (POD) directly eliminate excess ROS from fruit and vegetables to maintain homeostasis (Cao *et al.,* 2021; Zhang *et al.,* 2021). Ascorbic acid, glutathione, and phenolic compounds exhibit potent antioxidant properties in non-enzymatic systems. *(* Zhang *et al.,* 2022). Lo'Ay et al. found that CS/PVA coating, as a biosafety preservation coating, reduced the water loss, gas exchange and oxidation reaction rate of Superior seedless' grapes (Lo'Ay, Dawood, 2017). Carvalho et al. reported that CS-CIN coating improved the quality of fresh cut cantaloupe stored at 4°C for 20 days by inhibiting oxidative stress, while the CIN acted as a free radical scavenger and enzyme inhibitor, reducing free radical production and biofilm disintegration

(Carvalho et al., 2016). Based on these findings, it could be inferred that the CS/PVA or CS/CIN combination holds significant potential for senescence and maintenance of fruit quality caused by ROS overproduction. However, studies on ternary bioactive films for preservation and ROS in postharvest products remain limited.

In previous studies, we have observed that CS/PVA/CIN ternary films have excellent mechanical, antimicrobial, and antioxidant properties. In addition, CS, either alone or in combination with PVA or CIN, has been studied in postharvest fruit and vegetables. However, there are no data on their effect, alone or in combination with each other, on the quality and ROS scavenging capacity of 'Frutica' tomato (*S. lycopersicum*). Therefore, this study aimed to prolong the freshness of fresh tomatoes by preparing water barrier coatings and investigating their impact on the postharvest physiological and nutritional qualities of tomatoes. At the same time, the microstructures and water-blocking properties of the four different coatings and alterations in the nutritional quality of tomato, variations in the metabolism of ROS and the mechanisms were investigated under low temperature conditions (8 ± 2 °C).

4.2. Materials and methods

4.2.1. Coating and film preparation

1) For the 1.5% CS (w/v) solution, 1.5 g of CS was dissolved in 100 mL of slightly acidic water containing 1% acetic acid, heated at 80 °C for 4 h until complete dissolution, and then left to stand overnight before being filtered for impurities.

2) For the CS/PVA solution, PVA solution was obtained by dissolving 2 g of PVA powder in 100 mL of distilled water and heating it at 85 °C for 3 h until clear. The CS and PVA solutions blended well. After adding glycerol (0.3 g/g), the mixture was agitated for 30 min at 40 °C.

3) For CS/PVA/CIN, add 0.5 % CIN (v/v) and Tween 80 (0.1%) to the CS/PVA mixture, homogenized at 10,000 ×g for 5 min. The emulsion was degassed for 15 min in a vacuum-dehydrated oven to eliminate foam. It was then cast on a polystyrene petri dish and desiccated at room temperature (32 ± 2 °C; summer) for 48 h continuously. Continuous, homogeneous, transparent, and bubble-free films were obtained. Below are the details and labels for the samples in each respective group.

Control: distilled water;

CS: 1.5% CS (w/v);

CS/PVA: 1.5% CS (w/v) + 2% PVA (w/v);

CS/CIN: 1.5% CS (w/v) + 0.5% CIN (w/v);

CS/PVA/CIN: 1.5% CS (w/v) + 2% PVA (w/v) + 0.5% CIN (v/v).

4.2.2. Postharvest treatment of composite coating

'Frutica' tomatoes (*S. lycopersicum*) were obtained from the JA Fukuoka Yame Agriculture Store in Yame City. Harvested tomatoes (red stage) were transported to the laboratory, where they were inspected for uniformity in size, ripeness, and the absence of mechanical or visible defects.

The coating was made using the steps specified in Section 2.2, and the tomatoes were subjected to five different treatments: control (not coated), CS, CS/PVA, CS/CIN, and CS/PVA/CIN. Each group of tomatoes was immersed in its respective solution for 30 s. After coating, the tomatoes were placed vertically in perforated receptacles and fan-dried at room temperature. All the treated tomatoes were stored at 8 ± 2 °C and 75% RH for 30 d, and biochemical parameters were conducted and analyzed at 5 d intervals.

4.2.3 Sensory evaluation

Twelve evaluators, balanced in terms of gender, participated in the study, each with expertise in identifying quality attributes. A 10-point hedonic scale (10: excellent; 5: fair; 1: extremely bad) was used to assess the appearance, color, flavor, firmness, and overall quality. Changes in tomato appearance were photographed and recorded every 5 d.

4.2.4. Color

The color of tomatoes was measured using a color difference meter (Color reader CR-20, Japan) at room temperature. A white standard color plate (L^* = 94.2) was used for calibration before the measurement. The measurements were replicated three times on the surface of each fruit.

4.2.5. Weight loss

Weight loss: The reduction in sample weight was determined through weighing. The percentage of weight loss is then expressed using Eq:

$$Weight\ loss\ (\%) = \frac{\text{initial weight} - daily\ \text{weight}}{\text{initial weight}} \times 100$$

4.2.6. Firmness

A texture analyzer (RE-3305, YAMADEN Co. Ltd., Tokyo, Japan) with a with a 3 mm diameter needle probe was utilized to penetrate six equatorial locations on the tomatoes.

4.2.7. Total soluble solids

Total soluble solids (TSS): the TSS content of tomatoes was determined using a Brix moisture meter (ATAGO PAL-BX|ACID121, Co. Ltd., Japan) at 25 °C. The averages were expressed as percentages (%).

4.2.8. Titratable acid

Titratable acid (TA): the TA of the tomato samples was determined utilizing the titration method adopted by (Kumar, Neeraj, Pratibha, & Trajkovska Petkoska, 2021). Twenty milliliters of ground and filtered tomato juice were titrated with 0.01 N NaOH solution. As an indicator, 1% phenolphthalein was used to designate titration endpoints. Three replicates for each treatment group and TA as citric acid (%) were measured using Eq:

$$Titratable\ acid\ (\%) = \frac{V_{NaOH}(mL) \times C_{NaOH}(N) \times 0.064 \times 100}{10g}$$

where 0.064 is the conversion factor for citric acid.

4.2.9. Malondialdehyde

The malondialdehyde (MDA) content was determined using the method described by (Carvalho et al., 2016) with minor modifications. Tomatoes (1 g) were ground and homogenized in 10 mL of 100 g L^{-1} trichloroacetic acid (TCA) solution and then centrifuged at 2300 × g for 20 min at 4 °C. After extraction, 2 mL of the supernatant was combined with 2 mL of 0.67% (w/w) thiobarbituric acid (TBA), heated at 95 °C for 20 min, and then chilled to room temperature, before centrifuging again (2300 × g, 20 min, 4 °C). The absorbance of the supernatant was measured at 450, 532 and 600 nm. The MDA content was determined using Eq:

$$MDA\ content\ (\frac{\mu mol}{Kg}) = \frac{(6.45 \times (OD_{532} - OD_{600}) - 0.56 \times OD_{450}) \times V}{V_S \times m}$$

where OD_{450}, OD_{532} and OD_{600} represent the absorbance values at 450 nm, 532 nm and 600 nm, respectively; *V* represents the total volume of the extracted solution (mL); *Vs* is the volume of the extracted sample solution at the time of determination (mL); and *m* is the weight of the sample (kg).

4.2.10. Lipoxygenase

Lipoxygenase (LOX) content was determined according to the method described by (Zhao, Zhu, Hou, Wang, & Li, 2020). Briefly, 5.0 g of fruit tissue was homogenized with 5.0 ml of pre-cooled extraction buffer (containing 0.1 mol L^{-1} sodium acetate buffer (pH 5.5), 4% polyvinylpolypyrrolidone (PVPP), and 1% Triton X-100). The homogenized solution was centrifuged at 2300 × g for 30 min at 4 °C. The reaction included 2.75 mL of 0.1 mol L^{-1} sodium acetate buffer (pH 5.5) and 50 μL of 0.1 mol L^{-1} linoleic acid sodium salt, which was incubated at 30 °C for 10 min, and then added into 200 μL diluted enzyme extraction solution. LOX activity was measured by the increase in absorbance at 234 nm and expressed in units per gram (U kg^{-1}), where one enzymatic activity unit is defined as a 0.01 increase in absorbance per minute

4.2.11. Hydrogen peroxide

The hydrogen peroxide (H_2O_2) in tomatoes was evaluated using the method recommended by (Z. Li et al., 2022). Briefly, fresh tissues (5 g) were mixed with 5.0 mL of pre-cooled acetone (4 °C), homogenized in ice, and centrifuged at 12000 × g for 20 min. One milliliter of the supernatant was thoroughly mixed with 0.1 mL of 10% (w/v) titanium sulfate, 1 mL of pre-cooled acetone, and 0.2 mL of concentrated ammonia, followed by centrifugation at 12000 × g for 15 min at 4 °C. The precipitate was repeatedly rinsed with pre-cooled acetone until the pigment was removed. Then, 3 mL of H_2SO_4 (2 mol L^{-1}) was added to the washed precipitate. After dissolution, the absorbance was measured at 412 nm and the result was expressed as micromoles per gram (μmol kg^{-1}).

4.2.12. Superoxide anion

The amount of superoxide anion (O_2^-) was measured using a previously reported method (Zhou et al., 2014). First, fresh samples (5 g) were mixed with 5 mL of sodium phosphate buffer

solution (50 mM; pH 7.8), comprising 1.0 mM ethylenediamine tetraacetic acid (EDTA), 0.3% (v/v) Triton X-100, and 2% (w/v%) polyvinyl-pyrrolidone (PVP). The mixture was then centrifuged at 12000 × g for 20 min at 4 °C. One milliliter of the supernatant was mixed with 1 mL of sodium phosphate buffer (50 mM, pH 7.8) and 1 mL of hydroxylammonium chloride (1 mM), shaken well, and incubated at 25 °C for 1 h. Then, 1 mL of 17 mM 4-aminobenzenesulfonic acid and 1 mL of 7 mM a-naphthylamine were added to the mixture, and the color development reaction was carried out at 25 °C for 20 min. Finally, the absorbance was recorded at 530 nm without holding for 1 h as the control group. O_2^- production was expressed as nanomoles per gram per minute (nmol min^{-1} kg^{-1}).

4.2.13. Peroxidases activity

The peroxidases (POD) activity was measured according to the method described by (Wang *et al.,* 2023). Enzyme solution was prepared by homogenizing 3.0 g of Fresh tomato tissue with 3.0 ml of extraction buffer, containing 1 mmol polyethylene glycol (PEG_{6000}), 4% PVPP, 1% Triton X-100, and 0.1 mol L^{-1} sodium acetate buffer (pH 5.5). The homogenized mixture was ground under ice-bath cooling and subsequently centrifuged at 2300 × g for 30 min at 4 °C. For POD determination, the reaction system included 3.0 mL of 25 mmol L^{-1} guaiacol solution, 0.5 mL of supernatant, and 0.2 mL of 0.5 mol L^{-1} H_2O_2 solution. The activity and absorbance at 470 nm (POD) were recorded for 3 min at 30-s intervals, with distilled water as a blank reference. One unit of POD activity was defined as an increase in POD activity of 0.1 in the absorbance at 470 nm per minute (U kg^{-1}).

4.2.14. Catalase activity

The catalase (CAT) activity was measured using the method from (Jiang *et al.,* 2019) with slight modifications. To extract the enzymes, 3.0 g of sample tissue was homogenized with a mortar and pestle in 3.0 mL of cooled 0.1 mol L^{-1} sodium phosphate buffer (pH 7.5), containing 5 mmol L^{-1} DTT and 5% (w/w) PVPP, and then the mixture was centrifuged at 2300 × g for 30 min at 4 °C. The reaction included 2.9 mL of 20 mmol L^{-1} H_2O_2 solution and 100 µL of supernatant. One unit of CAT activity was defined as a 0.01 decrease in OD_{240} per second (U kg^{-1}).

4.2.15. Superoxide dismutase activity

The superoxide dismutase (SOD) activity was based on the inhibition of photochemical reduction using the nitroblue tetrazolium (NBT) method. Briefly, 5 g of flesh tissue was homogenized with 5.0 mL of cooled 100 mmol L^{-1} sodium phosphate buffer (pH 7.8) including 7 mmol L^{-1} DTT and 5% (w/w) PVP, before centrifuging at 2300 × g for 30 min. The SOD activity was determined as described by (Meng et al., 2022). One unit of activity was calculated as a 50% reduction in SOD inhibition by NBT (U kg^{-1}).

4.2.16. Ascorbate peroxidase activity

The ascorbate peroxidase (APX) activity was assayed as described by (Ma, Fu, Hussain, Huang, & Zhu, 2019). To acquire the enzyme solution, tomatoes (5 g) were homogenized in 5 mL of pre-cooled phosphate buffer (pH 7.5) containing 2% PVPP (w/v), 0.1 mol L^{-1} EDTA, and 1 mmol L^{-1} ascorbic acid. The reaction system was assembled using 0.1 mL of enzyme extract, 0.30 mL of 2 mmol L^{-1} H_2O_2 solution and 2.6 mL of 50 mmol L^{-1} phosphate buffer (pH 7.5) containing 0.1 mmol L^{-1} EDTA and 0.5 mmol L^{-1} ascorbic acid. Absorbance at 290 nm was recorded at 30-s

intervals for 3 min. One unit of APX activity was defined as a decrease of 0.01 in absorbance per minute (U kg^{-1}).

4.2.17. Glutathione reductase activity

Glutathione reductase (GR) activity was measured using the method from (Meng *et al.,* 2022) with slight modifications. In brief, 5 g of flesh tissue was homogenized with 5 mL of pre-cooled phosphate buffer (pH 7.5; 1 mmol L^{-1} EDTA) and subsequently centrifuged at 2300 × g for 30 min at 4 °C. Then, 0.2 mL of supernatant was mixed with 2.7 mL of 25 mmol L^{-1} phosphate buffer solution (pH 7.5, 1 mmol L^{-1} EDTA, and 5 mmol L^{-1} oxidized glutathione), and 0.4 mL of 4 mmol L^{-1} NADPH. Absorbance of the resulting mixture was measured at 340 nm, the activity of the enzymes was calculated and presented as (U kg^{-1}).

4.2.18. Statistical analysis

All experiments were performed in triplicate and statistically analyzed using SPSS 26.0. Data were analyzed using analysis of variance (ANOVA) and differences were considered significant at $P < 0.05$. Principal component analysis (PCA) and correlation analysis (GraphPad Prism 9) were used to explore the intricate connections between the qualitative attributes and physicochemical properties of the coated fruit.

4.3. Result and discussion

4.3.1. Food preservation after coating treatments

Figure 4.1 depicts the sensory characteristics of tomatoes in all treatment groups over 30 d at low temperatures. The yellow circles represent wrinkled tomatoes. At the beginning of storage, the tomato skin was glossy and smooth, indicating freshness and excellent texture. At the 15th day of storage, folds and pits were visible on the surface and inside the damaged parts of control tomatoes.

In the other coated treatment groups, there were no discernible changes in the damaged areas, and the epidermis and sliced portions of the tomatoes retained their color and texture. As time progressed, the appearance of all tomatoes began to deteriorate, with multiple pits appearing in the control tomatoes on day 25, where the sensory score was only 2 points, which is not accepted by the market and consumers. In the coated groups, substantial wrinkles due to water loss were visible and the score decreased. The cut surface of the control tomatoes had collapsed as a result of severe water loss, and 'running water' was observed by the 30 d. Notably, bioactive coatings with CIN (CS/CIN and CS/PVA/CIN treatment groups) did not result in substantial surface or slice changes in tomatoes, indicating that their storage quality was superior to that of the other groups (Fig. 4.2A). This suggests that the water-barrier coating can delay the rate of water loss, reduce wrinkling, and be more consumer-friendly.

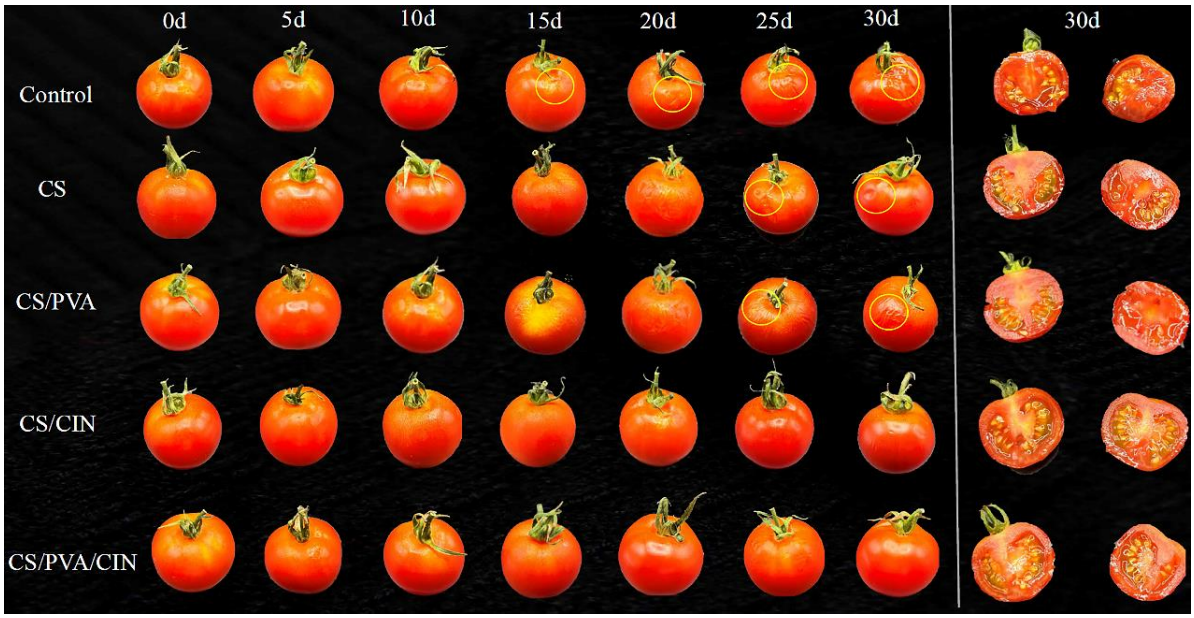

Figure 4.1. Sensory evaluation of tomatoes during the cold temperature.

4.3.2. Color

Assessing the color is paramount in evaluating the quality of fruit. The initial *L** ranged from 49.76 ± 1.50 to 48.66 ± 1.49 for all treatment groups at the beginning of storage, as shown in Fig. 4.2B. The greatest decrease in *L** was observed in the control group of fruit. Concerning *a** values, all treatment groups showed an increasing trend throughout the storage period (Fig. 4.2C). For the treatment group coated with CS/PVA/CIN, the *a** value (30.6 ± 0.50) increased slowly and was only 65% of that of the control group (44.9 ± 0.57) at the end of the storage period. In addition, the *b** value of the control sample was only 9.46 ± 0.53, while CS/CIN and CS/CIN/PVA coating groups reached around 17.63 at day 30 (Fig. 4.2D), indicating that the composite coating film containing CIN EOs had an effect on the color change of tomato during refrigerated preservation and can improve consumer acceptance.

The freshness of stored horticultural produce is primarily conveyed by its outward appearance and color. Tomatoes are prone to surface-water loss and wrinkling. Consequently, the *L** value (brightness) decreased during the storage. In this study, the higher *L** and lower a* values in the coated fruit can be due to the development of a protective layer of CIN, which inhibited POD enzyme activity and delayed changes in the color of tomatoes. Similar results have been reported for edible coatings, which maintain the attractive appearance of tomatoes (Pholsin *et al.,* 2024).

4.3.3. Weight loss

As shown in Fig. 4.2E, the weight loss of all the samples gradually increased throughout the storage period. The control group demonstrated a considerable weight reduction, reaching around 6.7% by the 30 d. However, all coating treatments delayed the weight loss of tomatoes, with the CS/PVA/CIN coating proving to be the most effective. The weight loss for the bioactive coating treatment group was only 4.57% on the 30 d. Moreover, the weight loss of samples with CS coating

(5.69%) was close to that of samples with CS/PVA coating after 30 d (5.92%), a correspondence that is visually evident in Fig. 4.1.

Horticultural crops are considered living entities because their metabolic processes persist post-harvest, resulting in weight loss owing to desiccation (Yadav et al., 2022). As expected, the CS/PVA/CIN coating exhibited significantly lower weight loss than the control group, which may be attributed to the addition of hydrophobic CIN, which increased the water-barrier properties of the film and limited the evaporation of water from the fruit surface, thus preventing surface shriveling and wrinkling of the fruit during postharvest storage. Therefore, the CS/CIN and CS/PVA/CIN treatment groups exhibited more favorable appearance during storage (Fig. 4.1). In contrast, the control and CS/PVA groups displayed greater weight loss than the other treatment groups. The control group exhibited rapid water loss due to exposure to air, whereas both CS and PVA were hydrophilic matrices with relatively high-water vapor permeability values. A previous study showed that coating with CIN-CS effectively reduced the water loss of fresh navel orange fruit while maintaining a high commodity value owing to its dense structure (Gao et al., 2018). Yan et al. (2022) reported that CS cross-linked coating reduced the weight loss of vibration-damaged ‘Nanguo’ pear. In addition, tomatoes exhibited slower weight loss during storage than in several previous studies (Aragüez et al., 2020; Mondal, Goud, Katiyar ., 2022), possibly because the tomatoes were exposed to lower temperatures in this study.

4.3.4. Firmness

As depicted in Fig. 4.2F, the firmness of the control group tomatoes rapidly dropped as the storage period progressed and reached 0 N by the end of the storage period. Nevertheless, the decrease rate in fruit was much slower in coated groups in comparison with that in control throughout the storage. The firmness of tomatoes coated with CS/PVA/CIN was preserved even

after 25 d (above 6 N), indicating that the water barrier coating group effectively preserved the firmness of fruit.

Fruit firmness plays a pivotal role in consumer acceptability (Wang *et al.,* 2023). CIN functions as both a scavenger of free radicals and an inhibitor of enzymes, thereby reducing the activity of cell wall hydrolases (Subash-Babu *et al.,* 2014). As determined by (Carvalho *et al.,* 2016), a coating comprising 2% CS with 500 mg L^{-1} CIN maintained the firmness values and structural integrity of the cell wall in freshly cut cantaloupes. In this investigation, the impact of the coating on mitigating the decrease in the firmness of tomato fruit was primarily due to the regulatory effect of CIN. Furthermore, the water content of fruit affects both cell density and firmness. CIN can inhibit the loss of water from the fruit to a certain degree and preserve firmness.

4.3.5. Total soluble solids analysis

The TSS content of tomatoes in all the treatment groups increased throughout the storage duration (Fig. 4.2G). The TSS of the control group increased from 6.7% to 8.4% over 30 d, whereas that of the CS/PVA/CIN group remained around 7.0% throughout the entire storage period. Based on these observations, it was expected that the CIN coating could effectively control the TSS content of tomatoes during storage.

An increase in the TSS content occurs naturally during fruit maturation and senescence. This was due to the hydrolysis of insoluble polysaccharides (starch) into monosaccharides. Moreover, the flavor of the fruit becomes more pronounced as storage time increases, and the production of glucose during ripening provides sweetness to the fruit. The control treatment group experienced a rapid increase in TSS from 6.8% to 7.8% at 15 d due to the water loss that occurs during storage, resulting in a rapid increase in TSS. Numerous studies have validated this phenomenon (Yousuf, Wu, Siddiqui, 2021). Consequently, the sluggish increase in the coating group with CIN during the

storage period and the smaller increases in TSS indicate that the coating with EOs has a stronger water-blocking property, which is consistent with the water vapor and WCA results. Wigati reported a slow increase in the TSS of strawberries after coating them with yam bean starch incorporated with agarwood *Aetoxylon bouya* EO (Wigati, Wardana, Tanaka, Tanaka, 2023).

4.3.6. Titratable acid analysis

As shown in Fig. 4.2H, TA levels decreased gradually and significantly throughout the storage period in all treatment groups, with the control group showing the lowest TA (0.182%) at the end of storage and having deteriorated completely. However, the CS, CS/CIN, and CS/PVA/CIN coatings maintained better TA values throughout the storage period.

Harvested tomatoes are extremely sensitive to increases in respiration activity, as the organic acids in the fruit, particularly citric acid, are metabolized to provide intermediates for the tricarboxylic acid cycle during such increases (Li *et al.,* 2017). In our study, the observed deceleration in the utilization of organic acids process of the coated fruit, in contrast to that of the control fruit, suggests a notable influence of the coating materials. These materials play a crucial role in reducing the respiration rate by forming a semipermeable layer on the skin of tomato fruit. In particular, the CS/CIN and CS/CIN/PVA bioactive coatings hindered the oxygen transport, resulting in slower metabolic activity. In this study, we inferred that the inclusion of CIN could slow the reduction of TA in tomatoes by controlling the ripening rate and metabolic activity, owing to the availability of CIN with antioxidant and biologically active compounds

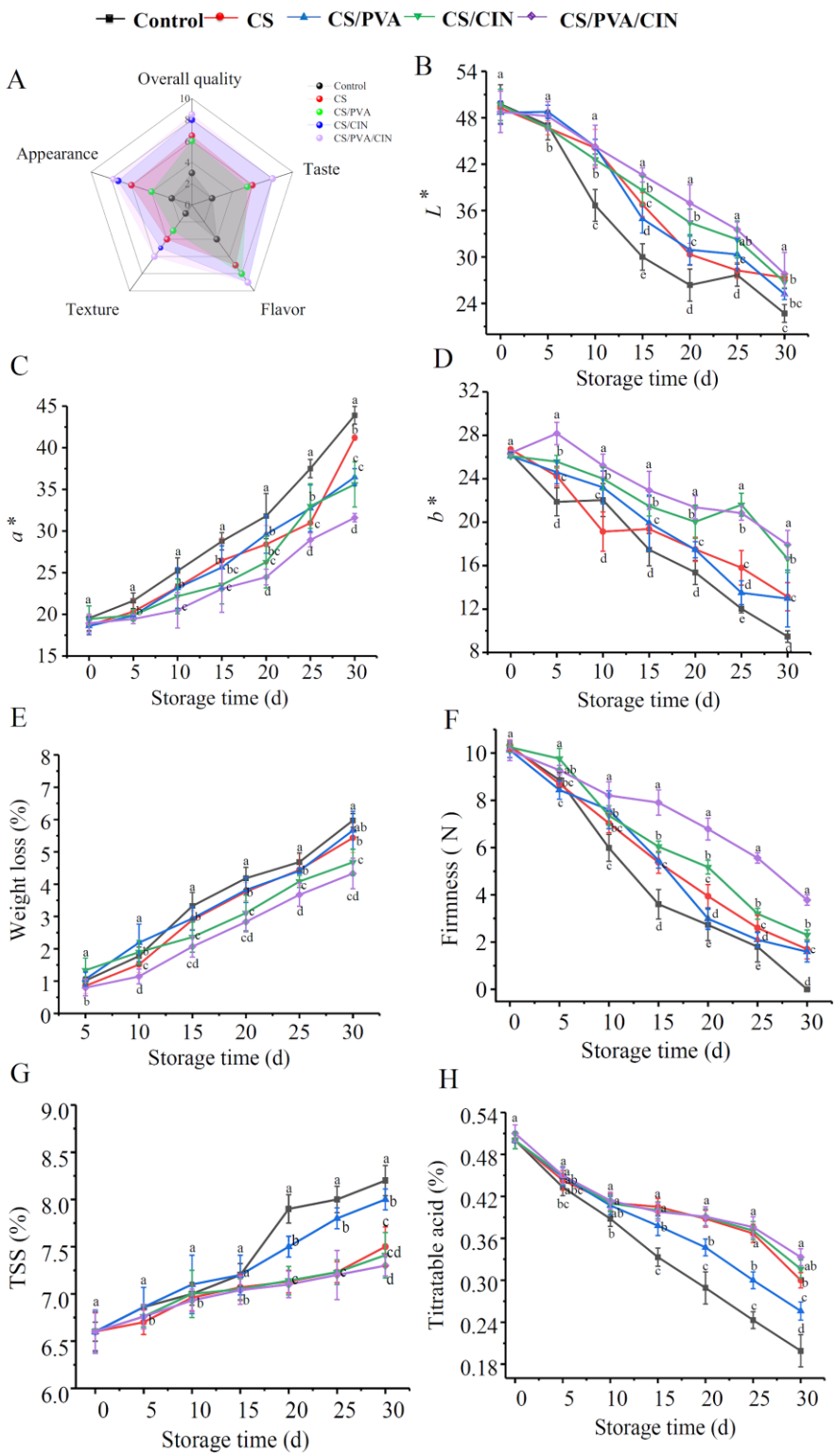

Figure 4.2. Sensory evaluation (A) at the end of the storage, L^* (B), a^* (C), b^* (D), weight loss (E), firmness (F), TSS (G), TA (H) value in tomatoes during the storage

4.3.7. Malondialdehyde analysis

Malondialdehyde (MDA) serves as a vital biomarker for assessing cell membrane lipid peroxidation during fruit storage. Alterations in MDA levels provide a direct reflection of the extent of lipid peroxidation occurring in fruit cell membranes. In general, high MDA content indicates high cell membrane permeability and severe senescence in fruit. As depicted in Fig. 4.3A, the MDA content of the control group showed a rapidly increasing trend with advanced storage, reaching 12.09 μmol kg^{-1} by the 30 d. However, the coated group exhibited a slow upward trend, especially after day 25, where the CS/PVA/CIN group had the lowest MDA content (7.97 μmol kg^{-1}).

4.3.8. Lipoxygenase analysis

Regarding LOX content, all treatment groups exhibited relatively low LOX levels in the initial 5 d (Fig. 4.3B). Nevertheless, the control samples exhibited a higher LOX content compared to the other coated groups after 5 d of storage. The LOX values of the pure CS samples were slightly higher than those of the CS/PVA group at the end of the storage period, suggesting that PVA had a weaker effect on the coated film. The CS/CIN and CS/PVA/CIN treatments showed a progressively slower trend after 25 d, with levels at only 42% of that observed in the control, resulting in lower LOX activity.

As shown in Fig. 4.3A and Fig. 4.3B, CS/PVA/CIN significantly inhibited LOX activity, reduced the MDA content, and prolonged fruit senescence in tomatoes. Changes in LOX activity were positively correlated with MDA content, as LOX has the capability to catalyze the transformation of unsaturated fatty acids into saturated fatty acid, thereby causing oxidative damage to cell membranes, increasing cell membrane permeability, and accelerating postharvest fruit senescence during fruit metabolism (Meng *et al.,* 2022).

4.3.9. Hydrogen peroxide analysis

Postharvest fruit and vegetables gradually senesce with storage time, leading to the accumulation of ROS and induction of physiological disorders of cellular metabolism, with the common phenomenon of higher H_2O_2 content and accelerated O_2^- levels. In this study, it was found that CIN-added films (CS/CIN and CS/PVA/CIN) helped to prevent oxidative damage to tomato cellular constituents, which may be because CIN acts as a free radical scavenger, neutralizing ROS to cope with the oxidative stress, thereby maintaining the integrity of tomato cellular membranes (Carvalho *et al.,* 2016).

As shown in Fig. 4.3 C, the H_2O_2 content showed an overall upward trend in all groups. Within the initial 5 d of storage, all groups displayed lower levels of H_2O_2 and there were no significant differences among the treated groups. For the control group, H_2O_2 content rapidly increased with the extension of storage, reaching 9.25 μmol kg^{-1} on 30 d. However, the H_2O_2 content in the CS/PVA/CIN groups was significantly lower ($P < 0.05$) than that in the other groups during the storage process.

4.3.10. Superoxide anion analysis

A similar trend is observed in the O_2^- generation rate, as illustrated in Fig. 4.3D; the control group exhibited a rapidly increasing trend, whereas that in the coated group increased slowly over the storage period. Twice as much ROS accumulated in the control group as in the CS/PVA/CIN group. In brief, the CS/PVA/CIN treatment effectively mitigated ROS accumulation and alleviated membrane damage during storage in comparison to the control group. Shao *et al.* found that the coating with CIN emulsion effectively inhibited the accumulation of ROS in fresh mushrooms (*Flammulina velutipes*) and maintained their storage quality (Shao *et al.,* 2023). These findings indicate that the innovative barrier coating incorporating CIN could effectively improve tomato's

ability to scavenge ROS, thereby maintaining cell membrane integrity, which is closely linked to limiting water loss. The storage of fresh horticultural produce after harvesting typically triggers the ripening process, followed by subsequent senescence (Wang *et al.,* 2019).

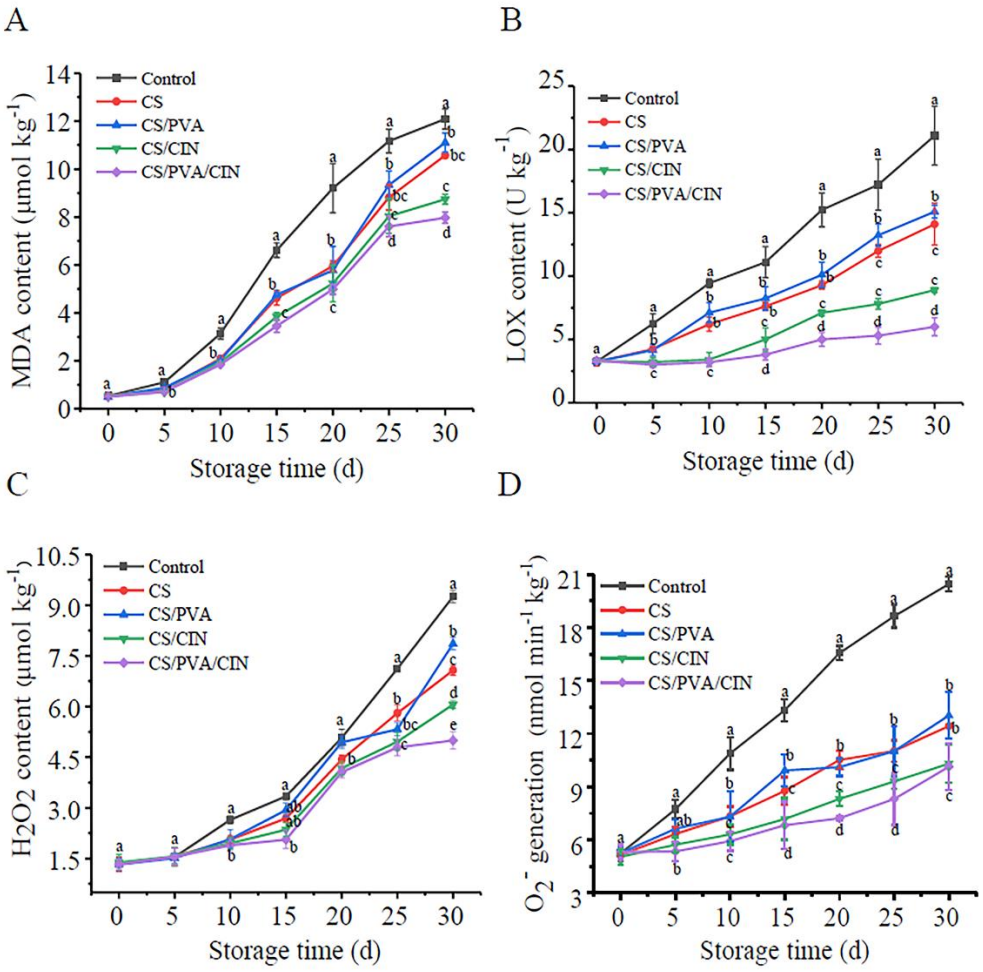

Figure 4.3. MDA content (A), LOX (B) activities, H_2O_2 content (C), O_2^- generation rate (D) in tomatoes during the storage

4.3.11. Catalase analysis

The CAT activities in the tomatoes exhibited a trend similar to that observed for SOD, POD, and GR activity throughout the storage period. As illustrated in Fig. 4.4 A, CAT activity initially

increased and then decreased. The control group achieved its highest CAT activity, measuring 263.93 U kg^{-1} on the 10th day and then declined rapidly. However, all the coating treatments reached their peak value on the 15 d. In particular, the CAT activity in the CS/PVA/CIN treatment group was 2.43 times greater than that observed in the control group by the end of the storage period.

4.3.12. Ascorbate peroxidase analysis

Throughout the storage period, the treatment group consistently exhibited higher APX activity in coated postharvest tomatoes than the control group (Fig. 4.4B). On the 10 d, the control group reached its peak APX activity, whereas the CS/PVA/CIN treatment group showed a 1.21-fold increase compared with the control group. At the conclusion of the storage duration, the APX values for each group were as follows: 49.12 U kg^{-1} (control), 65.37 U kg^{-1} (CS), 61.17 U kg^{-1} (CS/PVA), 79.13 (CS/CIN) U kg^{-1}, and 82.98 U kg^{-1} (CS/PVA/CIN).

4.3.13. Superoxide dismutase analysis

The antioxidant enzyme system acts directly to reduce ROS levels by neutralizing active oxygen-utilizing enzymes, such as SOD, CAT, POD, APX, and GR. Specifically, SOD plays a key role in converting O_2^- to H_2O_2, which can then be further broken down into H_2O and O_2 via the actions of CAT, POD, and APX. In addition, the breakdown of H_2O_2 to H_2O occurs through various pathways involving APX and GR, which regulate excessive H_2O_2 levels by oxidizing ascorbic acid to monodehydroascorbic acid and modulating reduced glutathione to oxidized glutathione, respectively (Zhao et al., 2020). In our investigation, the application of CIN coatings significantly enhanced the activities of CAT, SOD, POD, APX, and GR during storage (Fig. 4.4). Moreover, in terms of comprehensive quality performance (sensory and basic indicators), postharvest tomatoes

exhibited superior preservation in the CS/PVA/CIN and CS/CIN treatment groups. The observed enhancement in preservation is likely attributable to the increased capacity of the antioxidant enzyme system. Furthermore, these results were similar to the evaluation of CS-based coatings enriched with CIN treatments on mandarin fruit, navel orange fruit, strawberries, and mango fruit (Gao *et al.,* 2018 a; Gao *et al.,* 2018 b; Piechowiak Skóra, 2023; Xiao *et al.,* 2021).

As shown in Fig. 4.4C, SOD activity demonstrated an initial gradual increase, followed by a subsequent decline in all tested groups as storage time progressed. Notably, tomatoes treated with CS alone and those treated with CS combined with CIN and PVA consistently exhibited significantly higher SOD activities than the control group ($P < 0.05$). Towards the end of the storage period, the SOD activities of CS/PVA/CIN and CS/CIN were 512.33 and 494.00 U kg^{-1}, respectively.

4.3.14. Peroxidases analysis

As shown in Fig. 4.4D, the POD activity of the control group declined slightly for 5 d, reached the maximum value (85.30 U kg^{-1}) on the 10 d, and then rapidly declined to 64.98 U kg^{-1} on day 30, indicating that the tomatoes ripen on 10 d and then senesce rapidly. POD activity remained comparable among all coating groups within the initial 5 d storage period. However, after 15 d, the CS/PVA/CIN coating group exhibited the highest POD activity, followed by the CS/CIN, CS, CS/PVA, and control groups. Based on the storage period, the POD activity in the CIN coating was notably higher than that in the other treatment groups.

4.3.15. Glutathione reductase analysis

As shown in Fig. 4.4E, the GR activity of all groups was similar during the initial 5 d. After 5 d, the GR activity in the control group first increased and then decreased rapidly. In addition, at

a later stage of storage (20-30 d), both the CS/PVA/CIN and CS/CIN groups outperformed the CS coating group in terms of GR activity. However, the addition of PVA did not have a pronounced antioxidant effect on postharvest tomatoes.

These findings substantiate that CIN treatment contributes to an enhanced antioxidant capacity by sustaining elevated levels of enzymes associated with ROS scavenging (Fig. 4.4). This augmentation in enzymatic activity impedes the peroxidation of membrane lipids, thereby retarding the deterioration of membrane functionality, and consequently extending the overall senescence process of the fruit.

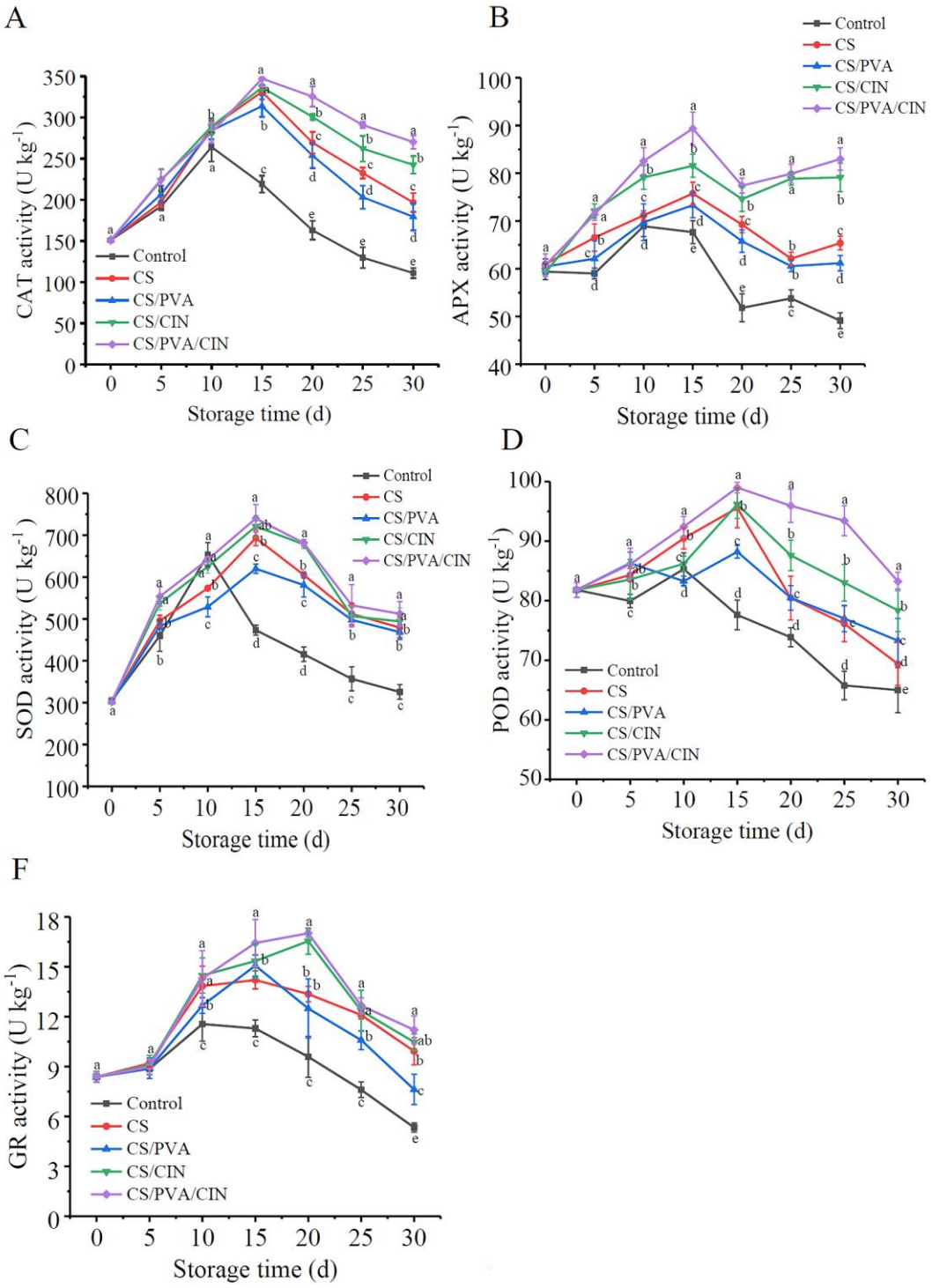

Figure 4.4. Various treatment on the antioxidant enzyme activities in tomatoes

4.3.16. Principal component analysis

As shown in Fig. 4.5, PCA was used to assess the impact of diverse materials on tomatoes during refrigeration. The results revealed that the first two principal components, PC1 and PC2, contributed 68.82% and 24.60%, respectively, with a cumulative variance proportion of 93.42%. The relationship between various each parameter and PC1 and PC2 is illustrated in Fig. 4.5A, where LOX, O_2^-, H_2O_2, *a** value, TSS, MDA and weight loss showed positive correlations with PC1, whereas *L** value firmness, sensory evaluation, TA, *b** value, POD activity, APX activity, GR activity, CAT activity and SOD activity exhibited negative correlations. The *L** value, firmness, sensory evaluation, TA, *b** value, LOX and O_2^- were positively correlated with PC2, whereas the POD activity, APX activity, GR activity, CAT activity, SOD activity, H_2O_2, *a** value, TSS, MDA and weight loss were negatively correlated with PC2.

The proximity of different samples on the scoring plots indicated similar behaviors of their effects on the tomato properties (Petriccione *et al.,* 2015). As shown in Figure 4.5B, there was a notable resemblance in scores among treatment groups on 0 d within the second quadrant. By day 5, the marked similarity observed between CS and CS/PVA, as well as CS/CIN and CS/PVA/CIN, with both coated and uncoated films positioned in the same quadrant, indicating that the insignificant differences between coated and uncoated films within the initial 5-day period. Similarly, in the first quadrant there was a control (15-20 days) group, a CS/PVA (25-30 days) group and a CS-treated group (30th day), illustrating that between the control and CS/PVA groups were not significant different during the 20–30-day storage period. On the contrary, the CS/CIN and CS/PVA/CIN treatment groups (10-30 days) were mainly concentrated in the third and fourth quadrants, indicating the variability of the group with CIN coating from the other three groups.

Physical and chemical parameters were distributed in different ways in the axis plane, indicating their variability in quality and nutraceutical traits. As depicted in Fig. 4.5, the CIN-coated group was mainly focused on POD, APX, GR, CAT and SOD enzyme activities after 20 days, indicating that CS/CIN and CS/PVA/CIN treatment group had a better effect on enzyme activities after 20 days, but not necessarily better for LOX, O_2^-, H_2O_2, *a** value, TSS, MDA, *L** value, *a** value, *b** value, sensory evaluation and weight loss. Moreover, the control samples in Fig. 4.5B seem to show a lower impact in POD, APX, GR, CAT and SOD enzyme activities during the storage period. Likewise, the control and CS/PVA treatment groups in Fig.4.5B seem to give higher LOX, MDA, H_2O_2, O_2^-, TSS, MDA and weight loss, which suggesting that the control and CS/PVA were ineffective in inhibiting weight loss, MDA, and other contents of postharvest tomato, and did not show improvement in delaying senescence. In summary, there was no significant difference between the control and coated groups within 5 days of storage. However, at a later stage (after 20 days), the CIN-coated group was significantly different from the other three groups with improved enzyme activity. Therefore, the CS/CIN and CS/PVA/CIN treatment groups proved to be more efficient in maintaining freshness and reducing ROS level in postharvest tomatoes.

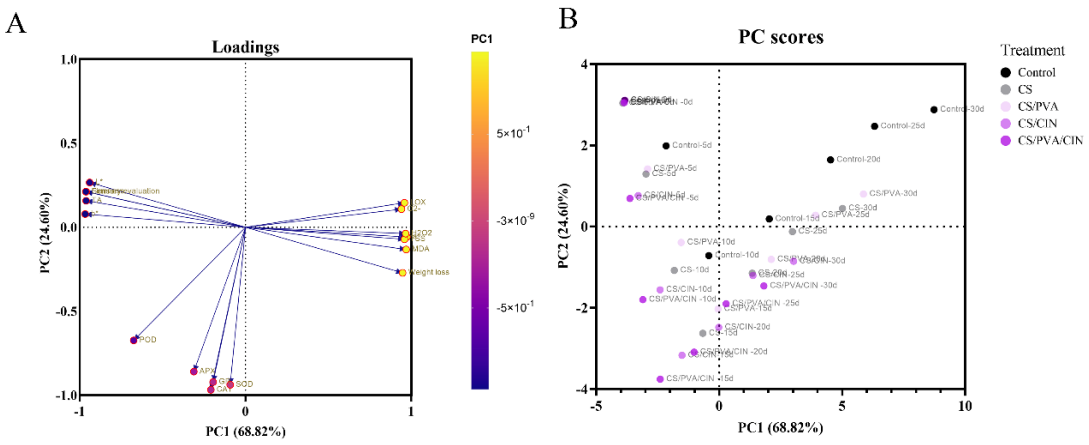

Figure 4.5. (A) Loading plots of sensory tests by PCA, (B) PCA scores of sensory tests of different treatment groups

4.3.17. Correlation heatmap analysis

Fig.4.6 shows a correlation heatmap analysis illustrating the interrelationships among the tomato parameters throughout the entire storage period. As shown in Fig. 4.6, weight loss was positively correlated with LOX activity (r = 0.84), O_2^- (r = 0.82), TSS (r = 0.91), MDA content (r = 0.97), *a** value (r = 0.95) and H_2O_2 (r = 0.95), whereas it was negatively correlated with *L** value (r = −0.97), sensory evaluation (r = −0.97), firmness (r = −0.97), *b** value (r = −0.92), TA (r = −0.94), POD activity (r = −0.47), APX activity (r = −0.03). Excessive softening is strongly associated with cell wall metabolism and quality deterioration of postharvest fruit. The firmness had a significantly negative correlation with weight loss (r = −0.97), MDA content (r = −0.96), H_2O_2 (r =-0.93), TSS (r =-0.92), LOX activity (r = −0.88) and O_2^- (-0.87). Moreover, antioxidant enzyme activities (GR, CAT, SOD, APX, POD activity) exhibited negative correlations with LOX content, MDA content, O_2^- generation rate and H_2O_2 content. These findings suggested that tomato senescence was accompanied by elevated ROS and reduced overall quality, and that ROS metabolism is strongly associated with tomato senescence. Integrating this with Figure 4.6, it can be inferred that the application of the water-barrier coating enhances ROS regulation, minimizes weight loss, delays senescence progression in tomatoes during storage, thereby substantially extending the shelf life of postharvest tomatoes.

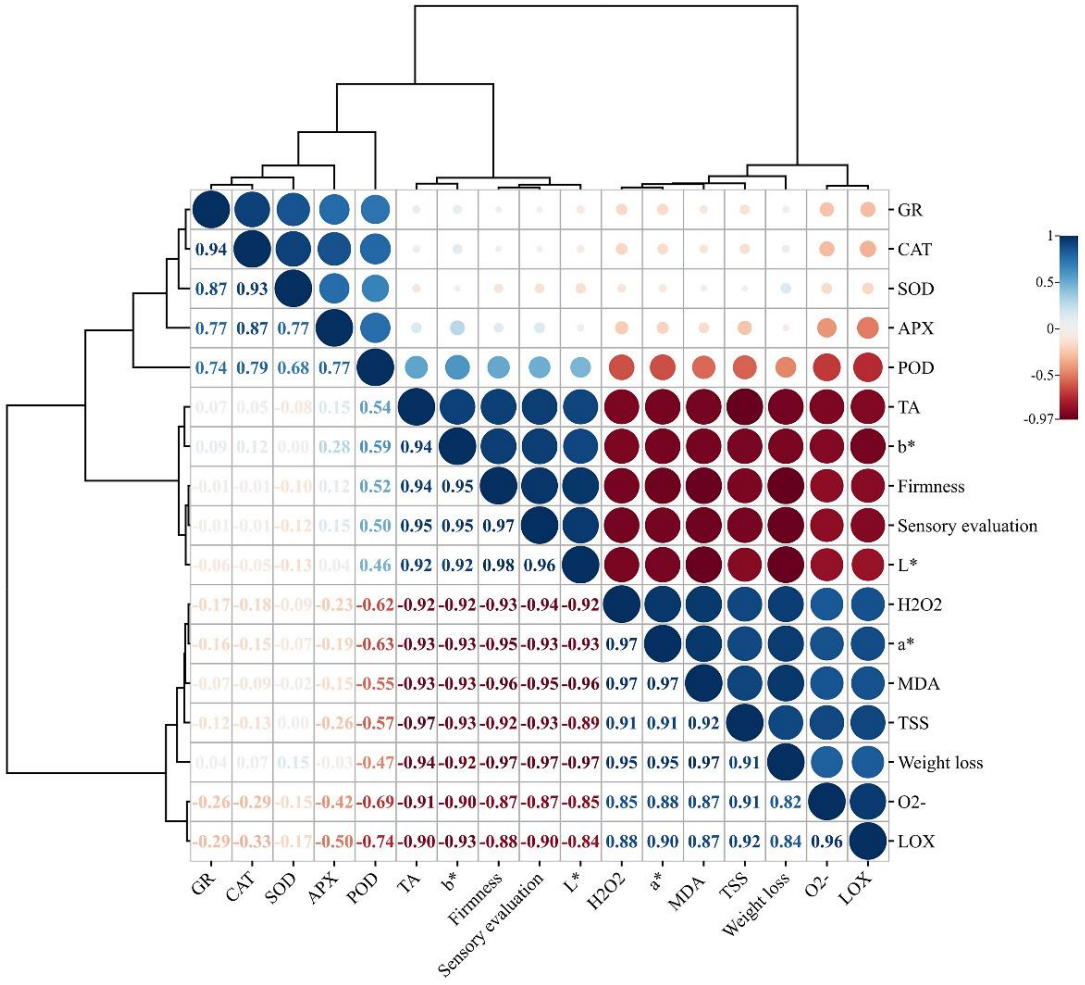

Figure 4.6. Heatmap of Pearson's correlations based on the measured parameters in tomatoes during the whole storage under the cold temperature 8 ± 2 ˚C.

4.4. Reference

Al-Bayati, F. A., & Mohammed, M. J. (2009). Isolation, identification, and purification of cinnamaldehyde from Cinnamomum zeylanicum bark oil. An antibacterial study. *Pharmaceutical Biology,* 47(1), 61-66.

Al-Dairi, M., Pathare, P. B., Al-Yahyai, R., & Opara, U. L. (2022). Mechanical damage of fresh produce in postharvest transportation: Current status and future prospects. *Trends in Food*

Science & Technology, 124, 195-207.

Aragüez, L., Colombo, A., Borneo, R., & Aguirre, A. (2020). Active packaging from triticale flour films for prolonging storage life of cherry tomato. *Food Packaging and Shelf Life,* 25, 100520.

Azeredo, H. M., & Waldron, K. W. (2016). Crosslinking in polysaccharide and protein films and coatings for food contact–A review. *Trends in Food Science & Technology,* 52, 109-122.

Cao, M., Wang, X., Su, J., Lu, Z., Li, Y., & Gao, H. (2021). Delayed senescence of kiwifruit by p-coumaric acid pretreatment during storage at 20° C: Toward regulating the ascorbate–glutathione cycle and phenolic anabolism. *Scientia Horticulturae,* 280, 109913.

Carvalho, R. L., Cabral, M. F., Germano, T. A., de Carvalho, W. M., Brasil, I. M., Gallão, M. I., . . . de Miranda, M. R. A. (2016). Chitosan coating with trans-cinnamaldehyde improves structural integrity and antioxidant metabolism of fresh-cut melon. *Postharvest Biology and Technology,* 113, 29-39.

Chandra, R. D., Prihastyanti, M. N. U., & Lukitasari, D. M. (2021). Effects of pH, high pressure processing, and ultraviolet light on carotenoids, chlorophylls, and anthocyanins of fresh fruit and vegetable juices. *EFood,* 2(3), 113-124.

Chauhan, D. S., Mazumder, M. J., Quraishi, M., & Ansari, K. (2020). Chitosan-cinnamaldehyde Schiff base: A bioinspired macromolecule as corrosion inhibitor for oil and gas industry. *International Journal of Biological Macromolecules,* 158, 127-138.

Chen, C.-K., & Huang, S.-C. (2016). Preparation of reductant–responsive N-maleoyl-functional chitosan/poly (vinyl alcohol) nanofibers for drug delivery. *Molecular Pharmaceutics,* 13(12), 4152-4167.

Elsabee, M. Z., & Abdou, E. S. (2013). Chitosan based edible films and coatings: A review.

Materials science and engineering: C, 33(4), 1819-1841.

Fadiji, T., Coetzee, C., Chen, L., Chukwu, O., & Opara, U. L. (2016). Susceptibility of apples to bruising inside ventilated corrugated paperboard packages during simulated transport damage. *Postharvest Biology and Technology,* 118, 111-119.

Gadkari, R. R., Suwalka, S., Yogi, M. R., Ali, W., Das, A., & Alagirusamy, R. (2019). Green synthesis of chitosan-cinnamaldehyde cross-linked nanoparticles: Characterization and antibacterial activity. *Carbohydrate Polymers,* 226, 115298.

Gao, Y., Kan, C., Chen, M., Chen, C., Chen, Y., Fu, Y., . . . Chen, J. (2018). Effects of chitosan-based coatings enriched with cinnamaldehyde on Mandarin fruit cv. Ponkan during room-temperature storage. *Coatings,* 8(10), 372.

Gao, Y., Kan, C., Wan, C., Chen, C., Chen, M., & Chen, J. (2018). Quality and biochemical changes of navel orange fruits during storage as affected by cinnamaldehyde-chitosan coating. *Scientia Horticulturae,* 239, 80-86.

Jiang, A., Zuo, J., Zheng, Q., Guo, L., Gao, L., Zhao, S., . . . Hu, W. (2019). Red LED irradiation maintains the postharvest quality of broccoli by elevating antioxidant enzyme activity and reducing the expression of senescence-related genes. *Scientia Horticulturae,* 251, 73-79.

Jin, W., & Wu, F. (2015). Characterization of miRNAs associated with Botrytis cinerea infection of tomato leaves. *BMC Plant Biology,* 15, 1-14.

Kaur, K., Jindal, R., Maiti, M., & Mahajan, S. (2019). Studies on the properties and biodegradability of PVA/Trapa natans starch (N-st) composite films and PVA/N-st-g-poly (EMA) composite films. *International Journal of Biological Macromolecules,* 123, 826-836.

Kumar, N., Neeraj, Pratibha, & Trajkovska Petkoska, A. (2021). Improved shelf life and quality of

tomato (Solanum lycopersicum L.) by using chitosan-pullulan composite edible coating enriched with pomegranate peel extract. *ACS Food Science & Technology,* 1(4), 500-510.

Kundu, P., Adhikary, N. K., & Maji, S. (2020). A critical review on use of edible coating to enhance shelf life of mango. *Current Journal of Applied Science and Technology,* 39(27), 116-128.

Li, C., Li, Q., Zhang, Y., Gong, Z., Ren, S., Li, P., & Xie, J. (2017). Characterization and function of Mycobacterium tuberculosis H37Rv lipase Rv1076 (LipU). *Microbiological research,* 196, 7-16.

Li, Z., Zhang, W., Li, X., Liu, H., Li, F., & Zhang, X. (2022). Combined effects of 1-methylcyclopropene and tea polyphenols coating treatment on the postharvest senescence and reactive oxygen species metabolism of bracken (Pteridium aquilinum var. latiusculum). *Postharvest Biology and Technology,* 185, 111813.

Liu, Y., Zhang, Y., Zhen, M., Wu, Y., Ma, M., Cheng, Y., & Jin, Y. (2023). Effect of catechin and tannins on the structural and functional properties of sodium alginate/gelatin/poly (vinylalcohol) blend films. *Food Hydrocolloids,* 135, 108141.

Lo'Ay, A., & Dawood, H. (2017). Active chitosan/PVA with ascorbic acid and berry quality of 'Superior seedless' grapes. *Scientia Horticulturae,* 224, 286-292.

López-Gálvez, F., Ragaert, P., Haque, M. A., Eriksson, M., van Labeke, M. C., & Devlieghere, F. (2015). High oxygen atmospheres can induce russet spotting development in minimally processed iceberg lettuce. *Postharvest Biology and Technology,* 100, 168-175.

Ma, Y., Fu, L., Hussain, Z., Huang, D., & Zhu, S. (2019). Enhancement of storability and antioxidant systems of sweet cherry fruit by nitric oxide-releasing chitosan nanoparticles (GSNO-CS NPs). *Food Chemistry,* 285, 10-21.

Meng, X., Chen, C., Song, T., Xu, J., Zhang, X., Wang, J., . . . Zhang, H. (2022). Effect of nano-

silica coating combined with pressurized Ar treatment on postharvest quality and reactive oxygen species metabolism in sweet cherry fruit. *Food Chemistry,* 374, 131715.

Mondal, K., Goud, V. V., & Katiyar, V. (2022). Effect of waste green algal biomass extract incorporated chitosan-based edible coating on the shelf life and quality attributes of tomato. *ACS Food Science & Technology,* 2(7), 1151-1165.

Monisha, M., Yadav, N., & Lochab, B. (2019). Sustainable framework of chitosan–benzoxazine with mutual benefits: Low curing temperature and improved thermal and mechanical properties. *ACS Sustainable Chemistry & Engineering,* 7(4), 4473-4485.

Narasagoudr, S. S., Hegde, V. G., Chougale, R. B., Masti, S. P., Vootla, S., & Malabadi, R. B. (2020). Physico-chemical and functional properties of rutin induced chitosan/poly (vinyl alcohol) bioactive films for food packaging applications. *Food Hydrocolloids,* 109, 106096.

Osugi, N., Dong, T., Hexig, B., & Inoue, Y. (2010). Generation and characterization of compositional gradient structure in the biodegradable chitosan/poly(ethylene oxide) blend. *Journal of Applied Polymer Science,* 104(5), 2939-2946.

Petriccione, M., Pasquariello, M. S., Mastrobuoni, F., Zampella, L., Di Patre, D., & Scortichini, M. (2015). Influence of a chitosan coating on the quality and nutraceutical traits of loquat fruit during postharvest life. *Scientia Horticulturae,* 197, 287-296.

Pholsin, R., Shiekh, K. A., Jafari, S., Kijpatanasilp, I., Nan, T. N., Suppavorasatit, I., & Assatarakul, K. (2024). Impact of pectin edible coating extracted from cacao shell powder on postharvest quality attributes of tomato (Lycopersicon esculentum Mill.) fruit during storage. *Food Control,* 155, 110023.

Piechowiak, T., Grzelak-Błaszczyk, K., Sójka, M., & Balawejder, M. (2020). Changes in phenolic compounds profile and glutathione status in raspberry fruit during storage in ozone-

enriched atmosphere. *Postharvest Biology and Technology,* 168, 111277.

Piechowiak, T., & Skóra, B. (2023). Edible coating enriched with cinnamon oil reduces the oxidative stress and improves the quality of strawberry fruit stored at room temperature. *Journal of the Science of Food and Agriculture,* 103(5), 2389-2400.

Ponce-Valadez, M., Escalona-Buendía, H. B., Villa-Hernández, J. M., de León-Sánchez, F. D., Rivera-Cabrera, F., Alia-Tejacal, I., & Pérez-Flores, L. J. (2016). Effect of refrigerated storage (12.5 C) on tomato (Solanum lycopersicum) fruit flavor: A biochemical and sensory analysis. *Postharvest Biology and Technology,* 111, 6-14.

Shao, X., Niu, B., Fang, X., Wu, W., Liu, R., Mu, H., . . . Chen, H. (2023). Pullulan-stabilized Soybean Phospholipids/Cinnamaldehyde emulsion for Flammulina velutipes preservation. *International Journal of Biological Macromolecules*, 125425.

Subash-Babu, P., Alshatwi, A. A., & Ignacimuthu, S. (2014). Beneficial antioxidative and antiperoxidative effect of cinnamaldehyde protect streptozotocin-induced pancreatic β-cells damage in wistar rats. *Biomolecules & therapeutics,* 22(1), 47.

Tapia, M. S., Alzamora, S. M., & Chirife, J. (2020). Effects of water activity (aw) on microbial stability as a hurdle in food preservation. *Water activity in foods: Fundamentals and applications*, 323-355.

Wang, C., Niu, Y., Meng, Q., & Zhang, L. (2019). Ethyl pyruvate (EP) suppressed post-harvest blue mold of sweet cherry fruit by inhibiting the growth of Penicillium oxalicum. *Journal of the Science of Food and Agriculture,* 99(7), 3517-3524.

Wang, H., Zhang, Y., Pu, Y., Chen, L., He, X., Cao, J., & Jiang, W. (2023). Composite coating of guar gum with salicylic acid alleviates the quality deterioration of vibration damage in ‘Huangguan’pear fruit through the regulation of antioxidant metabolism. *Postharvest*

Biology and Technology, 205, 112476.

Wang, J., Sun, X., Zhang, H., Dong, M., Li, L., Zhangsun, H., & Wang, L. (2022). Dual-functional intelligent gelatin based packaging film for maintaining and monitoring the shrimp freshness. *Food Hydrocolloids,* 124, 107258.

Wardana, A. A., Kingwascharapong, P., Wigati, L. P., Tanaka, F., & Tanaka, F. (2022). The antifungal effect against Penicillium italicum and characterization of fruit coating from chitosan/ZnO nanoparticle/Indonesian sandalwood essential oil composites. *Food Packaging and Shelf Life,* 32, 100849.

Wigati, L. P., Wardana, A. A., Tanaka, F., & Tanaka, F. (2023). Strawberry preservation using combination of yam bean starch, agarwood Aetoxylon bouya essential oil, and calcium propionate edible coating during cold storage evaluated by TOPSIS-Shannon entropy. *Progress in Organic Coatings,* 175, 107347.

Wu, G., & Wang, C. (2014). Investigating the effects of simulated transport vibration on tomato tissue damage based on vis/NIR spectroscopy. *Postharvest Biology and Technology,* 98, 41-47.

Xiao, J., Gu, C., Zhu, D., Huang, Y., Luo, Y., & Zhou, Q. (2021). Development and characterization of an edible chitosan/zein-cinnamaldehyde nano-cellulose composite film and its effects on mango quality during storage. *Lwt,* 140, 110809.

Xie, J., Wang, R., Li, Y., Ni, Z., Situ, W., Ye, S., & Song, X. (2022). A novel Ag2O-TiO2-Bi2WO6/polyvinyl alcohol composite film with ethylene photocatalytic degradation performance towards banana preservation. *Food Chemistry,* 375, 131708.

Xing, Y., Xu, Q., Yang, S. X., Chen, C., Tang, Y., Sun, S., . . . Li, X. (2016). Preservation mechanism of chitosan-based coating with cinnamon oil for fruits storage based on sensor

data. *Sensors,* 16(7), 1111.

Yadav, A., Kumar, N., Upadhyay, A., Pratibha, & Anurag, R. K. (2023). Edible packaging from fruit processing waste: A comprehensive review. *Food Reviews International,* 39(4), 2075-2106.

Yadav, A., Kumar, N., Upadhyay, A., Sethi, S., & Singh, A. (2022). Edible coating as postharvest management strategy for shelf-life extension of fresh tomato (Solanum lycopersicum L.): An overview. *Journal of Food Science,* 87(6), 2256-2290.

Yan, X., Wardana, A. A., Wigati, L. P., Meng, F., Leonard, S., Nkede, F. N., . . . Tanaka, F. (2023). Characterization and bio-functional performance of chitosan/poly (vinyl alcohol)/trans-cinnamaldehyde ternary biopolymeric films. *International Journal of Biological Macromolecules,* 246, 125680.

Yang, D., Liu, Q., Gao, Y., Wan, S., Meng, F., Weng, W., & Zhang, Y. (2023). Characterization of silver nanoparticles loaded chitosan/polyvinyl alcohol antibacterial films for food packaging. *Food Hydrocolloids,* 136, 108305.

Yousuf, B., Wu, S., & Siddiqui, M. W. (2021). Incorporating essential oils or compounds derived thereof into edible coatings: Effect on quality and shelf life of fresh/fresh-cut produce. *Trends in Food Science & Technology,* 108, 245-257.

Zhang, H., Liu, F., Wang, J., Yang, Q., Wang, P., Zhao, H., . . . Xu, X. (2021). Salicylic acid inhibits the postharvest decay of goji berry (Lycium barbarum L.) by modulating the antioxidant system and phenylpropanoid metabolites. *Postharvest Biology and Technology,* 178, 111558.

Zhang, X., Zhou, H., Han, Z., Huang, W., Gu, X., Li, B., . . . Zhang, H. (2022). Pichia caribbica combined with oligochitosan controlling black spot of tomatoes and the regulation on ROS

metabolism of the fruits. *Biological Control,* 176, 105109.

Zhao, Y., Zhu, X., Hou, Y., Wang, X., & Li, X. (2020). Postharvest nitric oxide treatment delays the senescence of winter jujube (Zizyphus jujuba Mill. cv. Dongzao) fruit during cold storage by regulating reactive oxygen species metabolism. *Scientia Horticulturae,* 261, 109009.

Zhou, Q., Ma, C., Cheng, S., Wei, B., Liu, X., & Ji, S. (2014). Changes in antioxidative metabolism accompanying pitting development in stored blueberry fruit. Postharvest Biology and Technology, 88, 88-95.

CHAPTER 5

CONCLUSIONS AND FUTURE WORKS

5.1 Conclusions

This thesis described the development and application of novel antioxidant/ antifungal coating film on fresh fruits. This work was focused on the following objectives:

1) Application of physicochemical characterization of coatings with CS, cross-linked-PEG, CIN and their application in banana preservation.

2) Investigation of physicochemical characterization of coating blend with CS, PVA and CIN formulations.

3) To further investigate the effect of CS, PVA and CIN coatings on postharvest fruit quality and reactive oxygen species metabolism.

The general conclusions of this present study were summarized as follows:

1) Ternary films with enhanced bioactivity were fabricated for banana preservation. These results demonstrate that incorporating CIN considerably enhances the mechanical properties, water barrier properties, and antimicrobial capacity of bioactive films. A ternary coating made from a

polymer compound of CS, PEG, and CIN reduced the respiration rate and delayed banana ripening. Additionally, it contributed to reduced weight loss, maintained peel color, and maintained levels of TSS, TA, and reduced sugars during the 12-24 days period. Sensory evaluation and quality analysis revealed that bananas coated with CS/PEG/CIN0.5, and CS/PEG/CIN1 had an extended shelf life of eight days at room temperature, but no significant differences were observed.

2) CIN concentration was varied to evaluate the impact on bio-active film physicochemical, mechanical, barrier, microstructural and anti-microbial/antioxidant properties. ATR-FTIR confirmed the good compatibility between CIN and the polymer components. SEM and AFM observed a uniform distribution of the CIN/CS/PVA. The homogeneous, intact, and compact bioactive films showed improved mechanical and oxygen barrier properties. Furthermore, CS/PVA/CIN ternary films demonstrated a better barrier capability of light transmittance at 350 nm. The addition of CIN improved the WVP and WCA of ternary film. The highest DPPH radical scavenging effect and reduction capacity was observed for the CS/PVA/CIN1.5 films. Both in vitro investigations on mycelial growth and spore germination demonstrated that the addition of CIN to bio-active composite films efficiently inhibited the growth of *P. italicum* and *B. cinerea* fungi, with the CS/PVA/CIN1.5 films achieving a maximum inhibition rate of more than 90 %. Therefore, the functional characteristics of biopolymer-based materials are improved by CIN.

3) The Schiff base (C=N) formed between the aldehyde group of CIN and the amino group of CS, combined with its dense structure and excellent water barrier properties, was effective in preventing water loss and softening of tomatoes. It also enhanced the appearance and physiological properties of tomatoes. Simultaneously, the consumption of substances such as TSS and TA was slowed. CIN-added coatings (CS/CIN and CS/PVA/CIN) reduced cell membrane permeability; decreased O_2^-, H_2O_2, LOX, and MDA content; and enhanced enzymatic ROS scavenging systems,

including SOD, CAT, POD, APX, and GR activities, which were highly correlated with reduced water loss. Thus, CS/PVA/CIN treatment effectively delayed the postharvest senescence of tomato fruit and is expected to be a novel freshness preservation technology. Nevertheless, the effect of PVA was attenuated in all the coating groups and may differ in other fruit and vegetables owing to multivariate factors.

5.2 Future works

1. From material:

Edible coatings are crafted from biodegradable and non-toxic materials, offering a sustainable solution for enhancing the shelf life and post-harvest quality of fruits, vegetables, and other food items. These coatings are formulated using a variety of biopolymer matrices, including polysaccharides, proteins, lipids, and composite materials.

1.1) Polysaccharide-based materials like pullulan, chitosan, and alginate, along with proteins such as collagen, gelatin, and soy protein, contribute to the formation of protective films that help preserve freshness and prevent spoilage.

1.2) Additionally, lipid-based materials like beeswax, carnauba wax, and jojoba oil provide further barrier properties to maintain product integrity. In future, by harnessing the natural properties of these materials, edible coatings not only extend the shelf life of food products but also minimize environmental impact. They offer a sustainable alternative to traditional packaging materials, aligning with the growing consumer demand for eco-friendly solutions.

2. From postharvest products:

In future, various types of edible coatings has proven effective in extending shelf life and enhancing post-harvest qualities across a spectrum of food items.

2.1) Fruits like mangoes, bananas, and strawberries, along with vegetables such as tomatoes, cucumbers, and carrots, have all benefited from these coatings.

2.2) Moreover, fresh meat cuts, as well as meat and fish products like trout fillets, beef, and chicken.

3. From technology:

3.1) Innovations in food preservation techniques may introduce new methods that are more efficient, sustainable, and capable of preserving the nutritional content and flavor of food products. This could include techniques such as high-pressure processing, pulsed electric fields, and cold plasma treatment.

3.2) Packaging will continue to evolve to meet the demands for longer shelf life, reduced food waste, and environmental sustainability. Smart packaging embedded with sensors and indicators to monitor freshness, as well as biodegradable and compostable packaging materials, are likely to become more prevalent.

3.3) Advances in data analytics, machine learning, and artificial intelligence may enable precision preservation techniques that tailor treatment conditions to the specific requirements of different food products, optimizing preservation while minimizing energy consumption and environmental impact.

3.4) Consumer demand for clean label products free from artificial additives and preservatives will drive the development of natural preservation methods using ingredients such as plant extracts, essential oils, and fermentation-based approaches.

Overall, the future of food preservation technology is likely to be characterized by a combination of advanced techniques, sustainable practices, and consumer-centric solutions aimed

at ensuring food security, reducing waste, and meeting the evolving needs of a growing global population.

SUPPLEMENTARY MATERIALS

Table S1. The sensory evaluation of bananas with different treatments.

Storage days	Sensory evaluation				
	Control	CS/PEG	CS/PEG/CIN 0.5	CS/PEG/CIN 1	CS/PEG/CIN 1.5
0	5.00 ± 0.01^{A}	5.00 ± 0.01^{A}	5.00 ± 0.01^{A}	5.00 ± 0.01^{A}	5.00 ± 0.01^{A}
4	3.82 ± 0.05^{C}	5.00 ± 0.21^{A}	4.89 ± 0.13^{B}	4.97 ± 0.18^{A}	4.91 ± 0.22^{B}
8	3.10 ± 0.15^{C}	3.42 ± 0.12^{B}	4.61 ± 0.28^{A}	4.57 ± 0.18^{A}	3.61 ± 0.58^{B}
12	2.23 ± 0.04^{C}	3.11 ± 0.12^{B}	4.15 ± 0.04^{A}	4.19 ± 0.12^{A}	3.20 ± 0.32^{B}
16	2.10 ± 0.02^{D}	2.78 ± 0.26^{C}	3.44 ± 0.04^{A}	3.42 ± 0.12^{A}	3.29 ± 0.12^{B}
20	1.22 ± 0.04^{E}	2.10 ± 0.18^{D}	2.90 ± 0.12^{A}	2.74 ± 0.02^{B}	2.30 ± 0.15^{C}
24	0.91 ± 0.03^{D}	1.61 ± 0.20^{C}	2.7 ± 0.11^{A}	2.78 ± 0.04^{A}	2.11 ± 0.25^{B}

Duncan's multiple range tests show that data with the same superscript letter in the same column are not statistically different ($p > 0.05$).

Table S2. The weight loss of bananas with different treatments.

Storage days	Weight loss (%)				
	Control	CS/PEG	CS/PEG/CIN 0.5	CS/PEG/CIN 1	CS/PEG/CIN 1.5
4	1.89 ± 0.41^{A}	1.61 ± 0.66^{C}	1.55 ± 0.10^{D}	1.58 ± 0.37^{CD}	1.67 ± 0.82^{B}
8	3.28 ± 0.83^{A}	2.77 ± 0.99^{C}	2.10 ± 0.39^{D}	2.02 ± 1.04^{CD}	2.13 ± 0.65^{B}
12	7.55 ± 0.94^{A}	4.86 ± 0.72^{B}	3.19 ± 0.69^{D}	3.29 ± 0.57^{D}	3.61 ± 1.00^{CD}
16	11.58 ± 1.22^{A}	8.98 ± 0.22^{B}	5.39 ± 0.26^{D}	5.43 ± 0.21^{D}	6.29 ± 0.23^{C}
20	16.30 ± 0.44^{A}	11.46 ± 0.62^{B}	9.20 ± 1.02^{C}	9.15 ± 0.70^{C}	10.59 ± 1.36^{B}
24	22.31 ± 0.31^{A}	15.41 ± 0.42^{B}	11.04 ± 0.24^{D}	11.01 ± 0.33^{D}	12.54 ± 1.09^{C}

Duncan's multiple range tests show that data with the same superscript letter in the same column are not statistically different ($p > 0.05$).

Table S3. The total soluble solid of bananas with different treatments

Storage days	TSS (%)				
	Control	CS/PEG	CS/PEG/CIN 0.5	CS/PEG/CIN 1	CS/PEG/CIN 1.5
0	0.50 ± 0.00^{A}	0.50 ± 0.00^{A}	0.50 ± 0.00^{A}	0.50 ± 0.00^{A}	0.50 ± 0.00^{A}
4	1.33 ± 0.05^{A}	1.40 ± 0.08^{A}	1.30 ± 0.00^{A}	1.40 ± 0.08^{A}	1.30 ± 0.00^{A}
8	1.87 ± 0.05^{A}	1.50 ± 0.00^{B}	1.30 ± 0.08^{CD}	1.20 ± 0.00^{D}	1.40 ± 0.08^{BC}
12	7.17 ± 0.09^{A}	6.50 ± 0.00^{B}	2.50 ± 0.14^{C}	1.93 ± 0.12^{D}	2.13 ± 0.12^{D}
16	10.50 ± 1.22^{A}	9.50 ± 0.22^{B}	6.67 ± 0.05^{C}	6.53 ± 0.12^{C}	6.80 ± 0.00^{C}
20	13.53 ± 0.44^{A}	11.40 ± 0.08^{B}	8.57 ± 0.12^{C}	8.50 ± 0.22^{C}	8.11 ± 0.05^{D}
24	14.00 ± 0.31^{A}	12.00 ± 0.00^{B}	9.00 ± 0.00^{C}	9.20 ± 0.00^{C}	9.50 ± 0.00^{D}

Duncan's multiple range tests show that data with the same superscript letter in the same column are not statistically different ($p > 0.05$).

Table S4. The Firmness of bananas with different treatments.

Storage days	Firmness (N)				
	Control	CS/PEG	CS/PEG/CIN 0.5	CS/PEG/CIN 1	CS/PEG/CIN 1.5
0	46.50 ± 1.08^{A}	46.67 ± 1.25^{A}	46.67 ± 1.25^{A}	46.67 ± 1.25^{A}	46.67 ± 1.25^{A}
4	41.70 ± 1.28^{A}	42.37 ± 0.52^{A}	42.33 ± 0.47^{A}	42.00 ± 0.41^{A}	41.60 ± 1.13^{A}
8	37.73 ± 0.61^{C}	39.47 ± 0.49^{B}	41.13 ± 0.12^{A}	41.01 ± 0.51^{A}	40.55 ± 0.46^{AB}
12	22.44 ± 0.91^{C}	33.96 ± 0.83^{B}	37.15 ± 0.55^{A}	38.06 ± 0.75^{A}	36.38 ± 0.70^{A}
16	11.87 ± 1.29^{C}	21.15 ± 0.76^{B}	30.67 ± 0.47^{A}	31.55 ± 0.33^{A}	30.07 ± 0.10^{A}
20	4.07 ± 0.09^{D}	8.92 ± 2.05^{C}	25.01 ± 0.63^{A}	25.21 ± 0.60^{A}	18.80 ± 0.58^{B}
24	2.1 ± 0.00^{D}	5.67 ± 1.24^{C}	11.78 ± 0.74^{A}	11.66 ± 0.95^{A}	9.67 ± 0.34^{B}

Duncan's multiple range tests show that data with the same superscript letter in the same column are not statistically different ($p > 0.05$).

Table S5. The Respiration rate of bananas with different treatments.

Storage days	Respiration rate (mg CO_2/kg/h)				
	Control	CS/PEG	CS/PEG/CIN 0.5	CS/PEG/CIN 1	CS/PEG/CIN 1.5
0	45.65 ± 0.41^{A}	45.35 ± 0.01^{A}	45.65 ± 0.01^{A}	45.55 ± 0.01^{A}	44.65 ± 0.01^{A}
4	63.33 ± 2.65^{A}	63.11 ± 2.58^{A}	62.30 ± 2.13^{A}	62.40 ± 2.18^{A}	62.79 ± 1.92^{A}
8	92.87 ± 3.15^{A}	81.29 ± 3.02^{B}	71.30 ± 2.18^{D}	72.20 ± 1.98^{D}	76.29 ± 2.58^{C}
12	82.17 ± 2.49^{B}	89.50 ± 2.72^{A}	76.50 ± 2.94^{C}	77.93 ± 2.62^{C}	82.13 ± 1.92^{B}
16	76.52 ± 2.02^{D}	79.50 ± 2.76^{C}	84.17 ± 2.00^{B}	85.13 ± 2.12^{AB}	86.80 ± 3.12^{A}
20	70.97 ± 2.94^{E}	73.40 ± 3.18^{D}	80.07 ± 2.12^{A}	78.50 ± 2.02^{B}	76.12 ± 2.15^{C}
24	61.62 ± 3.31^{D}	68.33 ± 1.20^{C}	74.00 ± 3.11^{A}	73.11 ± 2.11^{A}	70.50 ± 3.25^{B}

Duncan's multiple range tests show that data with the same superscript letter in the same column are not statistically different ($p > 0.05$).